



This document was produced
by scanning the original publication.

Ce document est le produit d'une
numérisation par balayage
de la publication originale.

GEOLOGICAL SURVEY OF CANADA
PAPER 91-12

ORIGIN OF THE LOWER PROTEROZOIC FLEMING CHERT-BRECCIA, NEWFOUNDLAND, LABRADOR-QUEBEC

Tyson C. Birkett

1991



Energy, Mines and
Resources Canada

Énergie, Mines et
Ressources Canada

Canada

THE ENERGY OF OUR RESOURCES

THE POWER OF OUR IDEAS



DEPARTMENT OF MINES
GOVERNMENT OF NEWFOUNDLAND AND LABRADOR

Contribution to Canada-Newfoundland Mineral
Development Agreement 1984-89, a subsidiary
agreement under the Economic and Regional
Development Agreement. Project funded by the
Geological Survey of Canada.



Energy, Mines and
Resources Canada

Énergie, Mines et
Ressources Canada

GEOLOGICAL SURVEY OF CANADA

PAPER 91-12

**ORIGIN OF THE LOWER PROTEROZOIC
FLEMING CHERT-BRECCIA,
NEWFOUNDLAND, LABRADOR-QUEBEC**

Tyson C. Birkett

1991

© Minister of Supply and Services Canada 1991

Available in Canada through

authorized bookstore agents and other bookstores

or by mail from

Canada Communications Group - Publishing
Ottawa, Canada K1A 0S9

and from

Geological Survey of Canada offices:

601 Booth Street
Ottawa, Canada K1A 0E8

3303-33rd Street N.W.,
Calgary, Alberta T2L 2A7

100 West Pender Street
Vancouver, B.C. V6B 1R8

A deposit copy of this publication is also available for reference
in public libraries across Canada

Cat. No. M44-91/12E
ISBN 0-660-14193-0

Price subject to change without notice

Critical Reader

Richard Bell
Denis Lavoie

Author address

*Geological Survey of Canada,
Quebec Geoscience Centre,
2700 rue Einstein,
C.P. 7500, Ste-Foy,
Québec, G1V 4C7.*

Cover Description

A clast of crust-type banded quartz lies in a matrix of chert-quartz sand, with chert cement. The clast exhibits unidirectional growth texture and repetitive growth events of euhedral quartz crystals. The two millimetres wide clast was photographed in doubly polarized light. The sample comes from northern Marble Lake. GSC 205130-T

Original manuscript received: 1990 - 11
Final version approved for publication: 1991 - 03

CONTENTS

1	Abstract / Resume
1	Introduction
1	Location and access
1	Previous studies
2	Stratigraphic position and geological setting
3	Terminology
4	General aspect of the Fleming Formation
5	Acknowledgments
5	Present investigation
5	Field investigation
5	Laboratory investigation
5	Areas studied in detail
6	North of Knox Mine
7	Slimy Lake area
8	Ridge at Bath Lake
9	Elizabeth Lake
10	North end of Marble Lake
10	Northern Marble Lake
11	West shore of Marble Lake
12	Northern Dyke Lake
13	Islands in Dyke Lake
16	Mineralogy
18	Texture and sedimentary structures
18	Lithological elements of the chert breccia
18	Cement
19	Matrix
19	Clasts
25	Diagenetic structures
27	Sedimentary structures
28	Chemistry
30	The origin of the Fleming Formation
31	Is the Fleming a lag deposit?
31	Is the Fleming a silicified dolomite?
32	Is the Fleming a silicified evaporite?
32	Is the Fleming a hot spring deposit?
32	Is the Fleming a magadi-type chert?
33	The origin of the Fleming formation
35	Why is the Fleming texturally unique?
35	Resource potential
36	Discussion
36	Conclusions
36	References
38	Appendices
38	1. Location and description of samples not plotted on figures
39	2. Analytical data

Figures

- 1a. Location map, 1b. Outcrop patterns of the Fleming and the (partly) equivalent Dolly Formation (*in pocket*)
2. Schematic stratigraphic column for portion of Kaniapiskau Supergroup
3. Sketch of geology on part of the large island in André Lake
3. 4. Chert breccia with cement of dominant iron carbonate and minor chert, Marion Lake
4. 5. Outcrop map of a portion of the prominent ridge north of the former Knox Mine
6. 6. Flat clast intraformational conglomerate within the Fleming Formation, north of Knox Mine
6. 7. Chert conglomerate, ridge north of Knox Mine
6. 8. Chert conglomerate, ridge north of Knox Mine
7. 9. Chert conglomerate, top of section, north of Knox Mine
7. 10. Disrupted chert beds slumping into chert-siltite, Knob Ridge
7. 11. Clast of debris-flow facies dolomite, Knob Ridge
7. 12. Clasts of dolomite, Knob Ridge
8. 13. Outcrop map of the exposures of Fleming Formation located north of Bath Lake
8. 14. Chert beds disrupted in chert cement, outcrop north of Bath Lake
8. 15. Outcrop map of the bedrock exposures examined in detail near Elizabeth Lake
9. 16. Chert arenites interbedded with chert siltites, north of Elizabeth Lake
9. 17. Outcrop map of the sequence of chert breccias examined at the north end of Marble Lake
10. 18. Crossbedding in chert arenites with floating chert clasts, north end of Marble Lake
10. 19. Outcrop map of the chert breccias examined along the shoreline of northern Marble Lake
10. 20. Lenses of chert breccia with chert arenite matrix and chert cement, in massive to slightly disrupted black chert, northern Marble Lake
11. 21. Various types of chert clasts in chert breccia, northern Marble Lake
11. 22. Massive black chert clasts in white chert cement, northern Marble Lake
11. 23. Outcrop map of the isolated bedrock exposure at the west shore of Marble Lake
12. 24. Dolomite clasts in chert breccia, west shore of Marble Lake
12. 25. Dolomite clasts in chert breccia, west shore of Marble Lake
12. 26. Chert clasts in dolomite beds, islands in central Dyke Lake
27. Outcrop and interpreted geology map of the area between Dyke and Petitskapau lakes (Northern Dyke Lake) (*in pocket*)
12. 28. Denault Formation stromatolites, Northern Dyke Lake
13. 29. Beds of chert oolites, northern Dyke Lake
13. 30. Chert oolite with multiple centres fused by chert cortex
14. 31. Chert oolites with multiple centres which originally enclosed sand size grains
14. 32. Chert oolites with sand size quartz grains and core replaced by coarse subhedral carbonate
15. 33. Fragment of algal mat, Northern Dyke Lake
15. 34. Silica nodules, islands in Dyke Lake
16. 35. Sparry dolomite containing concentrically banded chert nodules or pisoliths, islands in Dyke Lake
16. 36. Clast of quartz crust in chert arenite matrix
17. 37. Megaquartz crystal showing internal growth-bands and sub-grain formation
18. 38. Resedimented broken crusts in a chert-arenite matrix
19. 39. Clast of quartz crust in chert arenite to chert siltite matrix
20. 40. Broken crust in chert-arenite
20. 41. Clast of quartz crust in quartz-chert arenite with floating clasts
21. 42. Broken clast showing crystal terminations in graded chert-arenite

- 21 43. Banding resulting from the crystallization of a gel
- 21 44. Concentrically banded texture
- 22 45. Crystallized gel texture
- 22 46. Crystallized gel texture
- 22 47. Crust-type banded quartz
- 23 48. Composite clast
- 23 49. Composite clast, detail of Figure 48
- 24 50. Bilaterally growth-banded quartz
- 24 51. Bilaterally growth-banded quartz
- 24 52. Bilaterally growth-banded quartz
- 25 53. Crystallized gel textures
- 26 54. Crystallized gel textures with Liesegang-like bands
- 26 55. Detail of wavy loaded beds of chert arenites and chert breccias,
outcrop near Bath Lake
- 26 56. Layers of chert breccia and chert arenite, Knob Ridge
- 27 57. Detail of Figure 56
- 27 58. Fleming chert showing desiccation features
- 27 59. Blocks of Denault dolomite slumped in Fleming chert siltite,
with overlying chert breccias, Knob Ridge
- 27 60. Channel of Fleming chert breccia conglomerate cutting
Fleming flat clast intraformational conglomerate, Knob Ridge
- 28 61. Large clasts of Fleming intraformational rip-up conglomerate in
chert arenite, Knob Ridge
- 28 62. Detail of photo, Figure 61
- 28 63. Illustration of the limited lateral extent of bedded units,
Fleming Formation, Knob Ridge
- 29 64. Scatter diagram of La (ppm) versus Hf (ppm) for samples of the
Fleming Formation listed in Table 1 and 4 of Appendix 2
- 29 65. Scatter diagram of La (ppm) versus P₂O₅ (weight %) for samples of the
Fleming Formation listed in Tables 1 and 4 of Appendix 2
- 30 66. Scatter diagram of U (ppm) versus Th (ppm) concentrations in rocks
of the Fleming Formation listed in Tables 2 and 4 of Appendix 2
- 30 67. Histograms of Ba concentration in samples of the Fleming Formation
and associated rocks
- 31 68. Chondrite-normalized rare-earth spectra of samples from Table 4, Appendix 2
- 31 69. Chondrite-normalized rare-earths spectra of samples L1 55m, 5-1A and 5-1B
with chondrite-normalized La and Ce of other samples.

ORIGIN OF THE LOWER PROTEROZOIC FLEMING CHERT-BRECCIA, NEWFOUNDLAND, LABRADOR-QUEBEC

Abstract

The Fleming Formation of the Lower Proterozoic Kaniapiskau Supergroup of the Labrador Trough is composed of poorly bedded to locally well bedded cherts, chert breccias, and chert-quartz sandstones. Fleming Formation strata overlie a cherty phosphatic unit, traditionally considered part of the underlying dolomitic Denault Formation. The cherts and chert breccias of the Fleming Formation, although displaying some links to evaporites, appear to represent primary silica precipitates from the Lower Proterozoic ocean, and are best considered as precursors to banded iron formation. The chert-quartz sandstones with floating quartz clasts are penecontemporaneously reworked portions of the silica sequence.

Résumé

La Formation de Fleming du Supergroupe de Kaniapiskau (Protérozoïque inférieur) de la fosse du Labrador se compose de lithologies au litage peu défini à bien défini, dont notamment de cherts, de brèches siliceuses et de grès à chert et quartz. Les strates de la Formation de Fleming surmontent une unité de nature siliceuse et phosphatique, habituellement considérée comme faisant partie de la formation dolomitique sous-jacente de Denault. Bien que les cherts et les brèches siliceuses de la Formation de Fleming présentent des liens avec les évaporites, il semble que ces roches se soient formées à partir d'une précipitation de silice primaire dans l'océan au Protérozoïque inférieur et sont donc plutôt considérées comme des précurseurs des formations ferrifères rubanées. Les grès à chert et quartz contenant des clastes de quartz en suspension constituent des parties de la séquence de silice qui ont subi un remaniement pénécontemporain.

INTRODUCTION

The Fleming Formation of the Lower Proterozoic Kaniapiskau Supergroup in the western Labrador Trough is an enigmatic chert and chert breccia stratigraphic unit. Understanding the origin of these silica-rich sedimentary rocks should aid in the interpretation of the regional geological history, and consequently, several ingenious origins have been suggested for this formation.

Location and access

The Fleming Formation is largely restricted to the Knob Lake basin of the Labrador Trough (Fig. 1, in pocket). Adequate exposures can be found in the numerous imbricate sheets of the foreland fold and thrust belt of the Schefferville area, and most can be reached by road, although some critical exposures are best visited by float-equipped aircraft with local travel by boat.

Previous studies

Presumably because of its unusual and well developed textures, the Fleming Formation has attracted considerable, but mainly cursory examination in the past. Few researchers have taken the time to examine the cherts and chert breccias in a useful level of detail, and much of the work has been

coloured by preconceived ideas concerning the origin of cherts, of iron-formations, or the structural and stratigraphic setting of the unit.

The earliest systematic study dealing with the origin of the Fleming was by Howell (1954). Stratigraphic sections from Howell's work and a description of the unit in mineralogical and macroscopic terms can be found in Harrison et al. (1972). Gross (1968) and Baragar (1967) described the Fleming briefly in connection with studies of iron-formation and regional mapping, respectively. Dimroth (1971) discussed the Fleming in some detail and summarized much earlier work. In contrast to the approaches of many others, Zajac (1974) provided a description of the Fleming without genetic bias. The examination of the Fleming by most earlier workers was brief, as the studies were portions of regional mapping or mineral deposit projects, and all suffer from the drawback that examination of only a few outcrops often resulted in the extrapolation of local characteristics throughout the entire sedimentary sub-basin.

Wardle's (1982) compilation of the outcrop distribution of the Fleming Formation was based on published maps of the area and the unpublished work of geologists of the Iron Ore Company and of the Labrador Mining and Exploration Company. This compilation formed the basis for Figure 1b, which illustrates the present distribution of the Fleming and its (partly) laterally equivalent unit, the Dolly Formation (Harrison et al. 1972).

Stratigraphic position and geological setting

Stratigraphically the Fleming chert lies between the underlying Denault dolomite and the overlying Wishart quartzite of the Lower Proterozoic Kaniapiskau Supergroup of the Labrador Trough. Laterally, the Fleming Formation is probably equivalent in part with both the basinward siltstones and shales of the Dolly Formation and with the Denault Formation. The Fleming Formation has been reported to attain a thickness of 300 feet (91 m, Harrison et al. 1972), however, an overall average thickness is probably on the order of 25 to 50 m. Stratigraphic relationships are schematically shown in Figure 2. While this simplified stratigraphic column is successful in illustrating general lithologic relationships, the reader is referred to Howell (1954) or Dimroth (1971) for sobering commentaries on the actual stratigraphic complexity of the area. The Denault Formation is a dolomite containing stromatolitic reefs and other well developed sedimentary facies (fore-slope and backreef) (Donaldson, 1963,1966). In a few Denault localities, channels are exposed, which were cut into the dolomite and filled with debris-flow facies dolomite. The Wishart Formation is a shelf sandstone unit, transgressive onto the Archean basement, deposited under current to tide-dominated conditions (Simonson, 1985).

Following the work by Dufresne (1952), it was accepted that the Fleming seemed to be restricted to those areas where the Denault Formation was also present. The presence of an excellent section of typical Fleming chert breccias in a sequence of shales exposed in a railway cut some ten kilometres south of Schefferville (Fig. 1b) indicates that the situation is more complex than previously known.

Although contact relationships are not well exposed in the study area, the available evidence indicates that the Fleming Formation overlies the Denault conformably, and that the contact varies from sharp to gradational. Contact relationships across the tectonic grain are much more difficult to evaluate. The conformable contact between the Fleming and overlying Wishart Formation is gradational, with the basal few metres of the Wishart commonly quite cherty and locally containing interbeds of chert breccias identical to those of the Fleming.

The Fleming Formation is best developed laterally along the western margin of the Labrador Trough (Fig. 1b), but is also at least sporadically present along the eastern margin (Fig. 1). Eastern localities of the Fleming Formation, which were originally mapped as part of the Wishart Formation, include various facies of chert breccia found on the large island in André Lake (Fig. 1, 3) and along the northwestern shoreline of Marion Lake (Fig. 1, 4).

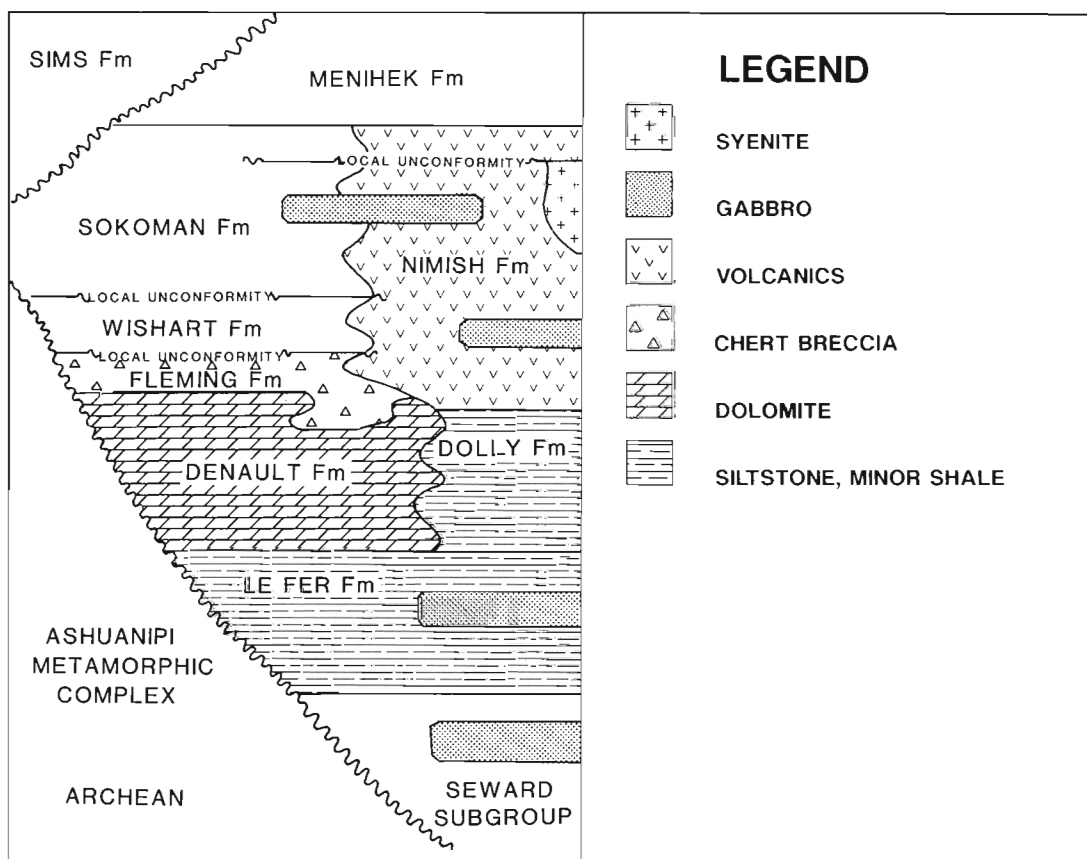


Figure 2. Schematic stratigraphic column for area south of Schefferville for the portion of the Kaniapiskau Supergroup including the Fleming Formation.

The Fleming may be more widespread than known in the eastern parts of the Trough stratigraphy, since it was not differentiated from the overlying Wishart by regional mapping parties when the majority of the present maps were made (Donaldson, 1966, p. 33).

According to Wardle's (1982) regional compilation, the Fleming has not been recognized in the area of the Nimish volcanics near Dyke and Astray lakes south of Schefferville. Perrault (1952) however, reported the presence of siliceous nodules at the top of the Denault Formation in islands in Dyke Lake, and siliceous oolites overlie stromatolitic dolomite at the north end of Dyke Lake. Thus there is reason to believe that the Fleming Formation is in some way represented in the central area around the Nimish volcanics. The lack of general reports of its presence may be due as well to local nondeposition as to erosion around the Nimish volcanic edifice.

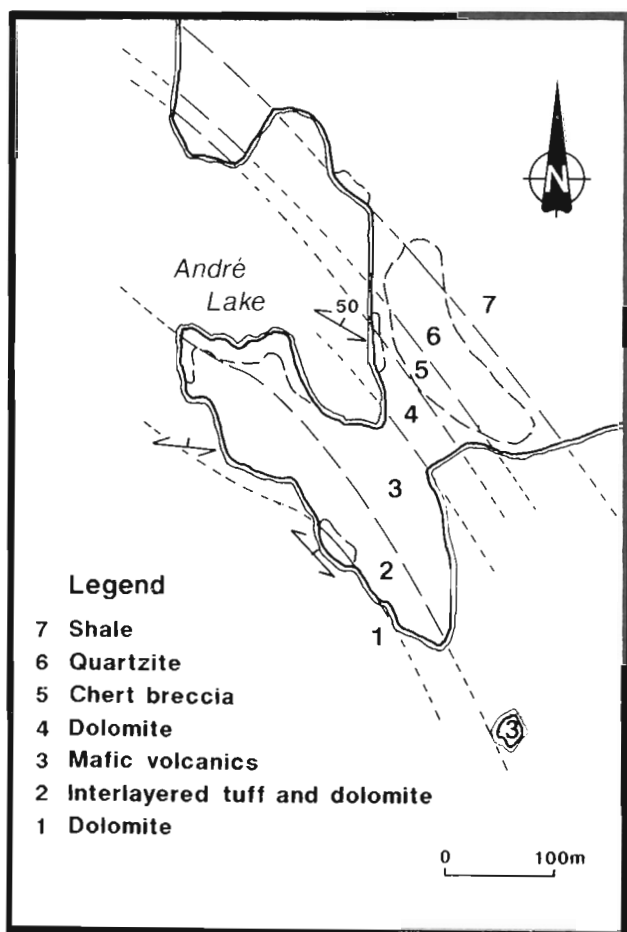


Figure 3. Sketch of the geology on part of the large island in André Lake (Fig. 1). The stratigraphy in this area differs from that of the Schefferville area in that there are mafic volcanic rocks interlayered with dolomite assigned to the Denault Formation by Wardle (1982). The stratigraphy is, however, recognizably similar to the Schefferville area in the overall lithologies and succession of units, with a chert breccia similar and equivalent to the Fleming, here exposed between the dolomite and quartzite.

The rocks of the Schefferville area lie near the Hudsonian front. All exposures of the Fleming Formation visited in this region are in the foreland-style fold and thrust belt of the Hudsonian orogeny, as illustrated by Harrison et al. (1972). The rocks of the area are generally best considered as non-metamorphosed, since all mineral assemblages encountered to date may be adequately attributed to burial and diagenesis, rather than metamorphism during an orogenic event. Based on studies of metamorphic petrology Klein and Fink, (1976 p. 485) estimated the maximum temperature reached by the Sokoman Formation in the autochthonous strata to the southwest of Schefferville at "150° C or somewhat less".

Terminology

The silica terminology proposed by Folk (1974) is utilized here. The generic term **quartz** refers to SiO₂ with or without structurally bound water. **Microcrystalline quartz**, contracted here to **microquartz**, has a grain size of 20 μm or less in equant or elongate crystals. **Chalcedonic quartz** consists of radiating bundles of fibres of quartz of extreme elongation relative to their diameters, without precise limits to grain size. **Megaquartz** has a grain size greater than 20 μm. **Chert** is the rock dominantly composed of microcrystalline quartz and/or chalcedony. **Chert sands**, or chert arenites are epiclastic sedimentary rocks whose particles are of sand size, the particles being aggregates of microquartz.

In addition to the terms of Folk (1974), the expression "**chert cement**" is utilized for microcrystalline quartz cementing a sedimentary rock where, on petrographic examination the microquartz appears to have precipitated in place. **Chert-quartz sands** are sedimentary rocks in which the sedimentary particles are composed of microquartz aggregates and of megaquartz grains. **Chert breccia**, as applied to the Fleming Formation, refers to a sedimentary rock with angular clasts of chert and megaquartz in a chert or chert-quartz matrix, or in a chert cement in cases where no sedimentary matrix is recognized.

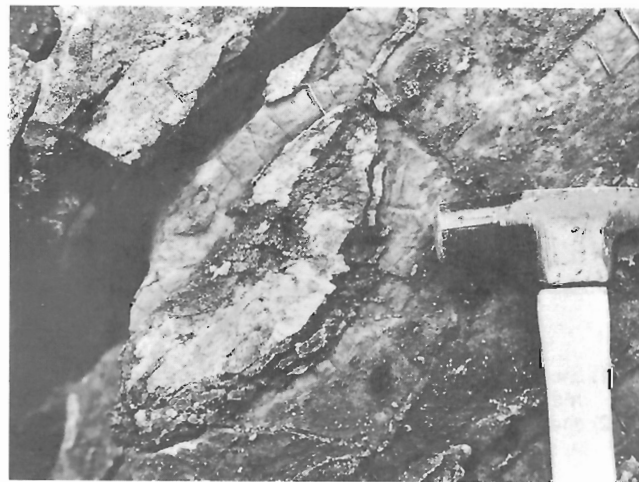
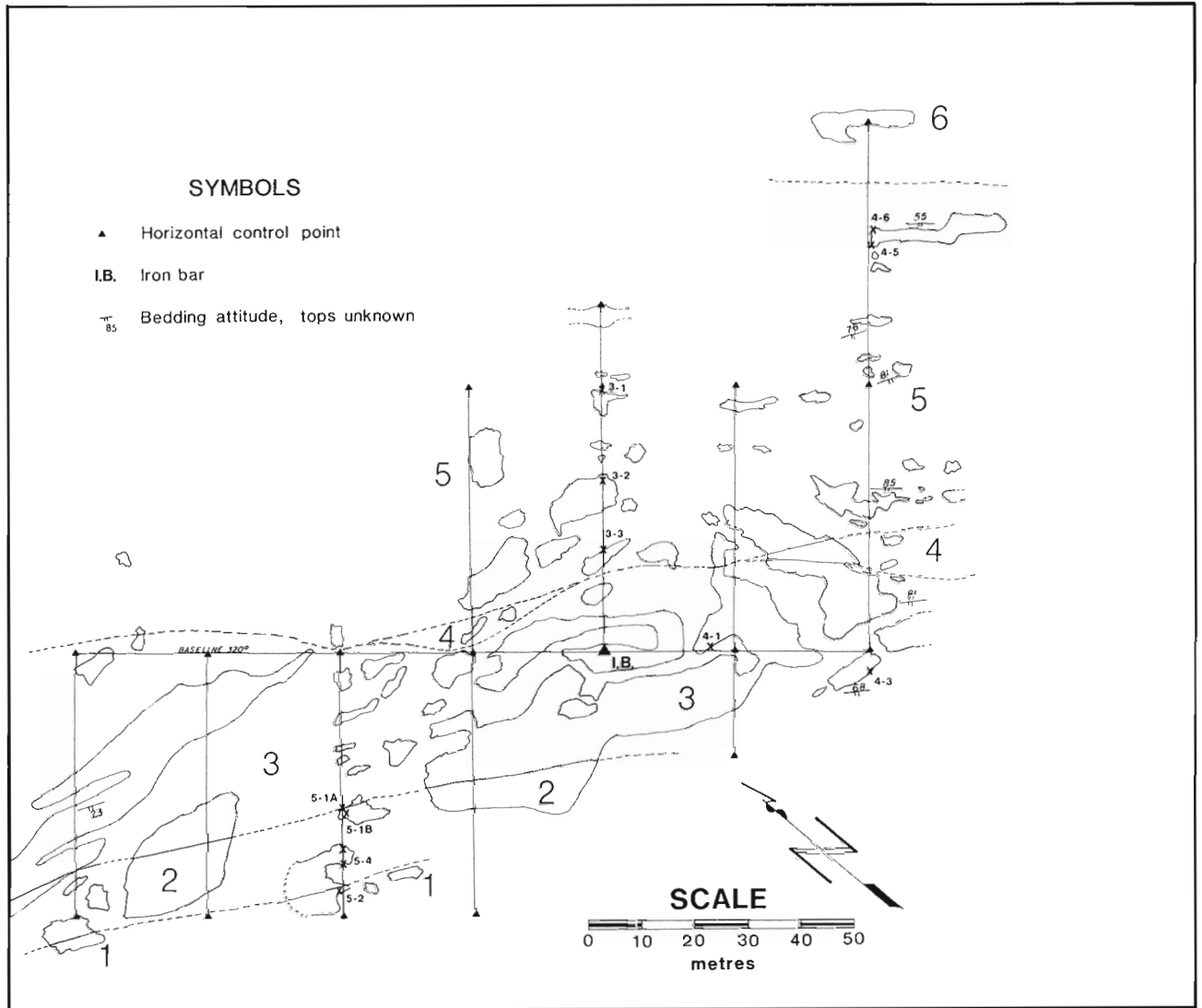


Figure 4. Chert breccia with cement of dominant iron carbonate and minor chert, Marion Lake, (see Fig. 1). GSC 205130-FF

General aspect of the Fleming Formation

Previous descriptions of the Fleming Formation reflect the complexity of the cherts and chert breccias, the limited lateral extent of recognizable units, and usually a general impression that the rocks themselves are not well organized. Zajac (1974, p. 11) described the Fleming as "a dense, massive rock with little evidence of bedding. It consists of chert fragments which are cemented by chert, quartzite, or various mixtures of the two." Gross (1968, p. 23) reports that the Fleming Formation "consists of 1 - to 1/2 - inch fragments of chert and quartz. The fragments consist of fine colloform bands of coarse and fine grey chert alternating with bands of radiating

needles of quartz and resembling chalcedony. As much as 75% of the rock may be composed of angular fragments that are cemented in a fine chert matrix." Dimroth et al. (1970, p. 65) write of "a slumped mass derived from an originally bedded sequence consisting of alternating shale, laminated chert, sandstone and chert breccia...now an unstratified body of irregularly interpenetrating masses of wildly contorted and brecciated laminated chert, of chert breccias cemented by chert, by cherty sandstone, and by shale, of sandstone with chert fragments, and of shale." The above descriptions contrast with studies by Howell (1954) who reported the Fleming in terms of a poorly stratified sedimentary sequence,



Lithological units:

- | | | |
|-------------------------------------------------------------|--------------------------------------------------------------------------------------|-------------------------------------------------------------------------------|
| (1) chert arenite with chert fragments and red chert cement | (3) cyclic units, varitextured chert fragments, variable matrix and cement relations | (5) chert pebble conglomerate, basal portion has much flat-clast conglomerate |
| (2) chert arenite with chert fragments | (4) chert arenite with chert fragments | (6) quartzite of the Wishart Formation |

Figure 5. Outcrop map of a portion of the prominent ridge north of the former Knox Mine. The stratigraphic younging direction is established by occurrences of graded bedding in the conglomerate making up the top part of the exposed section. Sample locations are indicated by X symbols. Solid triangles and lines illustrate the chained lines used to establish horizontal control.

but with recognizable and recurring internal features which he recognized in the various stratigraphic sections which he studied. Wardle and Bailey (1981, p. 339) describe the Fleming Formation as consisting of "massive to thick-bedded chert breccia of pebble- to boulder-sized clasts of colloform chert and drusy quartz set in an impure quartzite-chert matrix...In eastern exposures the formation consists of well-defined (1-2 m) breccia beds interbedded with quartzite and siltstone."

Evans (1978 p. 7, 8) reported the Fleming Formation as consisting "almost entirely of chert breccia with thin beds of massive cherty quartzite interbedded within the breccia....The breccia contains angular fragments of laminated to massive multicolored chert up to 0.5 m across, set in a fine grained recrystallized, quartzose matrix. No sedimentary structures or systematic regional grain size variations were recognized...In the Dyke Lake area, interbedding of Wishart quartzite and Fleming chert breccia and chert cement in the lower units of the Wishart imply a conformable, gradational contact."

These descriptions clearly show that the Fleming Formation is an extremely complex stratigraphic unit, and a general consensus concerning its description has not emerged. Furthermore, previous studies seemed to have been more concerned with the rocks in their regional or stratigraphic context, rather than their textural and chemical details.

Although internal variability may well make a brief description inadequate, it is still desirable to establish an overall summary of the Fleming Formation. The general impression which the geologist forms of the Fleming Formation is that of a poorly to moderately well stratified sedimentary sequence of chert sands and chert-quartz sands with many prominent clasts of chert and cockade megaquartz. A minor component of massive to faintly banded chert is generally evident. Bedding is unrecognizable to distinct. Where visible, beds are massive to thick bedded.

Acknowledgements

Fieldwork for this study was funded under the Canada-Newfoundland Mineral Development Agreement, 1984-89. It is a pleasure to acknowledge the assistance in the field of Jon Findlay, Ross Knight, Kim Nguyen, Mike Regular, Dan Richardson, Kevin Staples, and Don Watanabe. Michel Desjardins and Jean-Pierre Ricbourg of INRS-Géoresources provided instruction on the SEM. Neutron-activation analyses were provided by Mario Bergeron and Réal Gosselin of INRS-Géoresources. Discussions with Larry Aspler, Dick Bell, Fred Chandler, Quentin Gall, Paul Hoffman, Ross Knight, Dick Wardle and Steve Zajac have resulted in many improvements in my understanding of the Fleming Formation. These individuals do not necessarily agree with my interpretations. Critical reading of the manuscript by Dick Bell, Denis Lavoie, Ross Knight, and Dan Richardson has resulted in substantial improvement in presentation and considerable refinement in my thinking. Dan Richardson prepared the text, figures, references and appendices for publication.

PRESENT INVESTIGATION

Field investigation

Detailed study of the Fleming Formation was initiated in 1985, and continued through the seasons of 1986 to 1988 with supplementary observations being made each year. The field investigations are based on mapping of selected outcrops usually at a scale of 1 cm to 5 m. On the larger outcrops, horizontal control was maintained by establishing a grid consisting of a base line and cross lines at 25m spacings. On smaller outcrops or groups of scattered outcrops, detailed mapping was completed along chained lines. Outcrops, sample locations and geology were tied to the grids and sketched directly on the base maps in the field. Outcrop stratigraphy was established by reference to local and regional maps. In most cases, outcrops in the study area were found to be adequate for defining the underlying rock type. The lack of clean, glacially polished outcrop and the extensive development of lichens often inhibited the collection of desired observations. The areas of detailed mapping are located on the regional maps (Fig. 1a and 1b) and illustrated as Figures 3, 5, 13, 15, 17, 19, 23 and 27.

Although detailed observations of a limited number of outcrops are presented here, many other outcrops were examined both to select those for detailed studies, and to confirm and extend the conclusions derived from detailed mapping. The present study should in no way be considered a complete and definitive study of the Fleming Formation, if only for the reason that systematic and quantitative measurements of the lateral variability of the formation have not been undertaken. The interpretations presented here are intended as a conceptual framework for understanding the Fleming, and are subject to considerable amplification and extension, both in the field, and in the domain of geological hypotheses.

Laboratory investigation

Selected field samples were studied in polished slabs and in thin and polished thin sections through petrographic examination, X-ray diffraction, and cathodoluminescence. A suite of representative samples were chemically analysed for major and some trace elements (Table 1, 2, Appendix 2), and pyrite was separated from one sample and analysed for its sulphur isotopic composition (Table 2, Appendix 2). Four samples were studied using INRS-Géoresources' scanning electron microscope with energy-dispersive microanalyser (SEM).

Areas studied in detail

Selection of areas for detailed study was based on the quality of the outcrop available, regional coverage, and the presence of salient stratigraphic or petrographic features. The areas described below form the basis of the present study of the Fleming Formation and are based on detailed field examination of the rocks.

North of the Knox Mine

A prominent ridge north of the Knox Mine (Fig. 1b) was studied on a grid having a baseline 150 m long, with 7 cross lines (Fig. 5).

This outcrop, which does not expose the base or the top of the Fleming Formation, illustrates the typical shallowing-upward nature of these chert breccias. The stratigraphically lowest exposed unit (1 on Fig. 5) is a quartzite-chert arenite with fragments of chert and cockade megaquartz of various textures dispersed throughout the rock. A red cement (jasper) is common. A similar unit (2 on Fig. 5) but lacking the jasper cement overlies the lower unit. The central part of the outcrop is dominated by a series of "cyclic units" (3 on Fig. 5). The basal parts of these units are chert breccias with a clast population typically comprising massive, laminated, and concentrically banded (and broken) clasts in a chert arenite matrix with a chert (microquartz) cement. Stratigraphically upward over a distance of 1 to 5m, the clast population changes

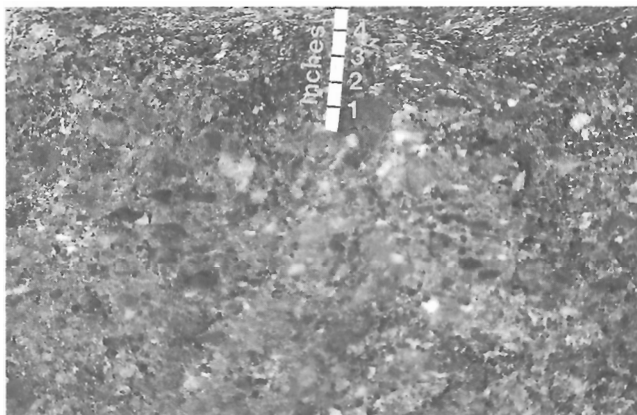


Figure 6. Flat clast intraformational conglomerate within Fleming. North of Knox Mine, and southeast of area shown in Figure 5. Photo by R. Knight. GSC 205130-U



Figure 7. Chert conglomerate, ridge north of Knox Mine, Figure 5, rounded chert pebbles with chert and minor carbonate cement. The carbonate component in the cement weathers recessively. GSC 205130-Y

gradationally to become monolithic massive to faintly banded chert and the chert arenite matrix disappears to leave only the clasts in a microquartz cement. Overlying the cyclic units is a unit of chert arenite (4 on Fig. 5) with dispersed clasts of various textures of chert and megaquartz. One hundred metres southeast of the area shown in Figure 5, the chert breccias are clearly flat clast conglomerates, developed in situ, (Fig. 6) although along strike to the northwest this is by no means evident from field examination of the outcrops. Small fault zones at high angles to the stratigraphy separate the area of flat clast conglomerates from the rest of the area studied, and detailed correlations cannot be made. The uppermost unit of the Fleming exposed at this site (5 on Fig. 5) is a chert pebble conglomerate (Fig. 7, 8, 9) carrying rounded pebbles and cobbles of various textures of chert, in a chert (microquartz) and carbonate cement. The clasts are well rounded, although often elongate rather than spherical, and are generally matrix supported, making up some 30 to 50% of the rock volume. This conglomerate truncates the underlying units and cuts down-section to the northwest. The contact with the overlying Wishart Formation lies concealed at the extreme northeast side of the outcrop zone. The contact may be a fault in this area. The Wishart at this location is a quartzite with clasts and partial cement of iron carbonate.



Figure 8. Chert conglomerate, ridge north of Knox Mine, Figure 5, illustrating general nature of bedding in this unit. Stratigraphic tops to bottom of photo. GSC 205130-W

Slimy Lake area

The outcrop to the north of Slimy Lake is known locally as Knob Ridge (Fig. 1b). Howell (1954) prepared a detailed map of the outcrop on this ridge, and proposed that many of the features could best be explained by silica replacement of dolomite. Although Howell's (1954) text does not permit exact and detailed comparison, it seems that one of the features for which he preferred a replacement origin (proposed partial replacement) occurs at the north end of the steep southwestern face of the ridge. At present, the satellite dish for the town of Schefferville is placed on the ridge crest near this site. Here the occurrence of several rounded but rather flat blocks of dolomite, which attain a maximum dimension of one-half metre for the largest clasts, do not display any record of silicification. The dolomite clasts are a mixture of two distinct sedimentary facies of carbonate rock, dololutite and debris flow (Fig. 10, 11, 12). In addition,

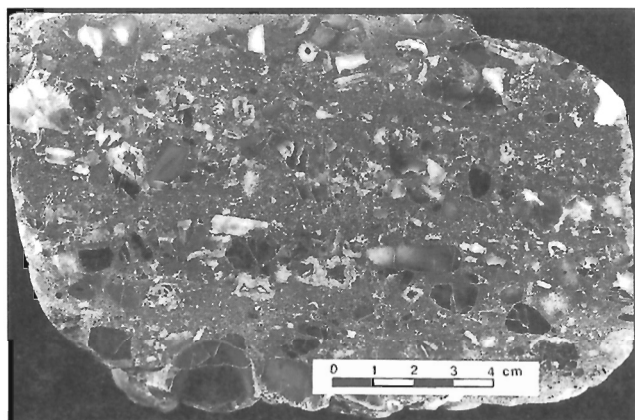


Figure 9. CHERT CONGLOMERATE Rounded pebbles of massive chert with a few pebbles of other chert textures comprise the layers in this conglomerate. Diagenetic mottling has produced rims on some fragments. Locality - north of Knox Mine, top of section. GSC 205130-I



Figure 10. Disrupted chert beds slumping into chert-siltite, Knob Ridge, (see Fig. 1b). GSC 205130-Z

adjacent clasts of dololutite record relative rotation of bedding. Thus the interpretation of this outcrop is that clasts of dolomite slid into the chert at the time of its formation. It is probable that the occurrence represents a channel cut into the Fleming and filled with debris deposits of Denault dolomite and chert.

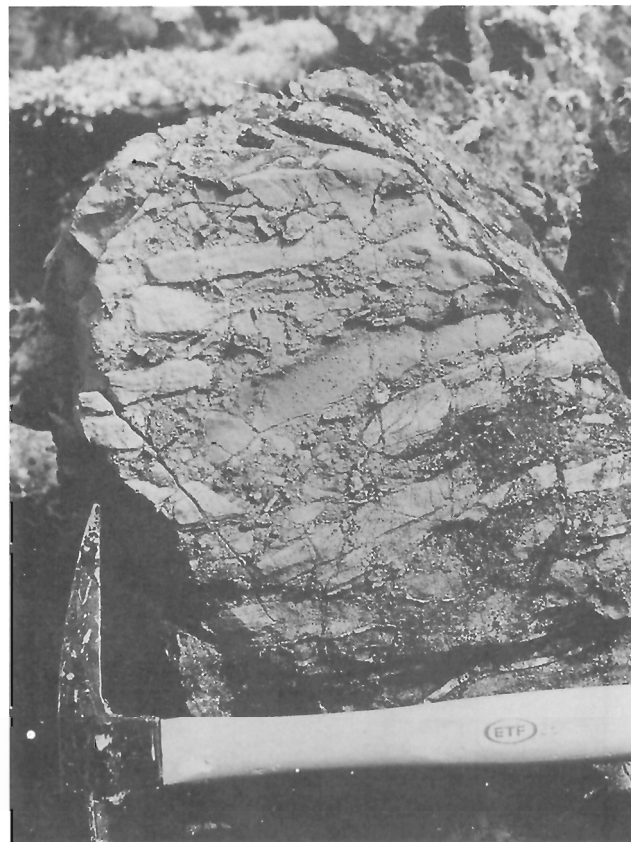


Figure 11. Clast of debris-flow facies dolomite, Knob Ridge, Figure 1b. The clast forms part of a layer of dolomite clasts and chert breccia which is enclosed in chert breccia. GSC 205130-V



Figure 12. Clasts of dololutite, Knob Ridge, Figure 1b. These clasts are part of the same layer illustrated in Figure 11. Chert and chert breccia of the Fleming are draped over the clasts. GSC 205130-A

At this locality, the well exposed contact between the Fleming and Wishart Formations is conformable and gradational. The lower portions of the Wishart are commonly cherty, and locally pass into chert breccias of limited lateral extent.

Ridge at Bath Lake

The prominent ridge north of Bath Lake is locally known as Roof Ridge. Here the Fleming Formation is well exposed (Fig. 13) and makes up the crest of the ridge. The upper contact of the Fleming with the Wishart quartzite is located along the northeastern side of the ridge crest. Though this contact is not well exposed, it can be determined that it is conformable and possibly gradational.

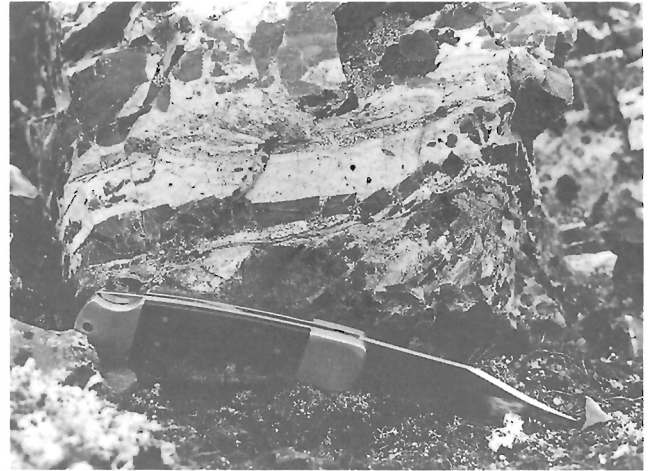
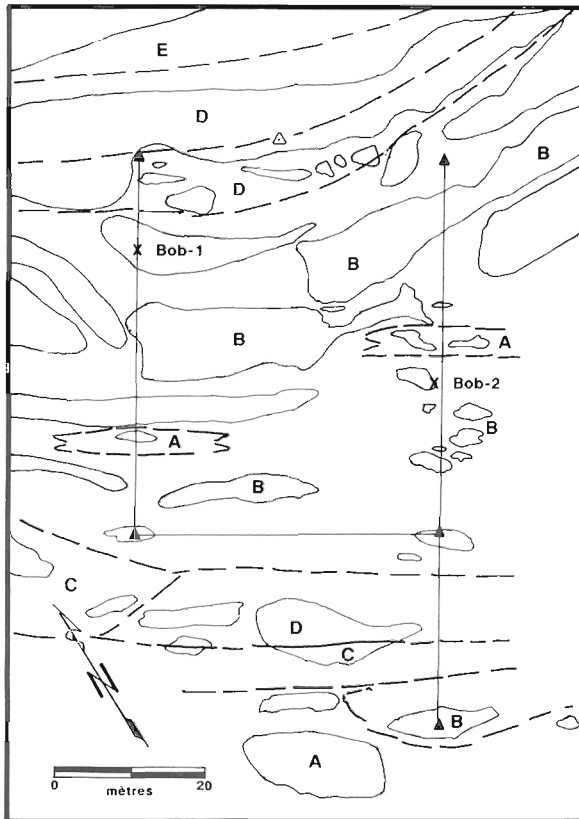


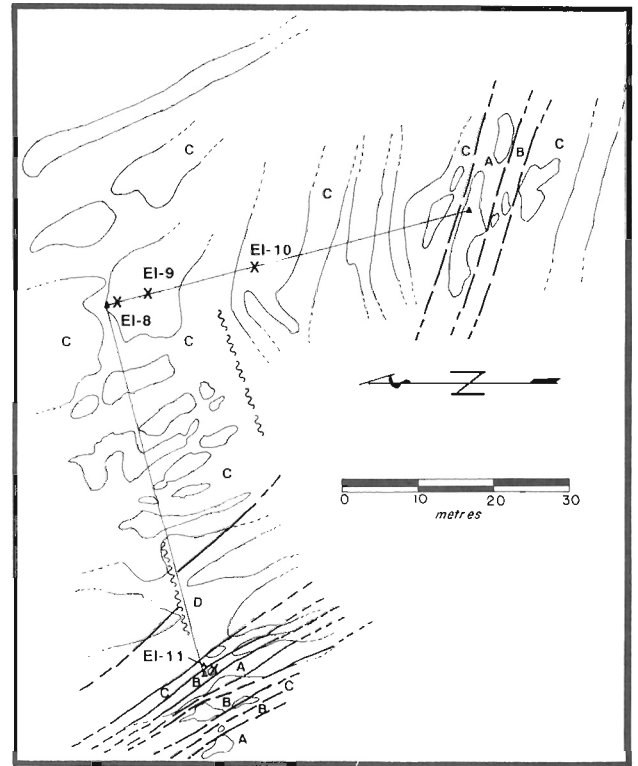
Figure 14. Chert beds disrupted in chert cement, outcrop north of Bath Lake, (see Fig. 13) GSC 205130-II



Lithologies:

- (A) massive to faintly laminated chert
 - (B) quartz-chert arenite to chert breccia with sand-size matrix
 - (C) chert breccia with no sand-size matrix, interlayered with disrupted to massive chert
 - (D) quartzite and quartz-chert arenites with floating clasts of chert or megaquartz
 - (E) quartzite of the Wishart Formation.
- Figure 14.** Chert beds disrupted in chert cement, outcrop north of Bath Lake, (see Fig. 13). GSC 205130-II

Figure 13. Outcrop map of the exposures of Fleming Formation located north of Bath Lake (Roof Ridge, Figure 1b). Sample locations are indicated by X symbols. Solid triangles and lines illustrate the chained lines used to establish horizontal control for the map.



Lithologies:

- (A) chert breccia, crudely bedded
- (B) quartz-chert siltite
- (C) quartz-chert arenite
- (D) chert breccia with jasper cement

Figure 15. Outcrop map of the bedrock exposures examined in detail near Elizabeth Lake. At this locality, bedding within the Fleming is well developed, and individual beds are laterally traceable over several tens of meters. Sample locations are indicated by X symbols. Solid triangles and lines illustrate the chained lines used to establish horizontal control for the map.

The lower portion of the Fleming exposed at this location illustrates the development of some of the textures commonly observed elsewhere. Banded chert, with lateral continuity of several metres, can be seen to be breaking into angular blocks of several centimetres maximum dimension, and slumping into a chert (microquartz) matrix/cement (Fig. 14). Further up-section, lenses of chert breccia and chert arenite illustrate the limited lateral extent of sedimentary units so typical of the majority of the Fleming Formation.

Elizabeth Lake

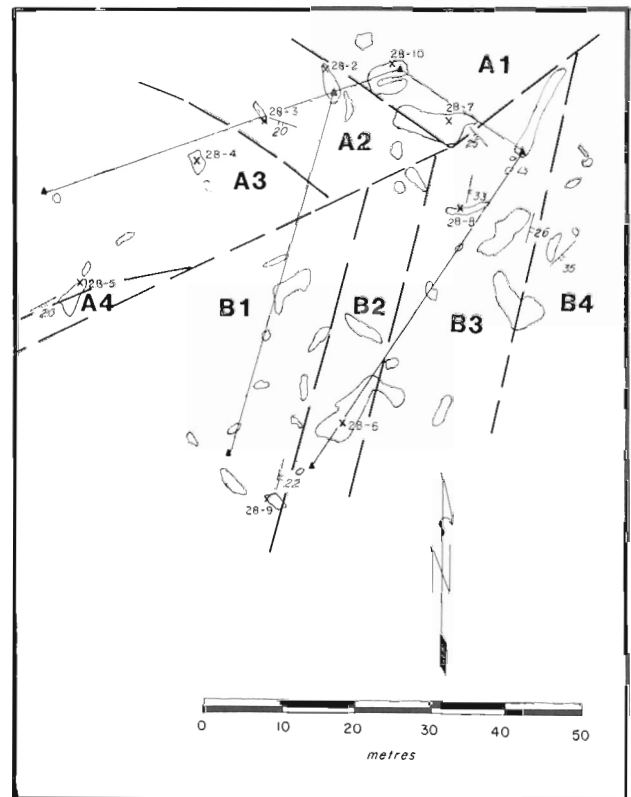
The northern end of a prominent ridge leading northwest from Elizabeth Lake (Fig. 15) was examined in considerable detail. In this area, three important features were noticed:

- i) Though not well exposed in the bottom of a small valley, the contact between the basal Fleming and underlying Denault is essentially planar over a length of nearly one kilometre.
- ii) Locally, the basal Fleming is strongly phosphatic. Elsewhere along this ridge, the basal Fleming is argillaceous with large clasts of cockade megaquartz scattered in a matrix of fine grained muscovite and chert.



Figure 16. Chert arenites interbedded with chert siltites, all with floating chert clasts, north of Elizabeth Lake, (see Fig. 15). The finer grained beds weather recessively. A bed of chert siltite about one metre thick is traceable over a distance of at least 100 metres up the hill. GSC 205130-CC

- iii) For most of its thickness, the Fleming consists of quartzite to sparse chert breccia, with scattered clasts (up to 5 cm in dimension) of various textures of chert and megaquartz. Bedding is well developed along the ridge, with individual bed thicknesses up to about 1m being easily traced for at least a few hundred metres in some areas (Fig. 16). Exclusive of the clasts, the grain size of the sedimentary particles in the different beds varies from silt to medium sand. Some of the finer beds display normal grading, while the coarser beds appear massive. The finest beds occur at the base of the sequence, near the phosphatic portion of the Fleming. Up-section there is a general increase in grain size which apparently does not markedly affect bed thickness.



Lithological units:

- | | |
|--------------------------------------------------|-----------------------------------------------------|
| (A1) massive chert-breccia | (B1) chert breccia with common chert arenite matrix |
| (A2) interbedded chert arenite and massive chert | (B2) chert breccia with lenses of chert arenite |
| (A3) chert breccia with chert arenite matrix | (B3) chert arenite with lenses of chert breccia |
| (A4) chert breccia with lenses of chert arenite | |

Figure 17. Outcrop map of the sequence of chert-breccias examined at the north end of Marble Lake. The contact separating the two main units defined here is not exposed, but is interpreted as an angular unconformity. No topographic feature suggestive of a fault is visible, nor is any tectonic brecciation evident in the rocks. Stereonet analysis of the bedding attitudes in the two main units suggests that they are not related by a fold. Sample locations are indicated by X symbols. Solid triangles and lines illustrate the chained lines used to establish horizontal control for the map.

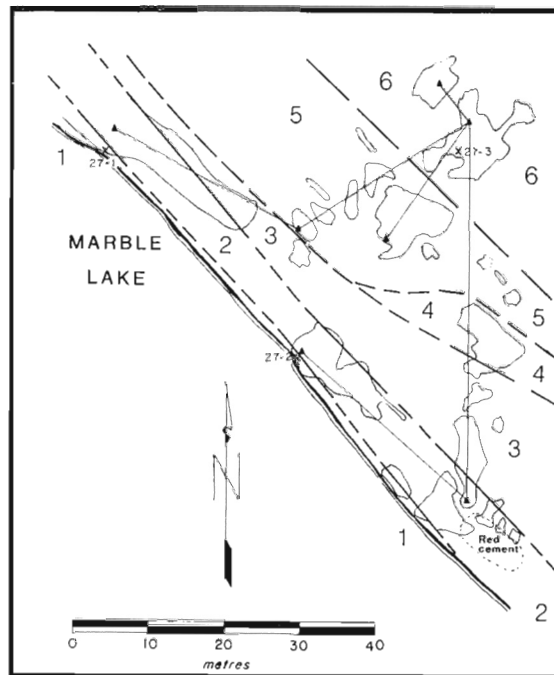
North end of Marble Lake

During the 1985 field season, a series of small outcrops at the north end of Marble Lake (Fig. 1b) were stripped and mapped in detail (Fig. 17). Here the Fleming consists of a series of poorly defined beds of chert breccias (A1 to A4 in Fig. 17) that are overlain by a series of relatively well bedded chert breccias, chert arenites, and quartzites (B1 to B4) that locally display crossbedding (Fig. 18). Since there is no topographic expression or fabric development suggestive of a fault and stereonet analysis suggests that the attitudes of the units are not related by folding, the unexposed contact between the two sets of units is interpreted to be an angular unconformity.

Northern Marble Lake

On the shore near the northern end of Marble Lake (Fig. 1b), a series of Fleming Formation outcrops (Fig. 19) illustrate particularly well the textural development of some of the chert breccias. Outcrop examination failed to establish a stratigraphic younging direction, and consequently units are described progressively inland from the shore of Marble Lake.

On the shore of the lake, a quartzite-chert arenite unit is exposed. This rock is massive and unbedded, and contains a few % of pyrite in the form of "nodules" scattered throughout the rock. The "nodules" are not massive, but are composed of numerous small grains of subhedral to euhedral pyrite concentrated in small areas of the rock.



Lithological units:

- (1) chert arenite with rare chert clasts, pyrite nodules in matrix
- (2) chert breccia, dark chert clasts often banded in light-colored chert cement with common reddish patches
- (3) chert breccia, light coloured chert clasts, chert-arenite matrix disappears up-section to leave only clasts and chert cement
- (4) chert breccia, tabular and concentric-banded fragments
- (5) chert breccia, abundant dark chert clasts in a sparse sand matrix with light-coloured chert cement
- (6) massive dark chert with some brecciated zones and light-coloured chert cement

Figure 19. Outcrop map of the chert-breccias examined along the shoreline of northern Marble Lake. Stratigraphic younging could not be established from observations on this outcrop. Sample locations are indicated by X symbols. Solid triangles and lines illustrate the chained lines used to establish horizontal control.



Figure 18. Crossbedding in chert arenites with floating chert clasts, north end of Marble Lake, (see Fig. 17). GSC 205130-P



Figure 20. Lenses of chert breccia with chert arenite matrix and chert cement, in massive to slightly disrupted black chert, northern Marble Lake, (see Fig. 19). GSC 205130-KK

Inland, a series of different chert breccia units can be defined and traced in outcrop on the basis of textures and colours of chert and megaquartz clasts. Some incomplete cyclic units have been tentatively identified within this sequence of breccias. The fabric of these rocks varies from clast-supported to matrix-supported, with the relative proportions of matrix and cement quite variable. The unit farthest from the shoreline consists dominantly of a massive, locally brecciated, dark chert cemented by white chert (microquartz) (Fig. 20, 21, 22). The contacts among the various units are sharp.

West shore of Marble Lake

A small outcrop on the west shore of Marble Lake (Fig. 1b, 23) is one of the few locations where evidence of the contemporaneity of the Fleming and Denault formations can be seen (Fig. 24 and 25). In this isolated bedrock exposure, a series of chert breccias and cherty quartzites/arenites are interlayered with one unit of chert breccia carrying abundant dolomite fragments. The fragments of dolomite are angular, up to 20 cm in maximum dimension, and are distributed relatively uniformly throughout the chert breccia unit. Outcrop lithologies are thought to represent a debris flow or series of debris flows, in which fragments of Denault dolomite were incorporated. Similar textures can be seen on islands in central Dyke Lake (Fig. 26).



Figure 21. Various types of chert clasts in chert breccia, northern Marble Lake, (see Fig. 19). Clasts of massive black, massive white and banded, broken crusts can be seen. GSC 205130-DD

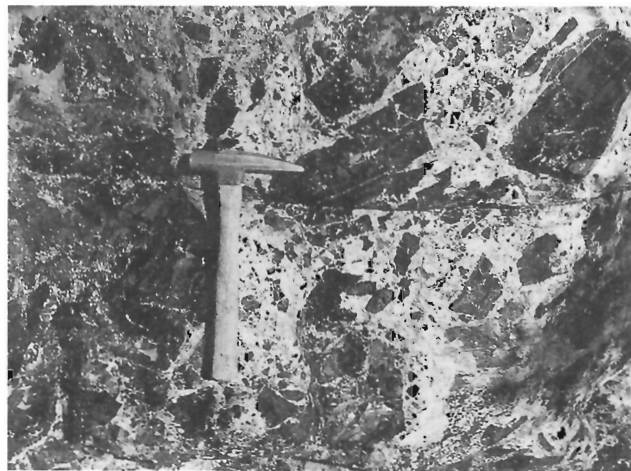


Figure 22. Massive black chert clasts in white chert cement, northern Marble Lake, (see Fig. 19). The angular black clasts can be locally reassembled (analogous to a jigsaw puzzle) and seem to represent a proximal slump facies of relatively well consolidated black chert in fluid pale chert. GSC 205130-JJ

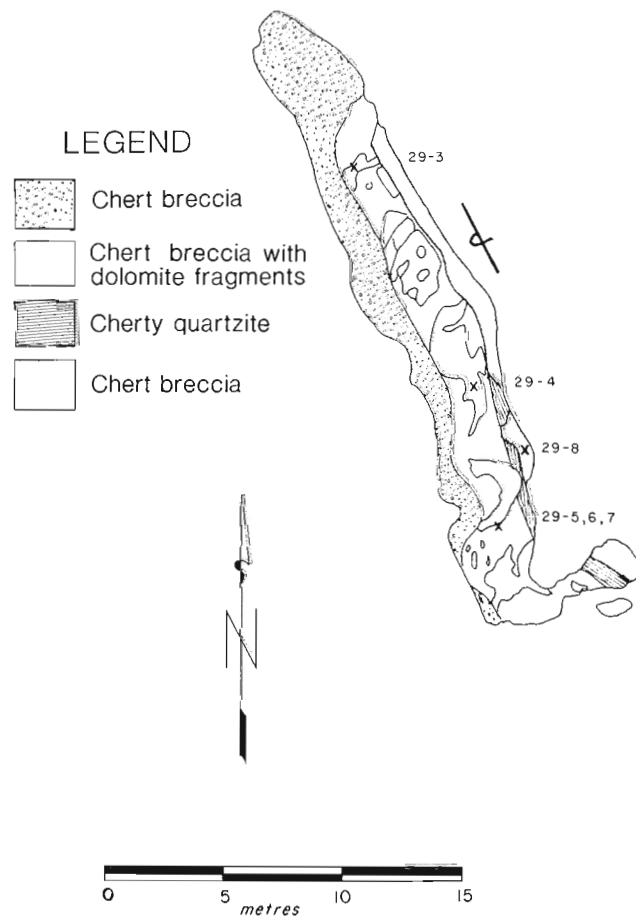


Figure 23. Outcrop map of the isolated bedrock exposure at the west shore of Marble Lake where a dolomite-bearing unit of chert breccia is interlayered with other beds lacking dolomite clasts. The entire stratigraphic sequence has been overturned. Sample locations are indicated by symbols.

Northern Dyke Lake

At the northern end of Dyke Lake (Fig. 1b), a previously unreported series of outcrops display local relationships between the stromatolitic facies of the Denault Formation and the Fleming.

During the summer months, low lake levels allow observation of the Knob Lake sedimentary sequence from Le Fer siltstones through the Denault, Fleming, Wishart, and Sokoman formations (Fig. 27). The entire lower portion of the sequence (Attikamagen Subgroup) seems to have been deposited in relatively shallow water, as indicated by the presence of ripple marks in the Le Fer, stromatolites in the Denault, and beds of silica (microquartz) oolites (Fig. 28, 29) in the Fleming. The Sokoman Formation at this locality

contains abundant magnetic greywacke, and is commonly cross bedded. Neither of these latter observations constrain water depth, nor do the textures and structures of the interbedded Nimish Formation volcanics give evidence of disposition.

Siliceous oolites, which attain a maximum diameter of about 4mm, have a concentric structure defined by subtle variations in crystal size. The oolites contain Ca and Ca-Mg carbonates as bands and patches and are cemented by carbonate. Locally, euhedral carbonate grains have been interpreted as replacing cement and oolites. The presence of broken silica oolite fragments however, attests to the presence of silica rather than carbonate during oolite formation. The presence of a few % of exotic oolite-sized chloritized basalt fragments also establishes the beginning of Nimish volcanism in the area as post-Denault.

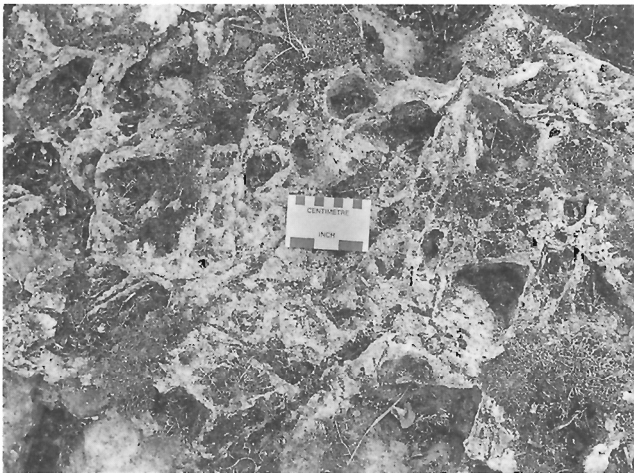


Figure 24. Dolomite clasts in chert breccia, west shore of Marble Lake, (see Fig. 23). Recessively weathered angular to subrounded clasts of dolomite, similar to the dolomite of the Denault Formation, occur in a matrix of chert. GSC 205130-G



Figure 26. Chert clasts in dolomite beds, islands in central Dyke Lake, Figure 1b. The angular and tabular chert clasts may have been deposited as a debris flow and/or storm bed. GSC 205130-AA



Figure 25. Dolomite clasts in chert breccia, west shore of Marble Lake, (see Fig. 23). The matrix to the dolomite clasts is mostly featureless chert that locally displays diagenetic mottling (left side of the photograph). GSC 205130-EE

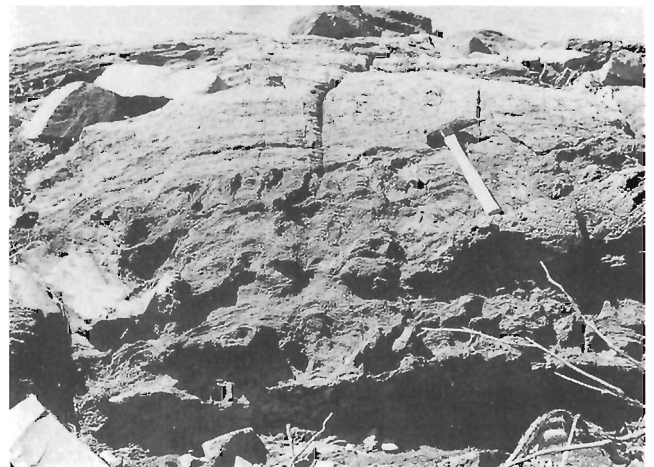
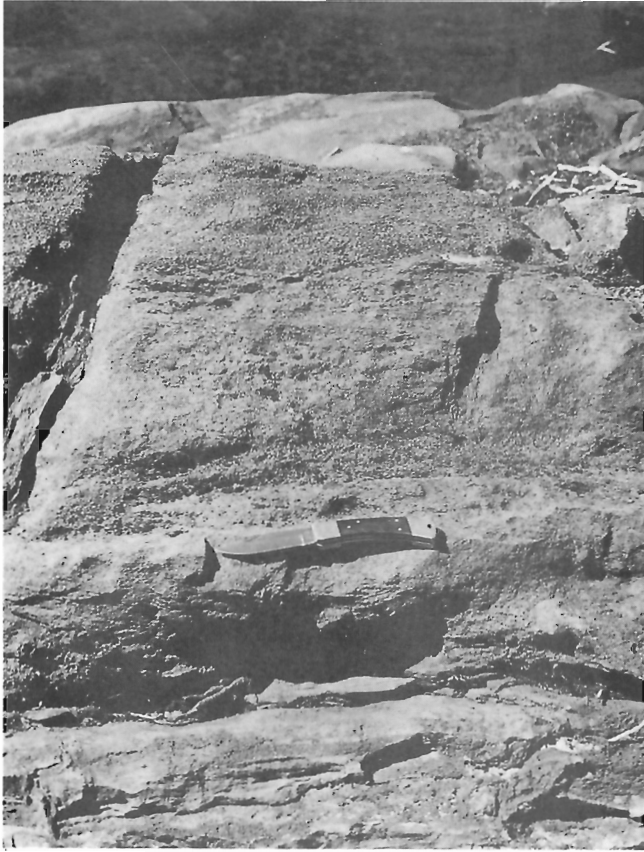


Figure 28. Denault Formation stromatolites including minor cryptalgal mats overlain concordantly by chert oolites of the Fleming Formation. Northern Dyke Lake, (see Fig. 27). GSC 205130-R



Other oolite rock components include grains of well rounded quartz that attain a maximum diameter of 1mm, and euhedral to subhedral crystals of pyrite in the cement, which constitute 5 to 10% of the rock. The well rounded quartz grains are particularly interesting as they are commonly somewhat elongate rather than spherical. In all probability, the shape of these grains represents relics from elongate mega quartz of other Fleming Formation facies (Fig. 30, 31, 32, 33).

Islands in Dyke Lake

In several small islands in central to northern Dyke Lake (Fig. 1b), significant amounts of siliceous chalcedonic nodules occur near the top of the exposed section of the Denault dolomite. The nodules, which comprise up to 75% of the rock, have diameters that range in size from 2 to 15 mm. In some locations, the nodules are confined to discrete strata and attain thicknesses of only a few centimetres, while elsewhere they comprise the majority of the rock and display no apparent lithological control. These nodules are relatively featureless assemblages of radiating masses of chalcedony, (Fig. 34) and can be reasonably interpreted as being of vadose

Figure 29. Beds of chert oolites, northern Dyke Lake, (see Fig. 27). The chert oolites (Fleming Formation) are overlain concordantly by quartzites of the Wishart Formation. GSC 205130-M

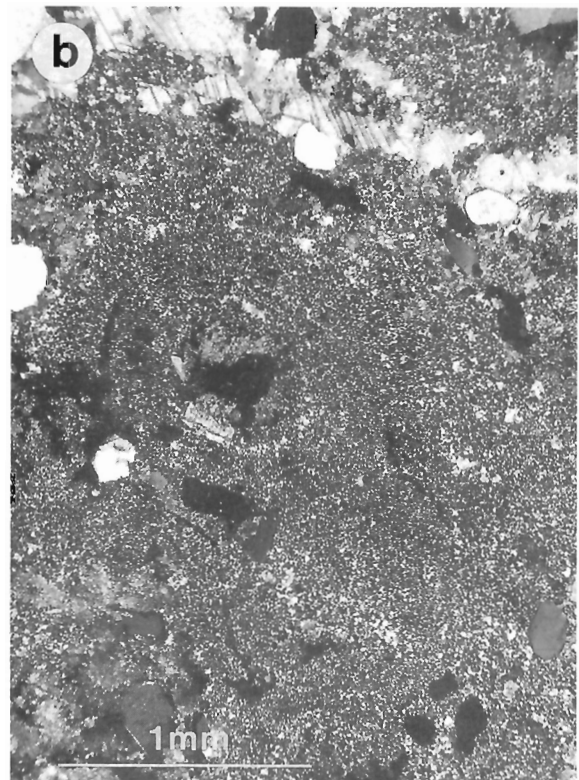
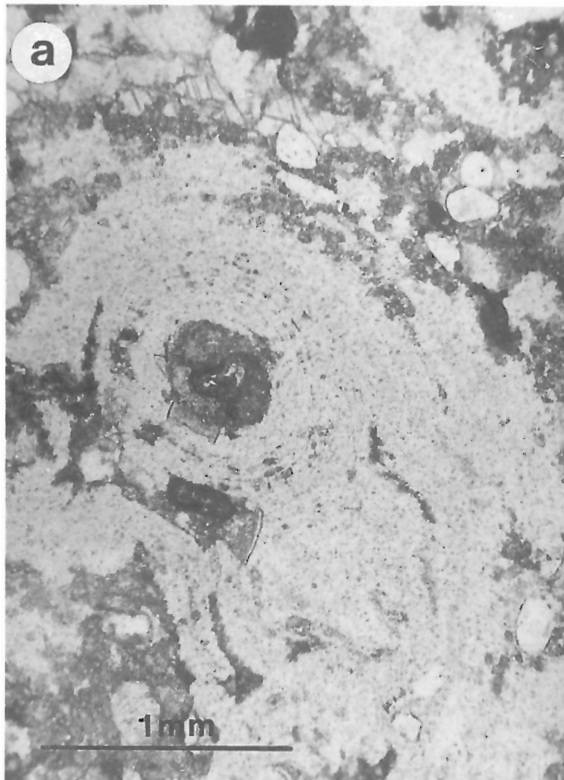


Figure 30. Chert oolite with multiple centres fused by chert cortex. Matrix is chert-arenite with chert and carbonate cement. A small carbonate vein is visible at the top of the photo (a) plane polarized light, (b) crossed nicols.

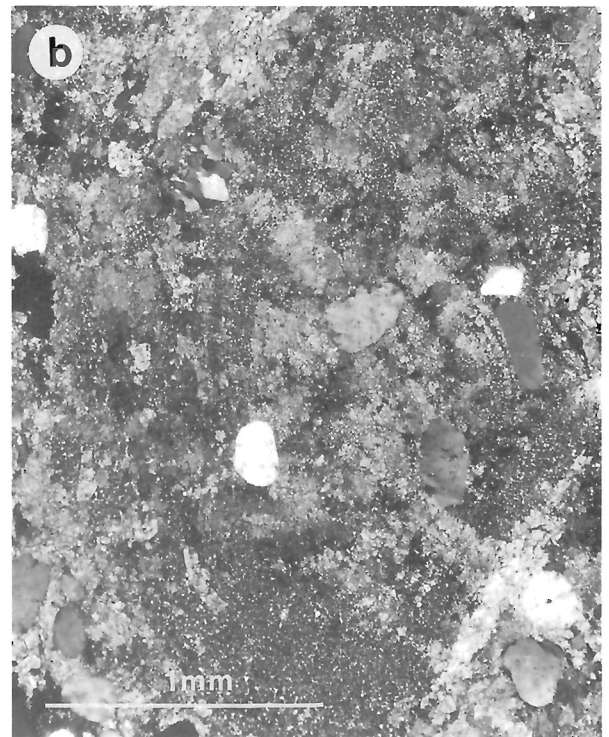
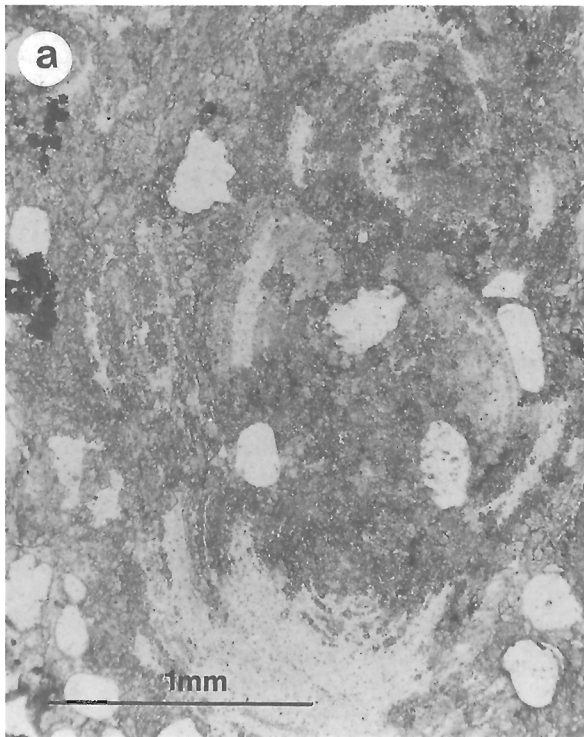


Figure 31. Chert oolites with multiple centres which originally enclosed sand size grains. Much of the oolite has been replaced by coarse, subhedral carbonate. Pyrite forming part of the cement in the rock is visible at the left of the photo **(a)** plane polarized light, **(b)** crossed nicols.

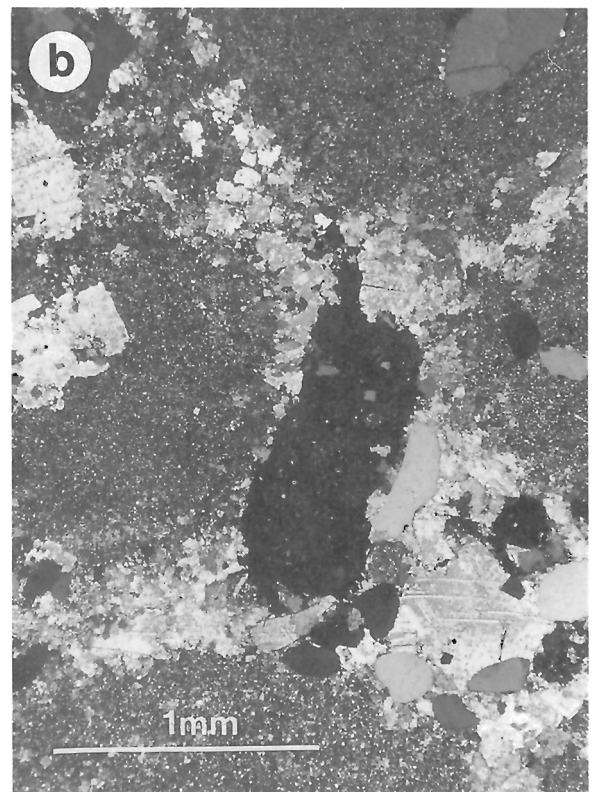
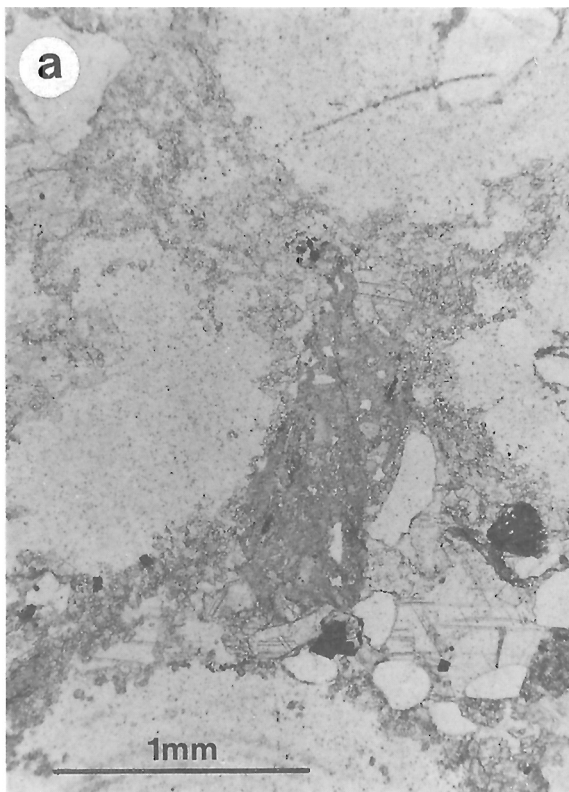


Figure 32. Chert oolites with sand size quartz grains (top of photos), and core replaced by coarse subhedral carbonate (left of photos). In centre is a clast of chloritized mafic volcanic rock **(a)** plane polarized light, **(b)** crossed nicols.

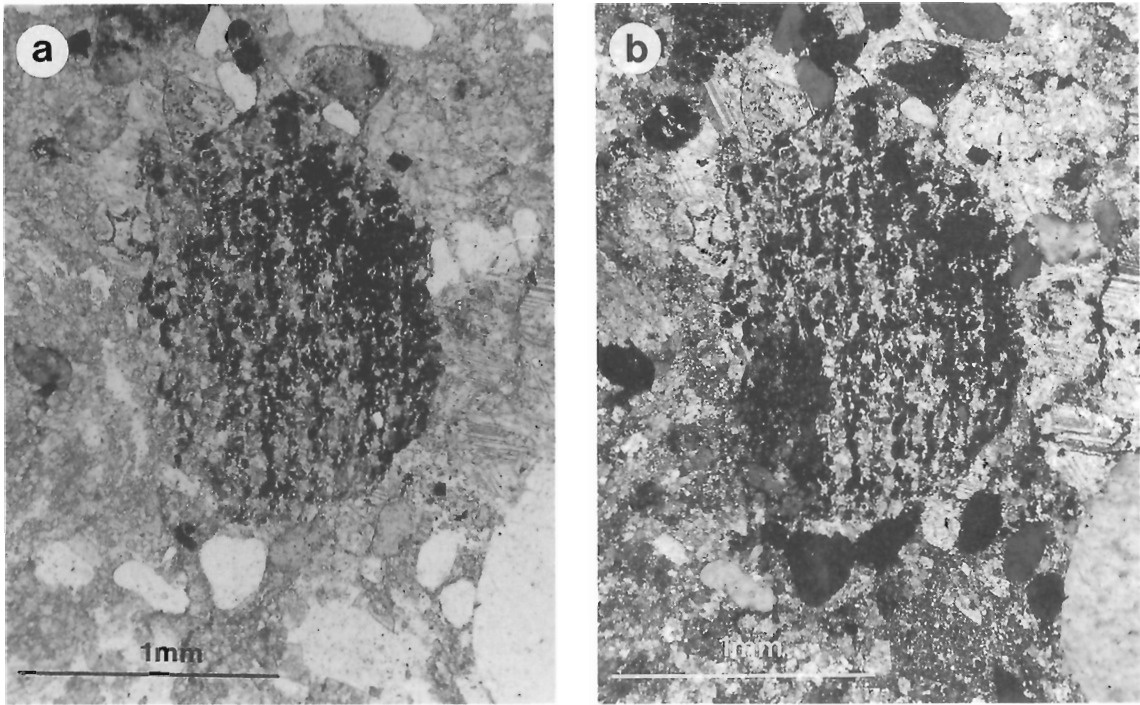


Figure 33. This fragment of algal mat is present as a clast in the oolitic cherts of the northern Dyke Lake area. The clast was probably eroded from material similar to the algal mats in the stromatolitic Denault dolomite immediately underlying the oolitic chert (a) plane polarized light, (b) crossed nicols.

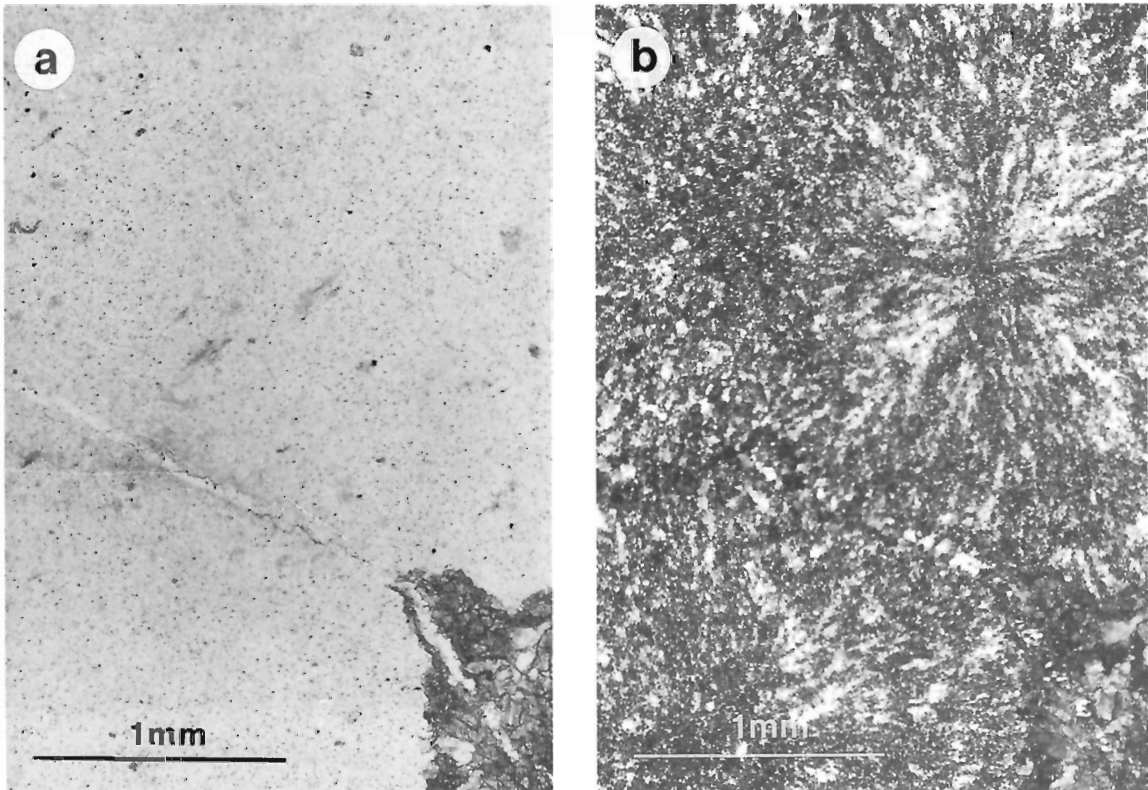


Figure 34. Silica nodules show concentric banding in outcrop and in polished slab (see Fig. 35) but in thin section are almost featureless. The banding results from subtle differences in grain size in the radiating aggregates which make up the nodules (a) plane polarized light, (b) crossed nicols. Locality - islands in Dyke Lake.

origin, although replacement of an evaporite component of the rock, as described by Chandler (1988a), cannot be dismissed. As shown in Figure 35, the silica nodules are associated with sparry dolomite and in some places apparently display reverse size grading (portion of the slab near the scale). Though not likely, it is possible that these nodules accumulated on the sediment-water interface and later controlled recrystallization of the host Denault to local sparry dolomite. Notwithstanding the details of their formation, the nodules attest to a major period of silica availability and mobility during the formation of the Denault.

Mineralogy

Thin sections and polished thin sections of samples from various outcrops of the Fleming Formation were examined by reflected and transmitted light microscopy, by cathodoluminescence, and in a few cases by scanning electron microscope (SEM).

Mineral grains with an extra-basinal origin are extremely rare. In the approximately fifty sections examined, clastic grains of K-feldspar, zircon, and epidote were identified in trace amounts only once.

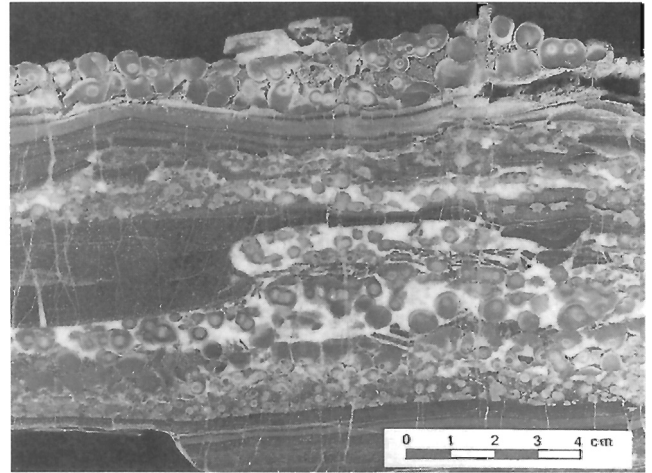


Figure 35. Sparry dolomite contains concentrically banded chert nodules or pisoliths (see Fig. 34). The banding in the silica nodules is defined by slight variations in grain size or concentration of impurities. There is a suggestion of reverse size grading in the chert nodules. The overall impression is that the fine grained dolomite is being replaced by silica with consequent recrystallization to sparry dolomite. Locality - islands in Dyke Lake. GSC 205130-N

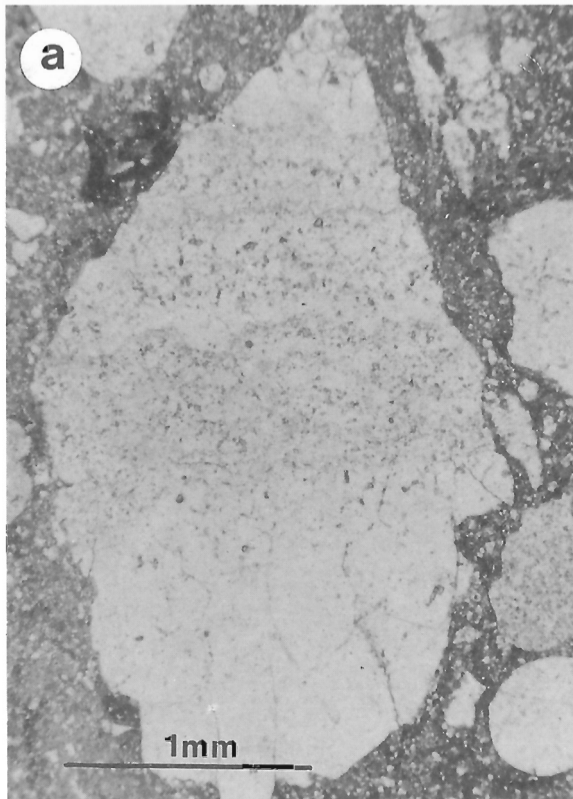


Figure 36. CRUST TYPE BANDED QUARTZ Clast of quartz crust in chert arenite matrix. Unidirection growth textures in quartz lead to large, elongate crystals with internal lamellae (a) plane polarized light, (b) crossed nicols.

The dominant mineral of the Fleming Formation is quartz, which is present as chalcedony, microquartz and megaquartz of various textures. Much of the quartz obviously formed approximately in situ, as crusts, banded geode-type material, or products eroded from these occurrences. The megaquartz formed early in the history of the rock, as it has commonly been eroded and redeposited with second-generation megaquartz overgrowths. Clasts of megaquartz crystals having large length to thickness ratios are well preserved, and could not have undergone significant transport as sedimentary particles. Though chert-quartz arenites probably consist of both extra-basinal quartz grains mixed with those of local derivation, an estimate of their relative proportions cannot be made.

In most cases, the larger quartz crystals found in the Fleming Formation rocks are uniform, unstrained, and show no signs of recrystallization. However, in crust-type clasts, described in detail below, some of the larger crystals display internal lamellar textures (Fig. 36 and 37) that could be interpreted as resulting from postdepositional strain within the crystals. Yet the identification of similar lamellar structures in sand size particles derived from the penecontemporaneous erosion of quartz crusts, and the lack of any evidence of strain within the rocks refutes the hypothesis that lamellae formation is the result of tectonic straining during thrust faulting. Alternatively, the impingement of crystal on one another during growth may have caused the formation of the lamellae.

Although the various textures of quartz, described below, allow for the formulation of a number of genetic hypotheses, it should be emphasized that textures suggestive of displacive growth of crystals with consequent volume change, or physical distortion of the rock have not been recognized in any part of the Fleming Formation, either in primary minerals or as pseudomorphic replacements.

Other common minerals within the Fleming Formation are iron oxides and dolomite. Iron oxides occur as minute grains to small irregular patches within the cement. Both magnetite and hematite have been identified through reflected-light microscopy. Dolomite occurs as part of the cement, and where textural relations can be seen invariably replaces silica (microquartz, chalcedony, or megaquartz, Fig. 31).

Locally, pyrite occurs as isolated crystals, as patches concentrated within the cement, and as a significant component of the cement in the chert oolites. Muscovite, stilpnomelane and apatite are widely distributed minor components of the rock, but locally can comprise a major constituent.

"Organic matter" or graphite is a common trace component of the Fleming rocks. Due to the difficulties in separating soft trace minerals from chert and quartz, detailed mineralogical studies of graphite were not completed. Darker varieties of chert are commonly coloured by disseminated graphite, and SEM examination disclosed widespread very fine grained materials of low atomic number

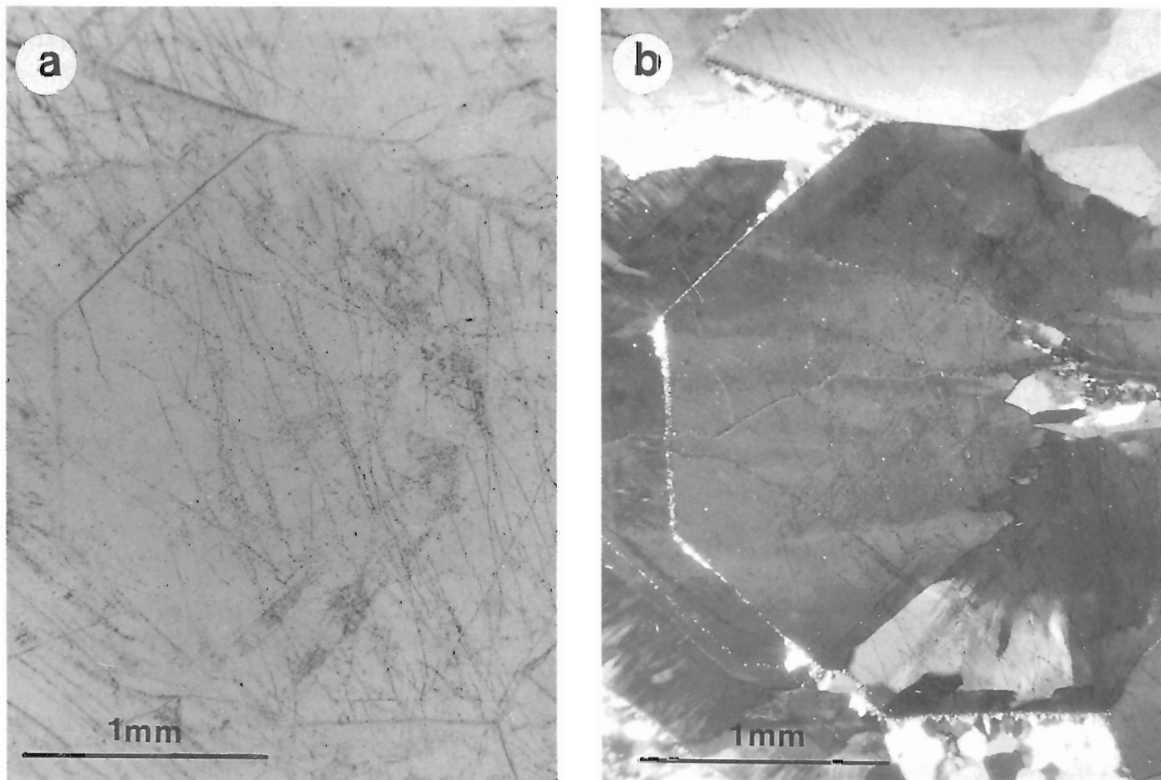


Figure 37. CRUST-TYPE BANDED QUARTZ - megaquartz crystals with c-axis approximately in the plane of the thin section showing internal growth-bands and sub-grain formation (a) plane polarized light, (b) crossed nicols.

in trace amounts. Scanning electron microscope examination also revealed the presence of trace amounts of previously unreported barite.

An unidentified polymorph of TiO_2 was encountered in all samples examined by SEM. This fine grained mineral, which apparently is only identifiable by chemical microanalysis, may be rutile, anatase, or brookite. It is present in the cherts and cements of the Fleming as tiny grains, less than $5\ \mu\text{m}$ in maximum dimension. The texture and distribution of the TiO_2 polymorph suggest that rather than being a clastic component of the rocks, it precipitated in place.

Presently regarded as a mineralogical curiosity, one grain of iridium has been identified during SEM examination. This opaque grain has a maximum dimension of $30\ \mu\text{m}$. It occurs as an isolated grain in a muscovite-iron oxide clast within quartz-chert arenite.

Examination of specimens by cathodoluminescence revealed that U and Th are generally present in small radioactive crystals of cubic habit. These grains are visible in cathodoluminescence because of the radiation-damage haloes in the surrounding quartz. Haloes are dull red to dull orange, and stand out in strong contrast to the black to dull blue of quartz. Because of their low concentration in the rock and very fine grain size, normal petrographic examination would not distinguish these minerals from iron oxides. No estimate is made of the proportion of radioactive materials present in oxides as compared to that in phosphates or other minerals such as zircon.

Texture and sedimentary structures

Strong emphasis must be placed on the textural variability and complexity of the Fleming Formation rocks. In a single outcrop, textures range from massive chert through various types of breccias to chert arenites. Partly disrupted bedding is common although difficult to see. Textures of broken-up crusts (from slumping or contraction) are common, as are textures of open-space filling. Unidirectional growth textures define bands which can, in some cases, be followed a few metres across an outcrop. These strings of fragments represent broken crusts that have retained their relative positions.

Sedimentary features in the Fleming Formation include crossbedding, local small-scale angular unconformities, and shallowing upward and coarsening upward cycles which locally culminated in a chert conglomerate with chert cement. Although bedding is not easily recognized within most exposures of the Fleming Formation, wavy bedding is present in places.

The author has tentatively identified cyclic units within the Fleming Formation. These stratigraphic units, though attaining thicknesses of up to 2m, generally have very limited lateral extent (a few metres to about ten metres). The base consists of a chert breccia with a varied assemblage of clasts (banded, broken crusts, recrystallized or open space filled), a chert arenite matrix and microquartz cement. Succeeding

upward, the clast population becomes restricted to fewer clast types and massive to faintly banded chert predominates, while the chert arenite matrix disappears, leaving only a microquartz cement. The upper tens of centimetres to about one-half metre of the cyclical unit consists of intact to brecciated, massive to faintly banded chert. Contact with the next cyclic unit upward is sharp. Laterally the cyclic units grade into chert breccias with sand sized matrix and chert cement, with a mixed clast population.

Lithological elements of the Fleming chert breccia

A systematic description of the Fleming Formation, and an interpretation of the origins and significance of this formation is based on an analysis of the lithological elements which compose the rocks. Discussion of the rocks is in terms of clasts, matrix and cement.

Cement

The cement of the Fleming is almost entirely chert (microquartz). In some areas, as at the section north of Knox Mine (Fig. 5) and at Marion Lake (Fig. 1), the cement locally contains a carbonate component which is indicated by recessive weathering, and a reddish coloration. Carbonate always replaces silica (based on observations of textures). The chert cement is locally coloured by finely divided iron oxides or carbon (presumably graphite derived from organic matter). Low abundance and the fine grained nature of the organic matter have precluded further investigation. Most of the trace minerals identified are locked in the cement and do not cross grain boundaries into the matrix or clasts (contrary to statements by Harrison et al., 1972). These minerals are sufficiently fine grained that they could be considered as part

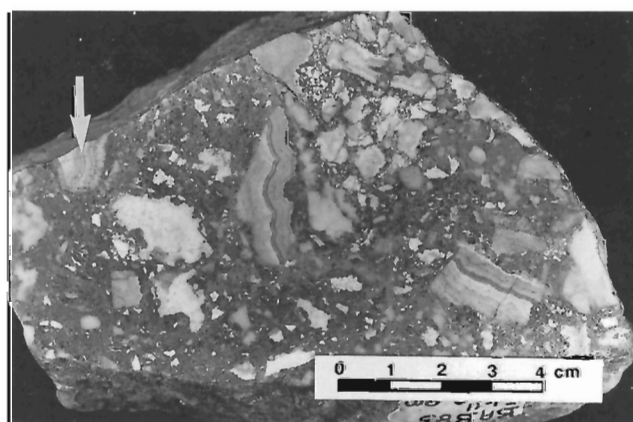


Figure 38. CRUST-TYPE BANDED QUARTZ - Resedimented broken crusts in a chert-arenite matrix with intact and resedimented concentrically banded quartz. Some of the pieces of broken crust are morphologically identical and may have come from the same crust. The clast indicated by the arrow, is noteworthy, as it illustrates the multiple events of erosion and sedimentation. This clast has bands (vertical in this image) which can be seen to terminate at a broken edge. In turn, the entire clast has been rimmed/overgrown by an outward-facing array of unidirectionally crystallized megaquartz. GSC 205130-J

of the cement. It seems more likely, however, that some of them, especially the phyllosilicates, were present as fine particles and are part of the matrix, while others such as TiO₂ (rutile?) and apatite were precipitated in place.

Matrix

The matrix of the Fleming Formation chert breccias consists of silica, present as either chert or quartz. The particles are generally in the sand to silt size, and normally well rounded. Quartz grains are commonly monocrystalline, although two or more crystals in a grain are by no means rare. Chert is polycrystalline. The internal textures of the quartz grains are compatible with their origin as erosional products of megaquartz from within the clasts of the Fleming Formation. The chert grains can be interpreted as having a similar origin, being eroded and redeposited locally.

Clasts

There are several distinct types of clasts in the Fleming, each of which had a specific origin.

It is important to note that clasts are simple, composed of single types of each of the structures listed below, and that complex clasts, indicative of erosion and redeposition of **consolidated lithified** materials, are not observed. There are,

however, many clasts which have been eroded (or slumped) and redeposited penecontemporaneously with their initial precipitation.

- (1) **massive chert:** one of the more common types described from the Fleming Formation, this clast type ranges in colour from white through shades of buff or grey to black. Internally they are cryptocrystalline, with conchoidal fracture. The shapes of the clasts of massive chert are commonly blocky, angular, to very poorly rounded.
- (2) **laminated chert:** clasts of chert which display a faint to distinct banding on the millimetre to centimetre scale. These clasts are occasionally observed as beds within the Fleming, or as trails of clasts defining a relict bedding.
- (3) **banded chert and quartz:** A large proportion of clasts in the Fleming display megascopic banding and can be subdivided into several types. These can be subdivided into several types.
 - (3a) **broken geode-type:** broken and resedimented geode-type clasts are a common part of the clast population in the Fleming. Otherwise identical to geode-type diagenetic mottling, layering terminates abruptly at a high angle to a broken surface. Commonly both intact and broken geode-type clasts occur in the same rock (Fig. 38).

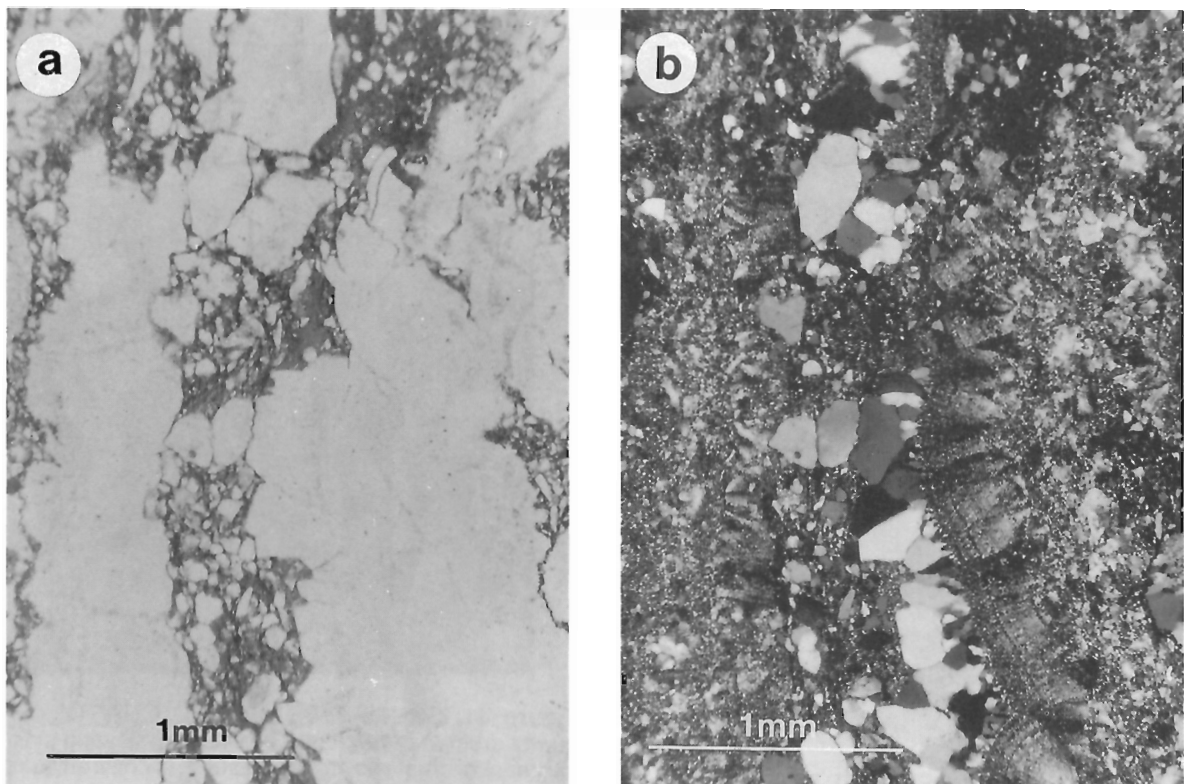


Figure 39. CRUST-TYPE BANDED QUARTZ - Clast of quartz crust in chert arenite to chert siltite matrix. The crust nucleated on poorly organized chert, grew through a stage of radiating chalcedony fibres, to become quartz crystals with unidirectional growth texture, becoming larger (and fewer) with increased distance from the base (a) plane polarized light, (b) crossed nicols.

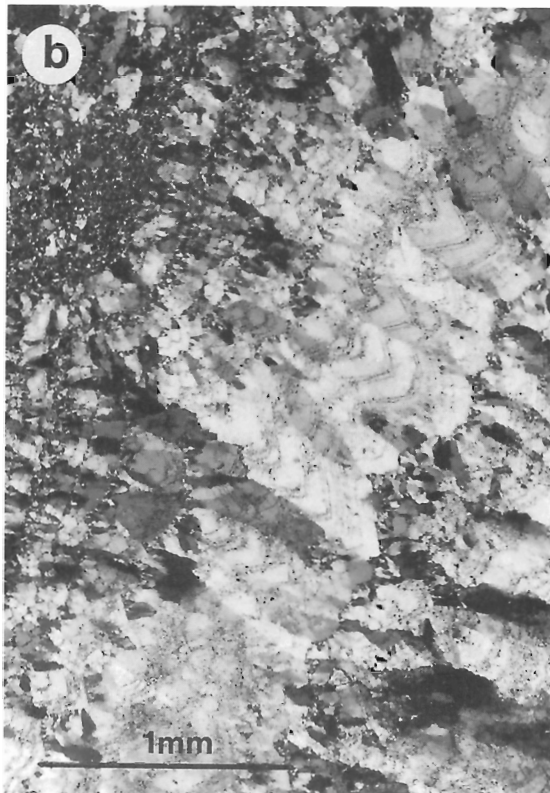
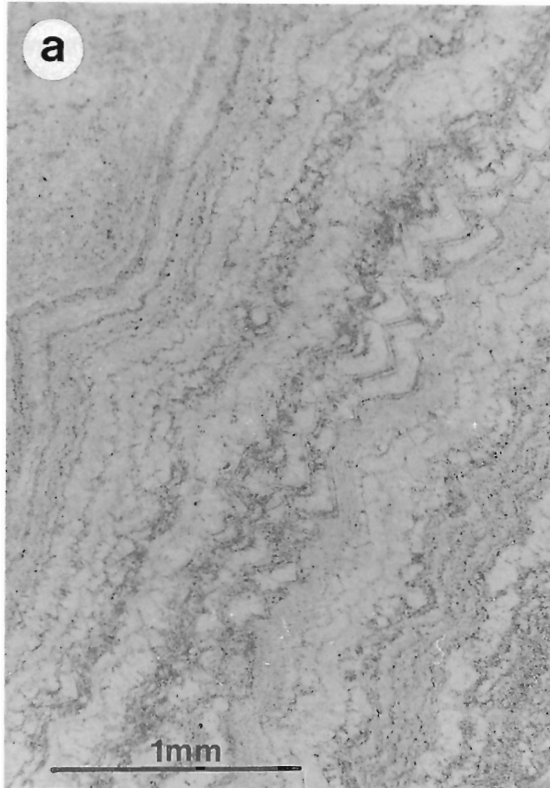


Figure 40. CRUST-TYPE BANDED QUARTZ - Broken crust in chert-arenite showing multiple growth episodes outlined by dark bands richer in fluid inclusions and also showing columnar structure of the elongate quartz crystals (a) plane polarized light,(b) crossed nicols.

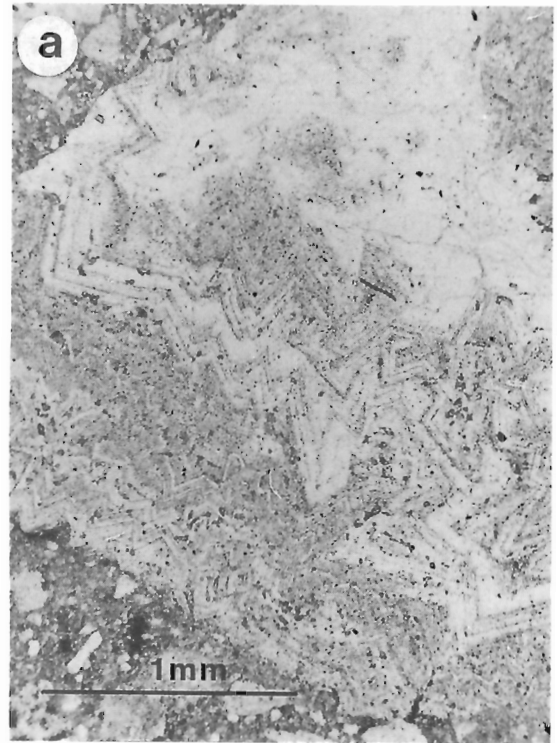


Figure 41. CRUST-TYPE BANDED QUARTZ - Clast of quartz crust in quartz-chert arenite with floating clasts. The fragment of crust shows development of chevron quartz, with some similarities to hopper crystals in modern evaporites. Some of the quartz in the matrix (lower left corner) shows elongate form inherited from crystals of crusts. See Figure 48 and 49 for further discussion (a) plane polarized light, (b) crossed nicols.

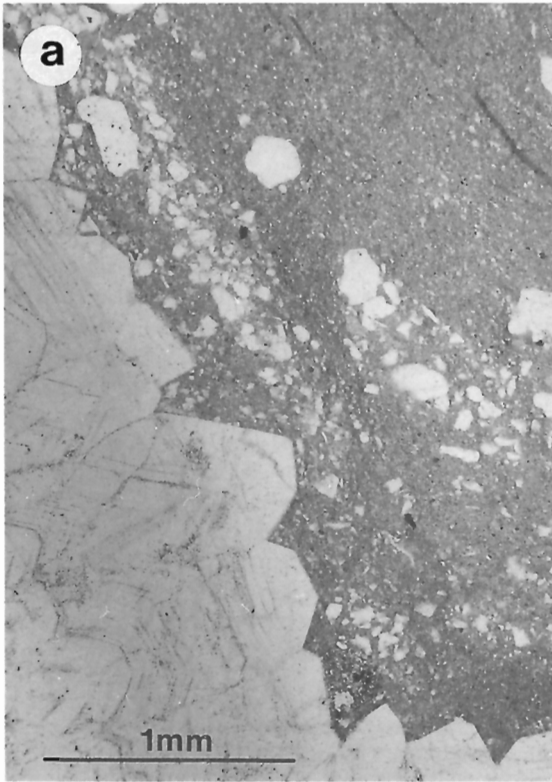


Figure 42. CRUST-TYPE BANDED QUARTZ - Broken clast showing crystal terminations in graded chert-arenite (a) plane polarized light, (b) crossed nicols.

Broken geode-type clasts can display a multi-stage history, with inward-directed quartz crystals in the primary stage followed by outward- or inward-directed growth at later stages, presumably at the time of disruption of the primary structure, or as a diagenetic overgrowth after deposition of the geode fragment as a clast.

- (3b) **crust-type banded quartz:** These clasts are distinguished by a generally planar arrangement of bands of quartz crystals (cockade megaquartz), rarely with layers of chalcedony, showing unidirectional crystallization texture. The megaquartz crusts grow from a chert substratum which usually has defined a planar base. Bands are discerned through variations in crystal size, and through concentrations of fluid or rarely solid inclusions. Quartz crystals become larger and impinge upon one another away from the substratum. In some examples, this progression in crystal size is monotonous, while in others it is seen to be cyclical (Fig. 36 to 47).



Figure 43. CRYSTALLIZED GEL TEXTURE - Banding results from crystallization of a gel, with nucleation at many centres scattered throughout the sample. Concurrent volume reduction has produced slumping and broken banding within the rock as crystallization proceeded. GSC 205130-H

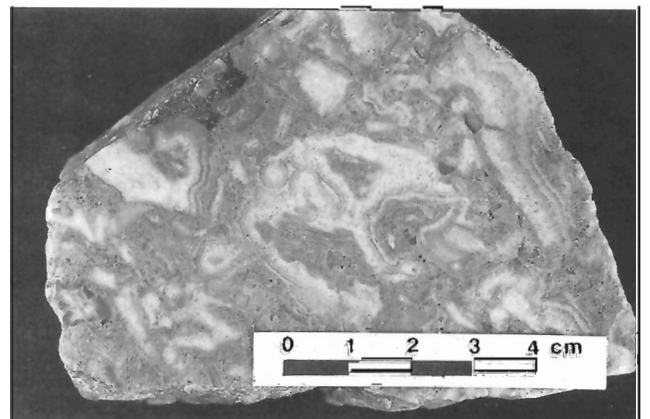


Figure 44. CONTENTRICALLY BANDED TEXTURE - Broken crusts (upper part of photo) occur with concentrically banded areas of diagenetic mottling, broken clasts of diagenetically mottled material, and a few clasts with other textures. GSC 205130

The bands of fluid inclusions show that the quartz crystals had euhedral forms throughout their growth. In rare examples, the fluid inclusions outline shapes with re-entrant features suggestive of, for example, the hopper crystals of halite in modern evaporitic environments. To date, the fluid inclusions observed have been too small for microthermometric studies. It is important, and must be emphasized, that all of the crystals examined show the morphology of quartz. No pseudomorphous replacement of a pre-existing mineral by quartz or by silica can be demonstrated in the samples examined. Specifically, no tabular or swallow-tail twinned shapes have been seen either as whole quartz crystals or as ghosts outlined by inclusions.

Crust-type banded quartz examples have lateral dimensions of up to a few centimetres, and thicknesses of up to about 1cm. In some locations, bands of identical

texture can be traced short distances across the outcrop, suggesting that they are only slightly removed from their place of formation. The size and form of these clasts suggest that they could not survive transport over any large distance without disintegrating.

Despite examination of many outcrops, crust-type banded quartz has not been found in its place or attitude of formation. No earlier report of the Fleming Formation mentions such clasts located in situ. Either the particular environment where clasts of this nature form has extremely low preservation potential, or the process leading to the formation of crust-type banded quartz creates, as well, instabilities such that the crusts are not preserved. One possibility (although others could be advanced) is that the crust-type banded quartz grew as upward-facing arrays of crystals in shallow water. Seasonal drying caused cracking of the underlying chert layers, and disruption of the crusts. Other possibilities involve the dissolution of evaporites with attendant open spaces quickly filled by crusts of quartz. Both theories, however, have the drawback that they predict that the crusts should be locally preserved in their growth positions.

- (3c) **composite clast:** one example has been observed of a mineralogically composite clast. This clast, which is illustrated in Figure 41, 48 and 49, carries a small proportion of a birefringent mineral as oriented inclusions. The mineral inclusions have not been identified as they have invariably been removed to leave a void where exposed on the surface of the polished thin section. It is presumed that the mineral is evaporite-related. The occurrence differs from the partly silicified nodules reported by Chandler (1988a) in that the inclusions do not retain a constant orientation throughout the clast, but instead are related to the morphology of the quartz in which they are contained. The inclusions are probably a co-precipitate with the quartz.

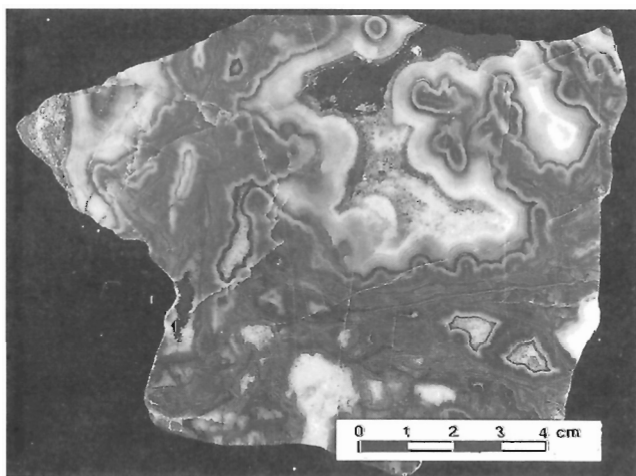


Figure 45. CRYSTALLIZED GEL TEXTURE - Largely intact, coarse mega-quartz has filled the open spaces resulting from volume reduction during crystallization. Darkest areas include higher concentrations of carbon. GSC 205130-HH

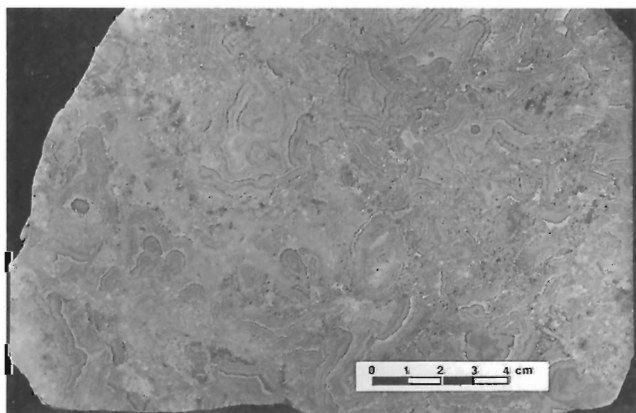


Figure 46. Virtually intact, CRYSTALLIZED GEL TEXTURE with minor disruption of banded material. GSC 205130-K

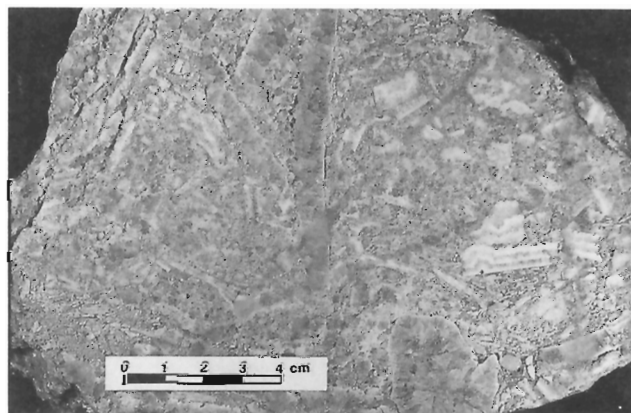


Figure 47. CRUST-TYPE BANDED QUARTZ - Broken quartz crusts resedimented into a matrix predominately composed of muscovite. A solitary quartz nodule is visible at the right of the photograph. GSC 205130-O

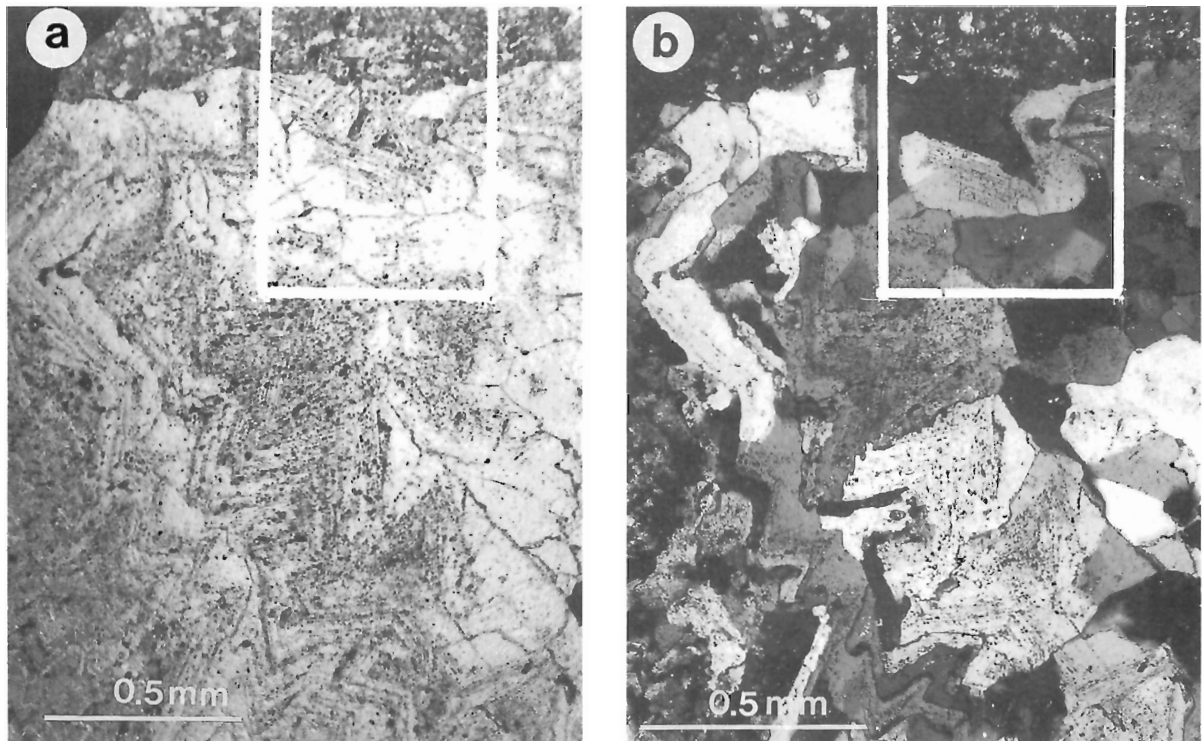


Figure 48. COMPOSITE CLAST - This composite clast is the only example recognized where a second mineral was co-precipitated with quartz. The small, elongate features parallel to the crystal outlines are a birefringent mineral. Scanning electron microscope examination has established that the mineral does not reach the surface of the polished thin section, every example now being a void. It is concluded that a slightly soluble evaporitic mineral coprecipitated with quartz in a crystal crust which was broken and resedimented to provide this clast. The rectangle outlines the area of Figure 49 (a) plane polarized light, (b) crossed nicols.

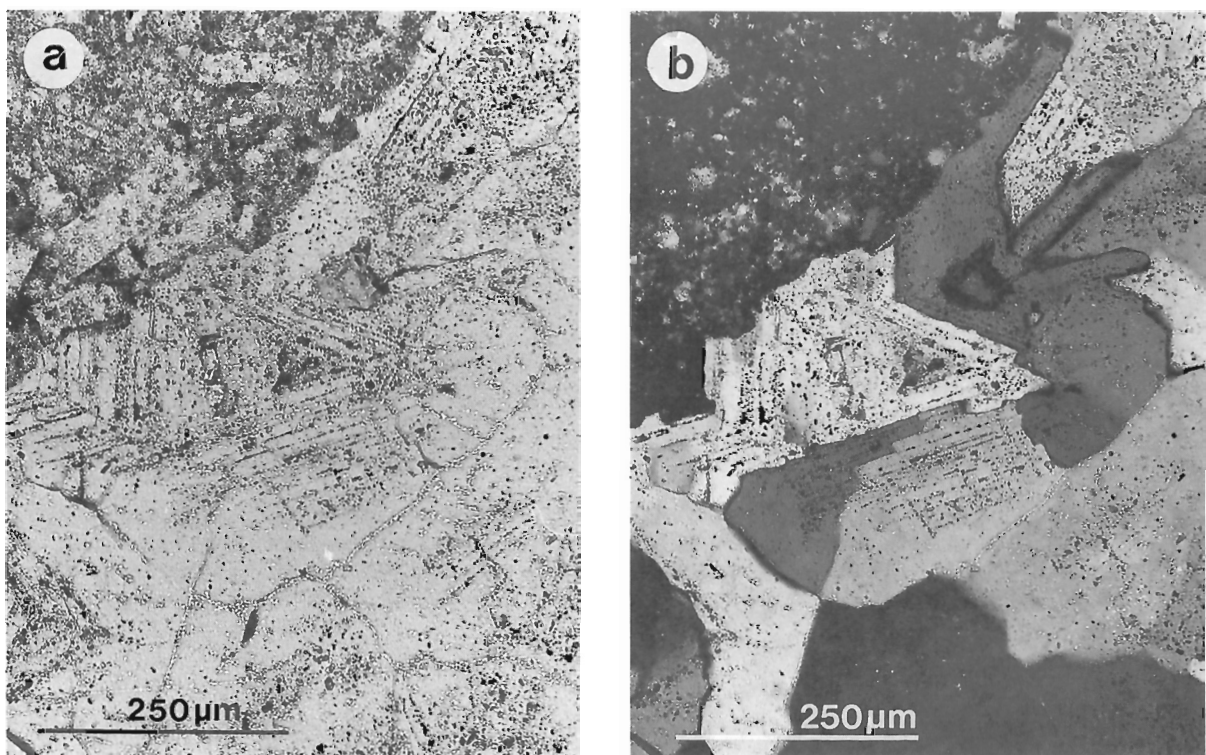


Figure 49. COMPOSITE CLAST - Detail of upper portion of Figure 48 illustrating the arrangement of the elongate grains around the crystal shape of the quartz (a) plane polarized light, (b) crossed nicols.

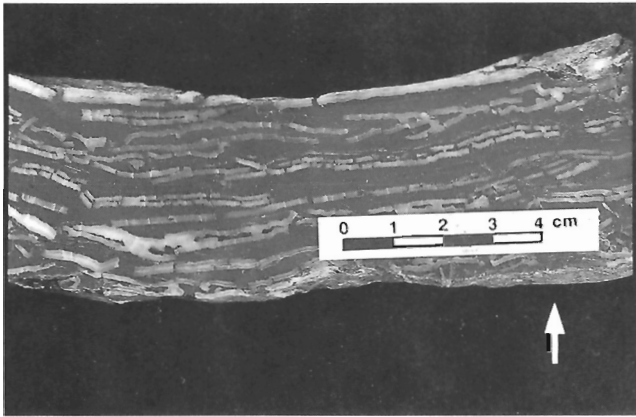


Figure 50. BILATERALLY GROWTH-BANDED QUARTZ - Desiccation of chert has provided a substratum for the growth of megaquartz in the open spaces provided by the cracking of the sediment. The stratigraphic younging direction is indicated by the arrow. GSC 205130-L

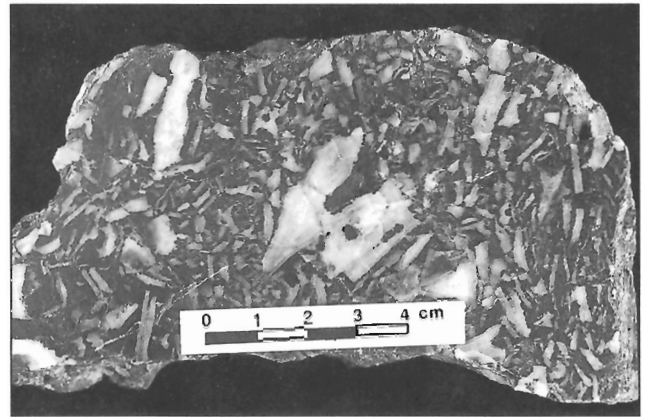


Figure 51. BILATERALLY GROWTH-BANDED QUARTZ - Features similar to those in Figure 50 can be seen in this sample where the layers have been resedimented and locally overprinted by a diagenetic mottling. GSC 205130-F

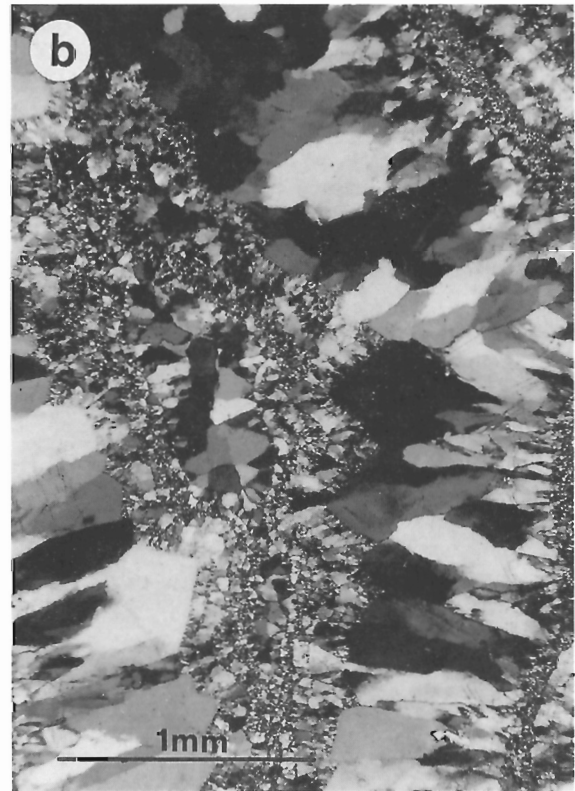


Figure 52. BILATERALLY GROWTH-BANDED QUARTZ - Megaquartz nucleated on a chert substratum has grown symmetrically toward the centres of open spaces produced during desiccation of the chert host. Quartz growth is rhythmic, with finer grained unidirectionally crystallized quartz filling the centre of the band (a) plane polarized light, (b) crossed nicols. The development of this texture is illustrated in Figure 50 and 51.

(3d) **bilaterally growth-banded quartz:** this is a rare clast type distinguished from the preceding by a bilaterally symmetrical disposition of growth bands and shapes inward from planar parallel bases toward a common central plane. This type of texture is observed in both clasts and in situ. When seen in situ, the quartz crystals are nucleated on the surfaces of contraction features in chert. It appears that due to volume loss during shrinkage, the cherts separated into flat layers as well as vertically-walled polygons. Quartz nucleated on the horizontal walls of the flat clasts and grew inward. This texture is illustrated in situ in Figure 50 and as clasts resedimented near their place of origin in Figure 51. Figure 52 illustrates the texture in thin section.

Diagenetic structures

Intact geode-type banded quartz: this results from a diagenetic mottling in the form of patches of banded chalcedony and megaquartz in the matrix of the rock. Examples are commonly of about 1 to 2cm in maximum dimension. The geode type is readily distinguishable from crust-type megaquartz by its ameboid shape, and symmetrical banding within the outline of the geode. There is an increase in crystal size from chalcedony to megaquartz toward the

centre of the geode, which in some cases is a void lined with the terminations of euhedral quartz crystals (Fig. 38, 51, and 53). Bands of fluid inclusions outlining the growth stages of the quartz crystals are less abundant in geode-type banded quartz than in the crust-type clasts.

The geode-type structures are reasonably interpreted to be formed through open-space filling. Three mechanisms may create the open spaces which are filled.

Firstly, mass movement within the sediments may lead to openings which can be filled by quartz. This seems unlikely because if the sediment has the cohesion to fracture, structural control of the openings should be evident. Field investigations indicate that this is not the case.

Secondly, evaporitic minerals or nodules may have been removed by solution to leave voids. The distribution of geode-type structures throughout the rocks is highly irregular. It would have to be postulated that the evaporitic nodules or patches were deposited as clasts or formed in early diagenesis, then removed by dissolution. The presence in many samples of broken and resedimented geode-type quartz with similar material in situ indicates the complexity of processes leading to the geode-type textures. A repetitive process of geode formation, erosion and resedimentation is required.

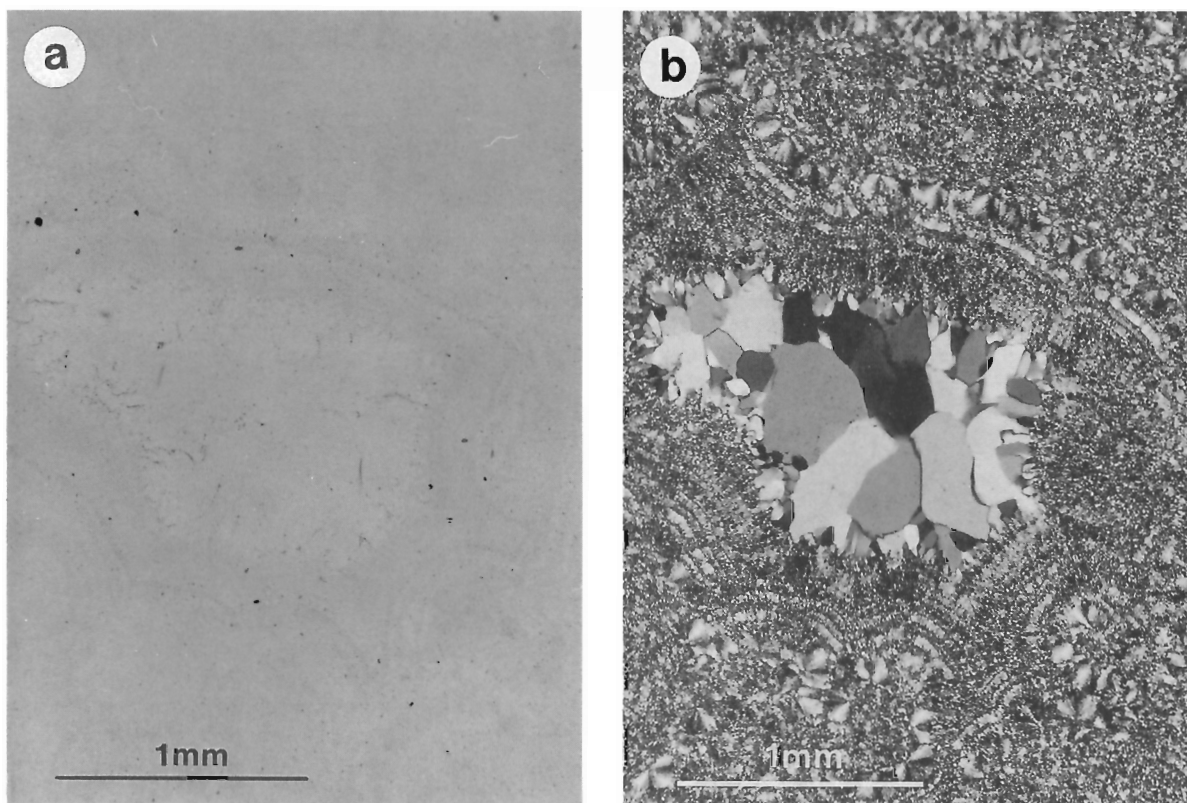


Figure 53. CRYSTALLIZED GEL TEXTURES - Textures of finely banded quartz crystallized from a gel. Multiple centres of nucleation give rise to complex interference shapes of crystallizing domains. The general direction of crystallization was inward (possibly controlled by the gross morphology of the area crystallizing), with the last area to crystallize being the centre of the photomicrograph, now characterized by coarse, inward-growing mega-quartz (a) plane polarized light, (b) crossed nicols.

The third possible origin for open-spaces in the sediments of the Fleming Formation is that patches of silica gel formerly present were removed to create the voids. This hypothesis is a variation on the second, involving silica rather than some unidentified evaporitic precursor. There are two equally possible mechanisms for the removal of the silica gel. It may have been redissolved

if the waters became temporarily undersaturated in silica, or may have been desiccated, and broken to leave spaces. Although geopetal structures associated with geode-type quartz have not been recognized, the desiccated, poorly crystalline silica gels may not be preserved. This third possibility seems the most likely mechanism to have produced open spaces within the chert breccias.

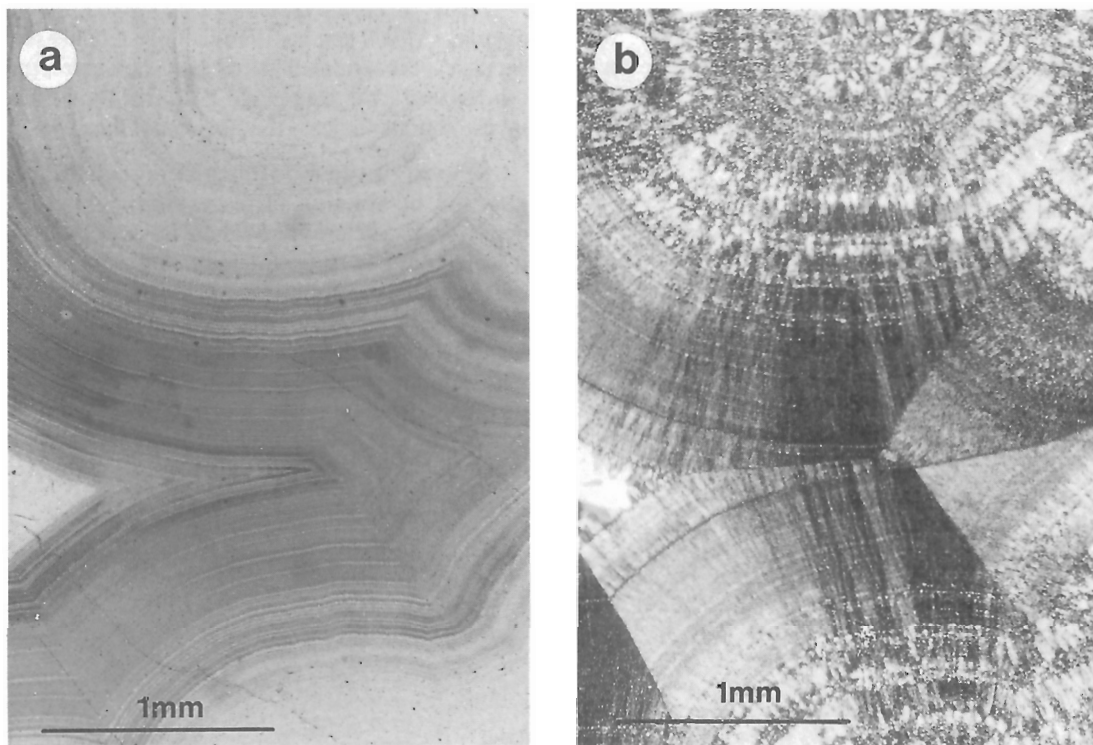


Figure 54. CRYSTALLIZED GEL TEXTURES - Domain interference developed during crystallization of a gel, with Liesegang-like bands marked by increased concentrations of solid and fluid microinclusions (a) plane polarized light, (b) crossed nicols.



Figure 55. Detail of wavy loaded beds of chert arenites and chert breccias, outcrop near Bath Lake (see Figure 13). GSC 205130-GG



Figure 56. Layers of chert breccia and chert arenite, Knob Ridge, Figure 1B. The larger clasts are broken crusts with unidirectional growth textured quartz, associated with flat-clast conglomerates, beds attain lateral dimensions of several metres. GSC: 205130-BB

"Crystallized gel" textures: a texture which is rarely preserved is that of a crystallized gel. Domains of this texture occur as patchy, poorly defined zones of irregular geometry within chert breccias at Knob Ridge, and at other locations. Nucleation at a large number of centres has led to concentric banding within the cherts (Fig. 43, 45, and 46) and produced mutually interfering zones of chalcedony (Fig. 53 and 54). Microbanding within these occurrences (Fig. 54) resembles Liesegang bands.

Sedimentary structures

The Fleming Formation, always described as a chert breccia, has generally not been studied as a bedded unit. Common sedimentary structures within the formation include: wavy bedding, chert arenite to chert siltite beds with loaded bases (Fig. 55), and intraformational conglomerates (documented north of the Knox Mine and at Knob Ridge). Desiccation features are preserved at Knob Ridge, as well as small channels within the Fleming. Combined desiccation and rip-up structures often produce wavy bedding. Several of these features are illustrated in Figure 56 to 62.

The aspect of sedimentary structures most difficult to evaluate in the Fleming is the lateral extent or continuity. Either through lack of outcrop or termination of units, beds cannot be followed more than metres or tens of metres in areas



Figure 57. Detail of Figure 56. GSC 205130-X



Figure 58. Fleming chert showing desiccation features. Slightly disrupted flat angular clasts with chert arenite matrix lie within chert breccias. Bedding is heaved upward and may reflect polygon formation or teepee structure. Locality - Knob Ridge. Photo by R. Knight. (GSC 205130-E)



Figure 59. Blocks of Denault dolomite slumped in Fleming chert siltite, with overlying chert breccias. Locality - Knob Ridge. Photo by R. Knight. GSC 205130-C



Figure 60. Channel of Fleming chert breccia conglomerate cutting Fleming flat clast intraformational conglomerate. Locality - Knob Ridge. Photo by R. Knight. GSC 205130-D

of apparent shallow-water sedimentation. This is illustrated in Figure 63, where interdigitating chert breccias and chert arenites are well exposed at Knob Ridge.

Chemistry

Major element analyses for a number of Fleming cherts and some related rocks are presented in Table 1, Appendix 2. Examination of these data reveals that typical of a chert, the Fleming is a very silica-rich rock type. The principal diluents of the silica are aluminum and associated potassium, probably of detrital origin as fine clays that settled out into

the chert muds, and carbonates of Ca, Mg, and Fe which are derived from early carbonate cements precipitated from the same waters that deposited the Fleming silica.

Elements normally occurring in trace amounts in rocks have been determined for a suite of samples from the Fleming and associated rocks, and are presented in Table 2, Appendix 2. It may be possible to evaluate the mineralogical hosts of certain trace elements from considerations of the correlations (or lack thereof) with other elements or with certain minerals. Such understanding can improve the interpretations of the sedimentology and diagenesis of the rocks under study.



Figure 61. Large clasts of Fleming intraformational rip-up conglomerate in chert arenite. The dark tones of the conglomerate are due to differences in grain size as contrasted with the chert arenites. The general hummocky nature of the bedding is well illustrated. Locality - Knob Ridge. Photo by R. Knight. GSC 205130-Q



Figure 62. Detail of photo Figure 61. Photo by R. Knight. GSC 205130-S

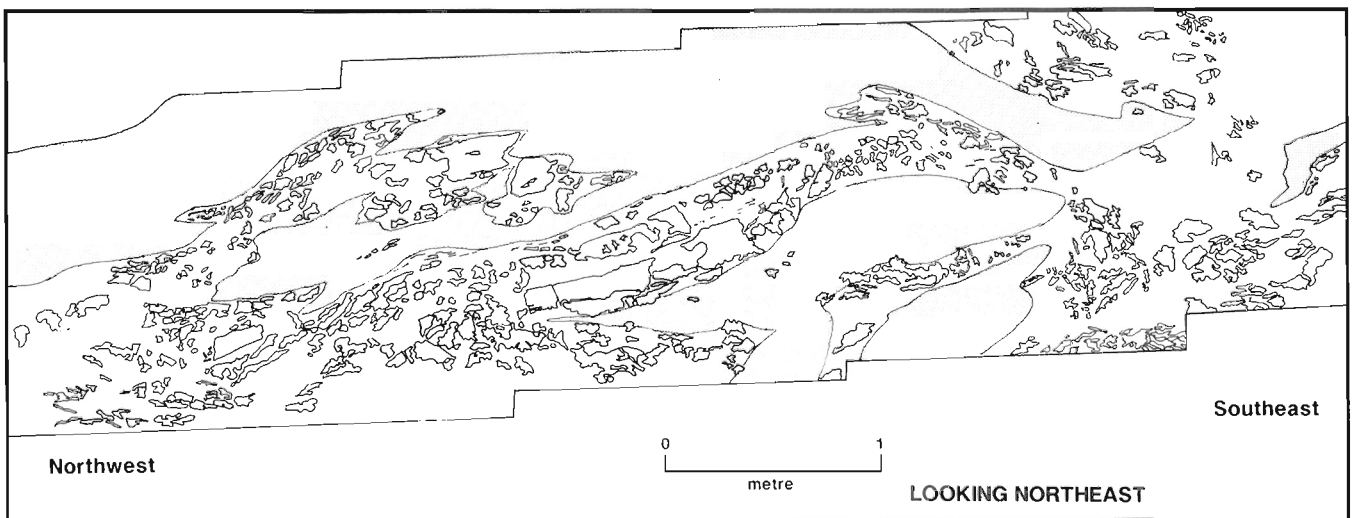


Figure 63. Illustration of the limited lateral extent of bedded units, Fleming Formation, Knob Ridge (Fig. 1b). This sketch was prepared from a photomosaic of the near-vertical outcrop. Bedding at this locality is subhorizontal, and thus the illustration approaches a cross-section. The stippled part of the drawing represents massive sands with floating chert clasts. The clear parts of the drawing represent massive to fragmental cherts, with the larger fragments and clasts indicated. Similar rocks nearby along strike are illustrated in Figures 56 and 57. Photographs were taken by R. Knight.

Concentrations of the common metals, and the high field strength elements in the Fleming are generally extremely low. In appropriate samples, however, higher concentrations of selected elements seem to correlate with the presence of above average clay content. Other mineralogical and chemical correlations are observed with zirconium and hafnium correlating with elevated rare-earths (Fig. 64), and phosphorus correlating with rare-earths (Fig. 66) in some samples. The concentrations of Ba, U, and Th, while still not elevated by most standards, are higher than expected for Fleming type rocks (Fig. 66, 67). The majority of the analysed samples plot within the 1 to 5 ppm range for U and for Th (Fig. 66), with a few samples higher or lower. The Ba content (Fig. 67) shows a bimodal population with a group of samples having Ba at or below the limit of detection for the analyses, and a main population with a mode of about 80 ppm Ba.

Replicate analyses of a rock sample L1-55m from the Fleming Formation are presented in Table 3, Appendix 2. This sample was analysed for a wider selection of elements to assure that major anomalies in the chemical composition of the Fleming rocks were not overlooked.

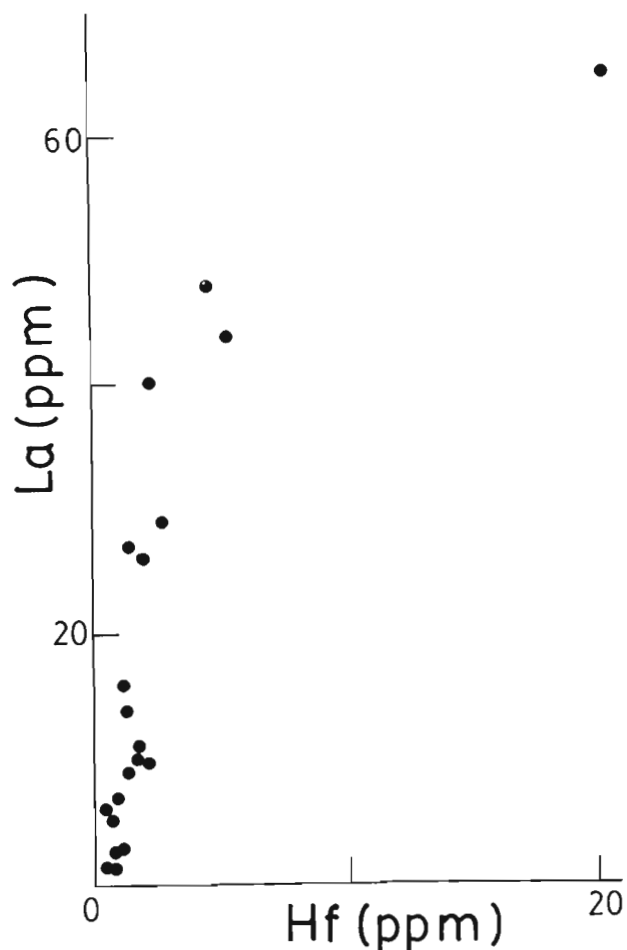


Figure 64. Scatter diagram of La(ppm) versus Hf(ppm) for samples from the Fleming Formation listed in Table 4, Appendix 2.

The distribution of phosphorous within the Fleming Formation is quite systematic with apatite-rich rocks being concentrated at the base of the unit. Apatite in the Fleming Formation hosts only a small proportion of the rare-earth elements, while the major proportion are held in zircon, probably of detrital origin. Concentrations of P_2O_5 within individual samples can attain 20 weight %. The distribution of apatite is well illustrated in stratigraphic sections in Harrison et al. (1972); in 6 of 8 sections, where the base of the Fleming can be clearly identified, phosphatic rocks are indicated at or just below the Fleming. The distribution of the phosphatic rocks is a primary feature, probably chemically controlled and a precursor to the conditions which allowed accumulation of the chert breccias.

The relationship between phosphorous and uranium and thorium is not clear. In general, samples of low P_2O_5 are low in U+Th. The two samples analyzed which contain the highest concentrations of P_2O_5 (samples E1-4A = 13.30 weight % P_2O_5 and E1-4C = 19.80 weight % P_2O_5) contain 2 to 16 ppm U+Th. The sample highest in U+Th (sample 3-2, U+Th = 39.9 ppm), however, contains only 0.05 weight % P_2O_5 but 880 ppm Zr.

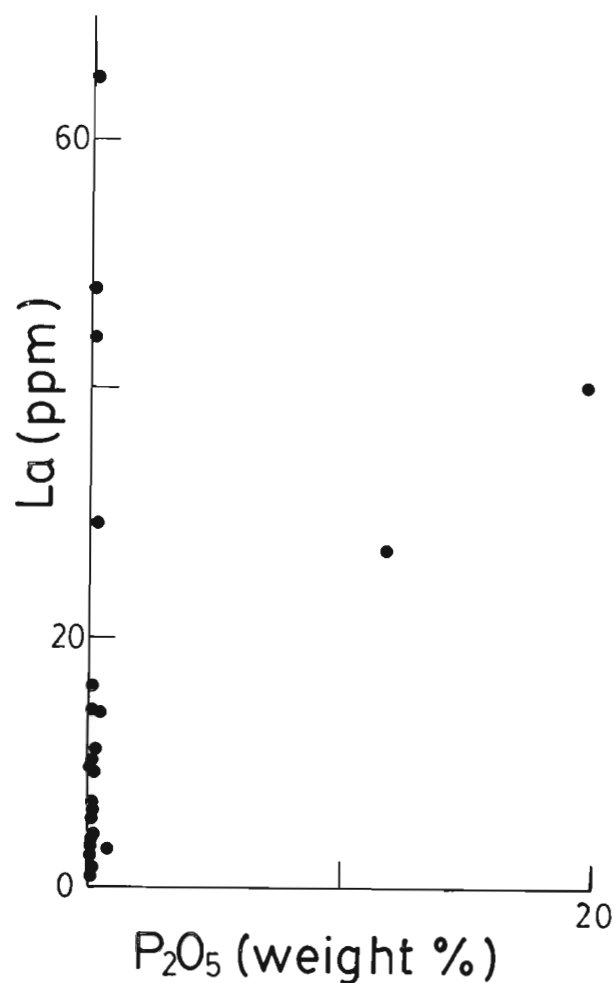


Figure 65. Scatter diagram of La(ppm) versus P_2O_5 (weight %) for samples of the Fleming Formation listed in Table 1 and 4, Appendix 2.

Consideration of the entire data set indicates that trace elements are found in three principal settings within the Fleming cherts. These settings are detrital minerals, carbonate cements, and phosphate as cement or clasts.

Detrital minerals are dominantly zircon and clays, although small proportions of apatite, monazite, or other dense, chemically stable minerals are also present. The presence of zircon, indicated by the concentration of hafnium in Figure 64, accounts for substantial proportion of the rare-earths and probably U and Th in the rocks. Adsorbed clay components are also believed to have contributed various proportions of trace elements.

Carbonate cements have trapped and held alkaline earth elements in the Fleming rocks.

Apatite, the only phosphate mineral identified to date within the Fleming Formation, is present as a cement and locally as resedimented clasts of local origin. Chemically, the apatite retains minor U, Th, and Ba as well as light and middle rare-earth elements (REEs).

Neutron activation analyses of the rare-earth elements (REE) and other elements (Sc, Cs, Hf, Ta, Th, and U) were obtained for a suite of Fleming samples (Table 4, Appendix 2). The REE spectra, presented in Figures 68 and 69, were chondrite-normalized using values from Taylor and Gorton (1977).

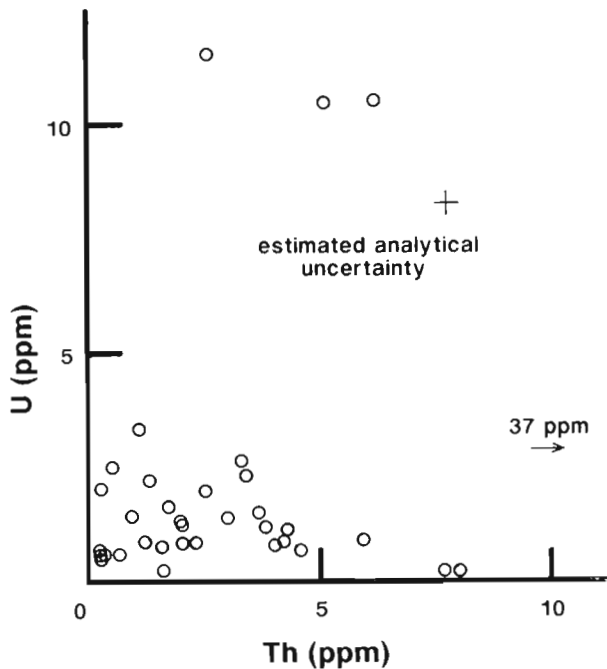


Figure 66. Scatter diagram of U(ppm) versus Th(ppm) concentrations in rocks of the Fleming Formation listed in Table 2 and 4, Appendix 2. There is no notable correlation, and the cherts and associated rocks typically contain between 1 and 5 ppm of each element. Exceptions occur, but still no systematic relationship emerges.

There are two principal rare earth element patterns in the rocks of the Fleming Formation. The most common, illustrated in Figure 68, shows a steep chondrite-normalized slope in the light rare-earths, and a relatively flat slope through the middle and heavy elements of the series. Cerium and Europium anomalies are commonly lacking in those samples where the REEs are contributed by detrital minerals. In samples where the REEs have been precipitated at the time of formation of the rock, or during its lithification, small negative Ce and Eu anomalies occur. Such anomalies are typical of rocks formed during the early Proterozoic when the atmosphere was more reducing than in the post-Precambrian. The second rare earth element pattern is illustrated in Figure 69. Here the rare earth element abundances are low, small negative Ce and Eu anomalies are present, and the chondrite-normalized spectra are flat to slightly elevated in the middle rare earths. Since this pattern occurs in rocks with relatively elevated iron contents, the mineralogic site of the REEs is probably iron oxides co-precipitated with the silica of the chert breccias.

THE ORIGIN OF THE FLEMING FORMATION

Presented below, in approximately their order of historical development, are several interesting theories proposed for the origin of the Fleming Formation.

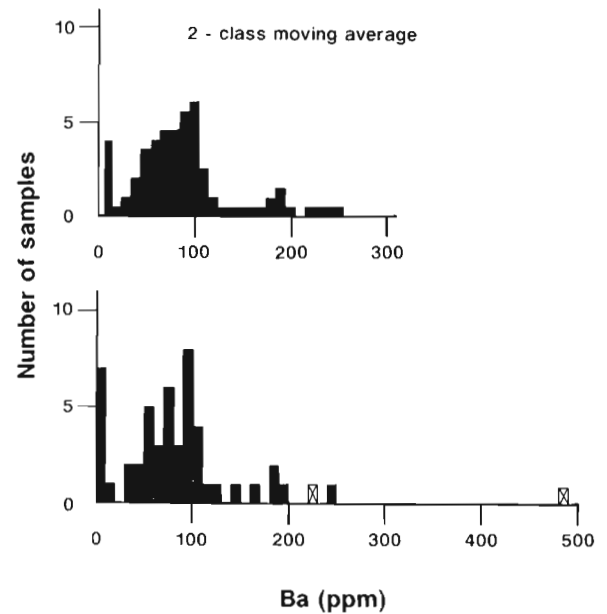


Figure 67. Histograms of Ba concentration in samples of the Fleming Formation and associated rocks. The upper histogram is a 2-class moving average of Ba concentrations, the bottom histogram is a plot of the raw Ba data. Solid boxes are Fleming cherts, while open boxes are shales above and below the Fleming at the rail cut south of Schefferville (Figure 1b). The population is bimodal, with one group of samples at or below the limit of detection (about 10 ppm), and a main population having a mode of about 80 ppm.

Is the Fleming a lag deposit?

The suggestion that the Fleming is a lag deposit resulting from the subaerial erosion of part of the Denault dolomite follows early suggestions by geologists of the Iron Ore Company of Canada. (Dufresne, 1952). According to this proposal, the Fleming represents chert and quartz scattered throughout the now-eroded portion of the dolomite that was concentrated as a residual layer on the erosional surface (Wardle and Bailey, 1981; P.H. Hoffman, pers. comm., 1986; Hoffman, 1987). Chandler (1988b) documented the presence of a chert lag at an unconformity within the Nastapoka Group, Richmond Gulf area. While the Nastapoka chert breccias are superficially similar to the Fleming, major differences exist. The Nastapoka chert breccias cut down through the

stratigraphically underlying carbonates and "appear identical to the tabular black chert occurring in the enclosing carbonates" (Chandler 1988b, p. 32). Fleming cherts and the small amounts of chert within the Denault are texturally quite dissimilar. Chandler also recognized karstic weathering temporally associated with the chert breccia. This is in marked contrast to the Fleming where there is no evidence for erosion associated with the dolomite-chert contact, and no unequivocal vuggy or open-space weathering textures are reported from the Denault Formation. Donaldson (1966) reported open spaces in the Denault are associated with silicification and possibly not with weathering. Texturally the Fleming cherts and the small amounts of chert within the Denault are distinct.

Detailed field examination of outcrops near the Fleming-Denault contact failed to detect the presence of irregular topography, paleosol development, local boxwork weathering, or rapid lateral thickness variations in either the Fleming or Denault. There is no indication that the Fleming Formation fills ancient topographic depressions on the Denault Formation or that it covers an eroded surface.

Is the Fleming a silicified dolomite?

The explanation for the origin of the Fleming Formation preferred by Howell (1954) and Dimroth (1971) is that these rocks are a silicified portion of the Denault. Howell seems to have assumed that quartz-filled joints in the Denault formed at the same time as the Fleming. This, however, is not necessarily the case in view of the systematic relationship between at least some of the joints and regional structure described by Howell (1954). Howell (1954) also interprets many textures to be replacement which can be equally well, if not considerably

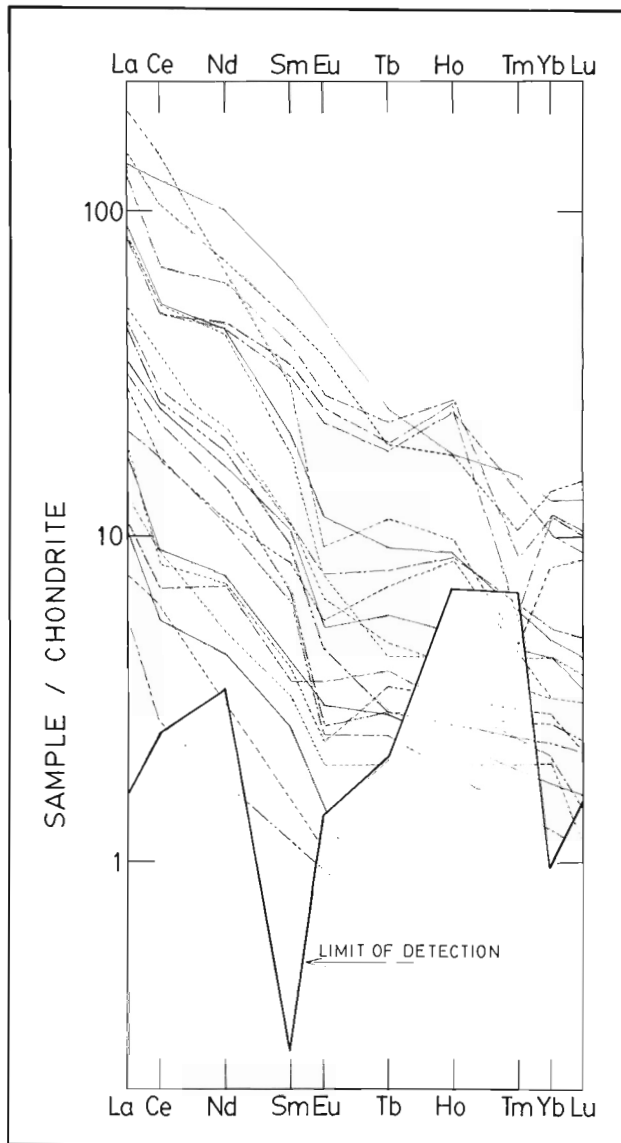


Figure 68. Chondrite-normalized rare-earth spectra of samples from Table 4, Appendix 2..

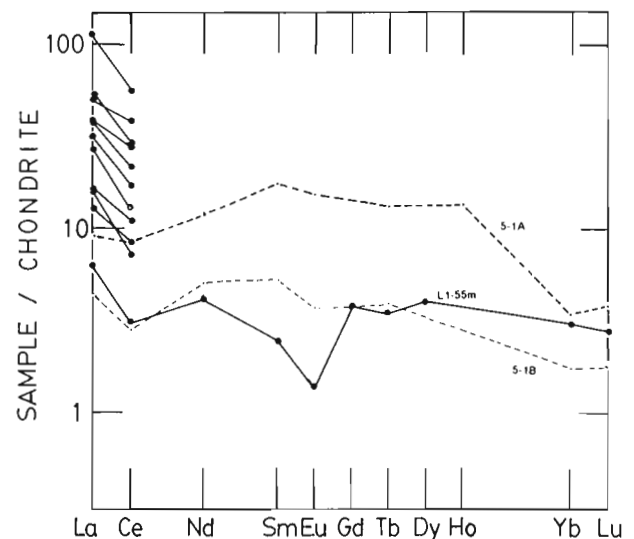


Figure 69. Chondrite-normalized rare-earth spectra of samples L1-55m (Table 3, Appendix 2), 5-1A and 5-1B (Table 4, Appendix 2), with chondrite-normalized La and Ce of other samples from Table 2, Appendix 2. The spectra are generally flat, with small negative Ce and Eu anomalies.

better, described as co-precipitation or even replacement of silicibyrrhombedral carbonates, in some cases followed by later silica replacement of the carbonates.

Donaldson (1966) described silicified portions of the Denault Formation and presented evidence that carbonate replacement as well as open-space filling have occurred. Though Donaldson's descriptions of silica-filled joints, remnant patches of dolomite and relict bedding in chert nodules within the Denault strongly support his interpretation, they also contrast strongly with all descriptions of the chert found in the Fleming Formation.

At the outlet of Marble Lake into Astray Lake (Fig. 2), near the top of the Denault Formation, dolomite and featureless, fine-grained chert are interbedded over several metres on a vertical scale of a few centimetres for each bed, and on a horizontal scale of at least tens of metres with good continuity of the beds. Both lithologies are relatively impure; the dolomite being seen to be siliceous in thin section, and the cherts dolomitic. This sequence is interpreted as a co-precipitation of chert and dolomite, with one or the other generally dominant at any given time.

Is the Fleming a silicified evaporite?

Dimroth (1978), followed by Wardle and Bailey (1981), slightly modified their views on the origin of the Fleming to include a component of previously present evaporites. The textural development of the Fleming was interpreted to include slumping of unconsolidated to semi-lithified sediments brought about by solution removal of evaporites. Whether all or only some rather small portion of the chert was thought to replace evaporites is unclear. The recognition of both length-fast and length-slow chalcedony was considered by Dimroth proof of the former presence of evaporites. Keene's (1983) work, which demonstrated the presence of both length-fast and length-slow chalcedony in modern deepsea siliceous oozes, contradicts the technical basis of Dimroth's argument. Dimroth's (1978) proposal for the origin of the Fleming Formation requires critical reappraisal. The hypothesis that more reactive components of the sedimentary package (evaporites and/or dolomite) were silicified and locally dissolved to promote slumping, while adjacent clastic units, presumably on a scale of less than a few metres, were not even cemented by silica is not readily acceptable. Solutions rich in silica would have cemented the sandy facies of the sedimentary package at least as quickly as they dissolved other components. Therefore the proposal that the Fleming Formation is predominately a silicified evaporite goes far beyond silicification controlled by chemical microenvironment. Another problem with the interpretation of the Fleming as a silicified evaporite is the proportion of silica which represents replaced earlier materials. It has become evident from the detailed studies reported here, in agreement with the interpretations of earlier investigators, that much of the quartz in the Fleming is redeposited megaquartz. Thus much of the supposed solution of evaporites or silicification of dolomite would have to have been contemporaneous with the deposition and reworking of the Fleming.

None of the foregoing should be understood as a complete rejection of the presence of former evaporitic minerals in the Fleming Formation. It would be most unusual if a rock interpreted as a silica precipitate never deposited more conventional evaporitic minerals. The challenge is to recognize the textural and mineralogical clues which allow for the quantification of those mineral proportions that have undergone dissolution or silicification.

Is the Fleming a hot spring deposit?

Based on textural features, particularly those displayed by concentric banded chert and quartz, and the partially contemporaneous nature of the Denault and Fleming formations, Simonson (1982) concluded that the Fleming was deposited from hot springs debouching onto the ocean floor.

According to Simonson (1982) the presence of the volcanic rocks of the Nimish allows the supposition of high regional heat flow that could support large-scale diffuse hydrothermal systems in a rift-style setting. Simonson (1982) further suggests that the Fleming Formation has effectively been separated from its root zones of igneous rocks by subsequent thrust faulting.

While the author is in agreement with Simonson's proposal that silica of the Fleming was precipitated from solution more or less in its present geological position, a hot spring origin for the Fleming Formation is rejected. Regional study of the Nimish volcanics has shown that there is no evidence of large scale hydrothermal systems in the area, (Evans, 1978 DH. Watanabe, pers. comm., 1989); Simonson's explanation of Fleming Formation root zone truncations fails to consider that the Fleming is commonly underlain by Denault dolomite which lacks any evidence indicative of the passage of hot, or even warm solutions. There is no evidence of thickness variations in the chert breccias, or that the original sites of deposition of the Fleming were aligned along, or controlled by lineaments or contemporaneous faults that would be expected to accompany major hot spring activity. Furthermore, the presence of Fleming rocks on the eastern side of Lake Attikamagan (at Marion and Andre lakes) implies that the unit has a significantly larger lateral dimension than is explainable by Simonson's model. If the Fleming was a hot spring deposit, it would be expected that components other than silica would be transported by the hot spring system. Geochemical analyses of the Fleming and examinations of many outcrops suggest, however, that no other elements were deposited with the cherts, neither common elements such as iron, potassium, sodium, or barium, nor rare-elements such as base metals, or gold.

Is the Fleming a magadi-type chert?

According to Shepard and Gude (1986, p. 336) a Magadi-type chert is one which formed from magadiite or some other similar hydrous sodium silicate minerals. Descriptions of cherts from the type area can be found in Eugster (1969) and Surdam and Eugster (1976).

In general Magadi-type cherts are formed from the diagenetic transformation of magadiite ($\text{NaSi}_7\text{O}_{13}(\text{OH})_3 \cdot 4\text{H}_2\text{O}$) or kenyaite ($\text{Na}_2\text{Si}_{22}\text{O}_{41}(\text{OH})_8 \cdot 6\text{H}_2\text{O}$) to quartz. The deposits are formed in lacustrine basins in areas of abundant volcanic detritus from waters of high pH dominated by sodium carbonate-bicarbonate. Magadiitic rocks are typically associated with other evaporitic rocks including trona, some zeolites, and evaporitic carbonates (particularly dolomite). Magadi-type cherts occur as thin, discontinuous beds generally up to 10 cm thick, frequently distributed around springs.

The contrasts between the Fleming cherts and the Magadi-type are striking. Direct crystallization of quartz as crusts is not reported from any Magadi-type occurrence, where all silica is precipitated as hydrous sodium silicates or silica gels. Magadiite rock association, particularly with sodium-rich evaporites and volcanics, contrasts markedly with the essentially nonvolcanic environment of the Fleming, where only portions of the Denault dolomite could be considered to have an evaporitic affinity.

Thus while the Fleming cannot be considered a Magadi-type chert based on the differences in geological environment between the two classes of rocks, there are suggestions of some similarities in the water chemistry of these two chert types. It is possible that the oceans of the Early Proterozoic were sodium carbonate rather than sodium chloride solutions (Kempe and Degens, 1985), with higher pH than at present and higher dissolved silica.

The origin of the Fleming Formation

Regional and detailed field investigations suggest that the Fleming is a direct silica precipitate, in some ways linked to evaporites. This is basically the origin proposed by Dufresne (1952) and accepted by Gross (1968), and Baragar (1967). Textural evidence supporting this hypothesis include the following:

- the quartz of the crusts does not seem to be pseudomorphous after any older mineral;
- the textures are all indicative of deposition, solution and redeposition of silica on a large horizontal scale in a local stratigraphic setting; and
- many of the textural elements described as clasts have been produced in situ, or transported only very short distances.

The Fleming appears to be a chemical sediment of shallow water origin, probably formed in a restricted basin, with virtually no clastic terrestrial component. The Fleming Formation can simplistically, yet accurately be described as an iron-formation without the iron.

In considering the origin of the Fleming Formation, it is useful to examine the stratigraphic settings of cherts in other iron-formation basins. The study of Trendall (1968) is particularly instructive in this regard. In comparing the

Hamersley, Animikie, and Transvaal basins, all of which include major iron formations, Trendall (1968, p. 1539) notes "Thus, of the two main iron formation constituents (silica and iron oxide), there is an indication from all three basins of the local deposition of silica before the onset of iron formation deposition". This suggests that the silica comprising the Fleming Formation, though texturally unique, is in a normal and expected stratigraphic setting. Based on Trendall's (1968) work, the stratigraphic unit which would seem to be unexpected is the Wishart quartzite. The Wishart quartzite however, does have features that appear to link it to the overlying Sokoman iron-formation including a common iron-carbonate chemical component and a chert component (Simonson, 1985; 1987). Although earlier workers based their theories of the origin of the Fleming Formation on careful field investigation, they were hampered in not having suitable information concerning the settings and internal organizations of other basins for comparative purposes. Had such data been available, theories such as a replacement, paleosol, or regolith origin for the Fleming would probably not have received wide acceptance. The foregoing does not in any way preclude or exclude a replacement origin for portions of the Denault which may be silicified as observed by Howell (1954) and Donaldson (1966). Undoubtedly downward-seeping silica-rich brines from the Fleming would contribute to silicification in the Denault. Interestingly enough, the present suggestion of the origin of the Fleming Formation does not offer much insight concerning a possible sub-Wishart unconformity. Though the periodic exposure of the Fleming and the presence of an unconformity at or near the base of the Wishart is suggested by the presence of chert pebble, chert-cemented conglomerate in the Knox Mine outcrop (Fig. 5), the regional extent of this sub-Wishart unconformity is unknown.

Application of the provocative term **silica precipitate or evaporite** to the Fleming is done deliberately in order to draw attention to the difficulties of accepting the theory that a major accumulation of chert could have occurred through direct precipitation from ocean waters. If evaporation were the mechanism of precipitation, huge amounts of water would be required to provide a source for such a thickness of chert, as silica is not sufficiently abundant in modern seawaters. This situation would also result in major amounts of other evaporitic minerals being associated with the rocks of the Fleming Formation, which is in marked contrast to the small proportion of these minerals that have been silicified or dissolved. A modification of this theory is that minor amounts of evaporation caused the precipitation of silica, the least soluble component in the solution, but that the process did not proceed to the point of depositing other minerals in significant amounts. The common presence of a phosphatic horizon at or near the base of the Fleming (see Harrison et al., 1972 for sections illustrating this) also raises the possibility that the silica of the Fleming was in some measure biogenically precipitated. However, thin section examination to date has not led to recognition of any fossils or definitive organic remains.

The proposed origin for the Fleming Formation which offers a simple solution to the above difficulties is that the silica was selectively precipitated from the Proterozoic oceans.

A conceptual framework proposed here for the origin of the Fleming Formation includes the following features:

(1) a chemical setting permitting abundant dissolved silica in ocean waters.

The general setting of the Fleming Formation was marine. Simonson (1985b) reached a similar conclusion on the setting of the Wishart and Sokoman formations. This conclusion is based on the lateral extent, chemistry, and sedimentology of the associated strata (Denault and Wishart), as well as the presence of the cherty phosphatic argillite commonly reported to underlie the cherts. Following Siever (1962), it is accepted that the oceans had higher concentrations of dissolved silica before the evolution of silica-precipitating organisms. Following Kempe and Degens (1985), the oceans of the Early Proterozoic possibly were dominantly carbonate-bicarbonate rather than halide. The resulting higher pH would have two principal consequences. Firstly, silica saturation would occur at much higher concentrations than in modern oceans (as illustrated by Degens (1968, p. 61) at pH above 9, SiO₂ solubility as silica gel is 200 ppm, increasing rapidly to 1000 ppm at pH 11). Secondly, at high pH many common silicate minerals are unstable, and would dissolve as has been documented in a modern lagoon precipitating dolomite and chert (Peterson and von der Borch, 1965). Similarly, Eugster and Jones (1968) have illustrated the corrosion of alkali trachyte boulders by hot alkaline spring waters at extremely rapid geological rates. The dissolution of detrital grains would serve to increase the concentration of Si and other elements in the waters associated with the Fleming Formation. Thus the apparent lack of detrital grains in the Fleming Formation (and possibly in many banded iron-formations) may be the result of the destruction of sedimentary particles, as well as relatively high rates of accumulation of the chemical sediments. The most likely regional setting for the deposition of Fleming Formation type rocks would be on a coast near an area of upwelling of deep ocean waters. Such waters would carry silica, dissolved CO₂ and nutrients to the deposition area. According to Heckel (1972), these conditions are favorable to the production of phosphorites, the development of organic blooms and the reduction of clastic sedimentation into the area of sedimentation by producing a dry climate on the neighboring continental landmass.

(2) primary precipitation of silica in very shallow to moderately deep water.

Though generally not preserved, areas of primary silica precipitation are found north of the Knox Mine, at Knob Ridge (Fig. 5), and in an apparently deeper water setting at northern Marble Lake (Fig. 17). In the shallow water examples, major portions of the Fleming consist of massive-to concentrically-banded cherts showing extreme small scale slumping. In order to explain the brittle and ductile behavior of adjacent layers, it is necessary to postulate deposition of silica both as chert and as a gel, or bed-selective early

diagenesis to chert of a series of gels. Such features are also well exposed at Roof Ridge (Fig. 13), and appear to have been best preserved below wave base. Deeper water accumulations of disrupted brittle, massive chert are exposed at northern Marble Lake (Fig. 17).

The dolomite and phosphate deposition which preceded the formation of cherts and their precursors may have been necessary to establish the conditions that allowed deposition of the Fleming Formation. Initial removal of Ca, Mg and CO₂ as dolomite from the waters that would later deposit the silica of the Fleming may have been an important preliminary step in raising pH and enhancing Si solubility. The factors causing subsequent deposition of silica are not clear, and several possibilities exist including: lowering of pH through mixing with less evolved waters, organic production of CO₂, or a marked change in temperature.

Selective deposition of silica as opposed to wholesale deposition of all components present in the water column through evaporation was probably an important factor in the process giving rise to the chert breccias of the Fleming Formation. Changes in pH imposed on the entire water column or on selective portions could have resulted in silica precipitation while other components, carbonates in particular, would not necessarily be precipitated. Acceptance of the latter coupled with the overall suggestion of high concentrations of silica in the waters removes the condition that other evaporitic minerals should be present in the Fleming in a significantly greater proportion. Both biological activity and the mixing of marine water with fresh water could have triggered silica deposition. The evidence for resorption of silica, as seen in the rounded quartz grains derived from megaquartz crystals, and the rounded chert grains in the resedimented portions of the Fleming, can be accepted as a normal part of a process in which changing conditions (mixing of waters) resulted in periods of silica undersaturation alternating with periods of supersaturation.

(3) local reworking of silica as well as chert and quartz due to slumping and wave action.

Desiccation of silica gel and consequent volume reduction were a major factor in the local slumping which produced many of the unique outcrop scale features of the Fleming. The shallowing-upward sequence culminating in a chert-pebble conglomerate north of the Knox Mine as well as the convolute structures and contraction features at Knob Ridge indicate that local exposure occurred. Much of the megaquartz in the Fleming Formation was formed as fillings of voids resulting from desiccation of silica gel, dissolution of other evaporitic minerals, or open spaces resulting from slumping of semiconsolidated sediments which had enough stiffness to fracture.

(4) transport of chert and quartz sands that formed through contemporaneous recrystallization of silica gel and chert and erosion of megaquartz from void filling.

Many outcrop exposures of the Fleming consist largely of resedimented materials (Fig. 15 and 17). In many locations quartz and chert make up silica-cemented arenites that also

contain variable proportions of vari-textured clasts. While a proportion of the clasts were transported with the rest of the sediments, many and probably most had a more local origin and formed in situ as crusts which were soon broken up by contraction or wave action. In most cases patches of chert, banded chert, or megaquartz also formed in situ. Channel fillings in the Fleming (Knob Ridge) and debris flows that incorporate Fleming material, illustrate the scale and magnitude of penecontemporaneous sedimentary processes.

Why is the Fleming Formation texturally unique?

Several features combine to make the Fleming Formation unique including: the common development of chert-quartz sands; the common presence of crust-type banded quartz as well as the other clast types; and the wide variations in sedimentary style not displayed by any other chert or siliceous sedimentary unit. Of these features, the development of crust-type banded quartz warrants further consideration. The presence of chert-quartz sands follows from penecontemporaneous erosion of the crusts, and the variety of styles of sedimentation can be attributed to the marine environment and the different water depths at which the Fleming Formation accumulated.

The behavior of silica in solution and through the various stages of precipitation is summarized in Krauskopf (1967 p. 166-170). Because quartz is much less soluble than silica gel and the kinetics of its precipitation are so slow, most chert occurrences forms as colloidal suspensions (gels or sols) rather than millimetre-scale quartz crystals which are common in Fleming Formation clasts. Though presently the explanation for the formation of Fleming crust-type clasts is uncertain, the leading possibilities seem to be that biological processes were involved, or that the crusts formed in a zone of fluid mixing. The presence of other components, possibly HCO_3 , CO_2 , Cl , or simple organic molecules may have allowed the formation of larger crystals. Laboratory experimentation to test these ideas has not been reported. While the simple growth of quartz crystals during evaporation cannot be excluded, it seems the least likely method to have produced the crusts, as no similar textures have been reported from laboratory studies of silica solutions, and the time involved to produce the crystals of the crusts would be prohibitively long.

If biological processes were involved in the formation of the crust-type banded quartz, no systematic association of crust-type clasts with organic remains can be recognized today. The possibility exists that a layer of organic material covered the water surface and increased the temperature in the underlying solutions by trapping and retaining heat. This heating could have greatly accelerated the growth of quartz from a chert substratum. Growth of quartz could be enhanced by electrochemical reactions in the organic mats, or by organic production of CO_2 leading to locally reduced pH and subsequent silica dumping.

If the quartz of the crusts was deposited in a zone of fluid mixing, simple dilution of the brines by fresher water would lower the pH and lead to silica precipitation. If mixing of the fluids occurred along the sediment-water interface, it may

have been by invasion of a denser brine into a less dense solution. While this process could allow quartz crystals to grow preferentially where the two fluids mixed, it would also facilitate preservation of crusts in their growth position, a situation not yet recognized in field studies.

While portions of iron-formations are highly siliceous, textures such as the crust-type clasts of the Fleming Formation are not reported elsewhere. The most likely cause of this difference is that the presence of enhanced Fe, CO_2 and other components in the waters depositing iron formations inhibited the mechanism of crust formation. An effective impediment would be the formation of abundant nuclei which would allow precipitation of fine grained chert and quartz instead of crusts.

The textural uniqueness and rarity of Fleming crusts implies that: 1) the conditions appropriate to their formation have not often been obtained, and 2) they have not been preserved throughout geologic time. Although the overall shallow water environment is recognizable, conditions here are not generally conducive to the preservation of the finer sedimentary structures. Furthermore, the abundant dissolved silica associated with the deposition of the Fleming Formation implies possible evaporitic conditions which only adds to the rarity of the environment.

RESOURCE POTENTIAL

The suggestion by Simonson (1982) that the Fleming Formation has a hydrothermal origin prompted this study. Although Simonson (1982) did not specifically discuss mineral resources, the parallel drawn between the Fleming and the siliceous rocks of Steamboat Springs, Nevada, warranted an investigation into the precious metal potential of the Fleming. Based on detailed field observations and the extremely low gold contents of all samples analyzed (Table 2, Appendix 2), Simonson's (1982) hypothesis is rejected and the precious metals potential of the Fleming appears to be negligible. If precious metals are to be sought in the Fleming Formation, the deposit type must be epigenetic, and associated with geological events not yet identified in the study area.

Study of the Fleming also facilitated an assessment of the mineral potential of the Denault dolomite. Dismissal of Simonson's (1982) hydrothermal origin for the Fleming diminishes the potential for the discovery of replacement-type mineralization in the Denault. The lack of any evidence indicative of hydrothermal activity in the Denault substantiates the latter. Suggestions by Hoffman (1987) of a foredeep-related origin for the Fleming (as a lag deposit) raised the possibility of an erosional surface on the Denault at or underlying the Fleming cherts. If this were the case, ground preparation suited to the deposition of Mississippi Valley type deposits of lead, zinc, barite, and fluorite could be envisaged. Field investigations, however, recorded no sign of Denault erosion or karstic weathering.

Donaldson's (1966, p. 33) report of a "slight erosional unconformity" separating the Denault and basal Wishart (correlated now with the Fleming) was based on the sharp

contact separating the two units, rather than on observation of an actual unconformity. The abundant field evidence of Denault slumping, particularly well documented at Knob Ridge (Fig. 11 and 12), is considered to be due to subaqueous debris flows moving down a reef slope rather than to the presence of an erosional unconformity.

The mineral resource potential of the Fleming as dimension stone and as a source of silica for electronic or glassmaking purposes was also evaluated. For both these applications, the rocks of the Fleming only locally and sporadically meet industry technical requirements. The hardness of the Fleming, fine grain size of impurities, and the heterogeneity of the unit on every scale render it of no interest for industrial materials. The phosphate-rich portions of the Fleming are neither thick nor continuous enough to warrant exploitation, and even if a substantial reserve could be defined, the hardness of the rock and the intimate association of phosphate and fine grained silica suggest that beneficiation would be problematic and non-economic.

DISCUSSION

Interpreting the origin of the Fleming Formation is made exceedingly difficult because the sedimentary rock record through geological time produces two mutually incompatible conclusions. Boulter and Glover's (1986) study of ancient Australian evaporites suggests that evaporites and related rocks have not changed greatly through geological time (late Archean to the present). Superior type iron-formations, however, suggest that the chemistry of the world ocean has evolved markedly with the major changes apparently taking place during the Proterozoic (e.g. Holland, 1984). There are significant uncertainties associated with the various lines of argument. In particular, the composition of the atmosphere in Archean and Early Proterozoic time must have had a pronounced effect on evaporitic rocks. Furthermore, in many cases it is by no means certain whether particular evaporitic sequences were formed in marine or lacustrine environments. Finally, interpretation of the importance of diagenetic alterations to sedimentary rocks introduces another complicating factor.

Although several notable attempts have been made to resolve the dichotomy in interpreting evaporitic rocks, to date no attempt is considered unequivocal. Eugster and co-workers (e.g. Eugster and Chou, 1973) drew parallels between present-day alkaline lakes and possible iron-formation forming systems. The scale of the larger iron-formations and their association with rocks of probable marine sedimentary origin argue against such an hypothesis. Though Kempe and Degens (1985) extended the conclusions of Eugster and co-workers to a global scale by arguing that the oceans of Archean and Early Proterozoic time were sodium carbonate-bicarbonate rich, they failed to address the problems of interpretations of ancient evaporites. The dominance of dolomite in the older carbonate sequences also led Tucker (1982) to suggest that the oceans of the Proterozoic differed chemically from the Phanerozoic

The rocks of the Fleming Formation bear on the problems of the origins of iron-formations and seem to provide a bridge linking modern and ancient evaporites. A simplistic workable model, that addresses the problems referred to above, is that the Early Proterozoic oceanic composition was sodium carbonate-bicarbonate rich, and that the evaporitic rocks preserved from that era are dominantly nonmarine.

CONCLUSIONS

During the Early Proterozoic, major amounts of silica were deposited in the Knob Lake Basin. This silica took the form of replacements of some portions of dolomite, common co-precipitation with dolomite, and much direct deposition as silica gels, chert and quartz.

Field and laboratory investigations suggest that:

(1) the rocks of the Fleming Formation accumulated in their present geological position, and are neither lag deposits nor transported accumulations of chert dominantly formed elsewhere; and

(2) the quartz of the crusts which make the Fleming a texturally unique unit was precipitated as quartz and does not replace an earlier mineral.

REFERENCES

- Baragar, W.R.A.**
1967: Wakuach Lake Map-area, Quebec-Labrador; Geological Survey of Canada, Memoir 344, 174 p.
- Boulter, C.A. and Glover, J.E.**
1986: Chert with relict hopper moulds from Rocklea Dome, Pilbara Craton, Western Australia: An Archean halite-bearing evaporite; *Geology*, v. 14, p. 128-131.
- Chandler, F.W.**
1988a: Diagenesis of sabkha-related sulphate nodules in the Early Proterozoic Gordon Lake Formation, Ontario, Canada; *Carbonates and Evaporites*, v. 3, p. 75-94.
1988b: The Early Proterozoic Richmond Gulf graben, east coast of Hudson Bay, Quebec; Geological Survey of Canada, Bulletin 362, 76 p.
- Degens, E.T.**
1968: *Geochemie der Sedimente*, [Geochemistry of sediments]; Ferdinand Enke Verlag, Stuttgart, 282 p.
- Dimroth, E.**
1971: The Attikamagen - Ferriman Transition in Part of the Central Labrador Trough; *Canadian Journal of Earth Sciences*, v. 8, p. 1432-1454.
1978: Region de la Fosse de Labrador, Ministère des Richesses Naturelles, Québec; *Rapport Géologique* 193, 396 p.
- Dimroth, E., Baragar, W.R.A., Bergeron, R., and Jackson, G.**
1970: The Filling of the Circum-Ungava Geosyncline; in *Symposium on Basins and Geosynclines of the Canadian Shield*, A.J. Baer (ed.), Geological Survey of Canada, Paper 70-40, p. 45-142.
- Donaldson, J.A.**
1963: Stromatolites in the Denault Formation, Marion Lake, Coast of Labrador, Newfoundland; Geological Survey of Canada, Bulletin 102, 33 p.
1966: Marion Lake Map-area, Quebec-Newfoundland; Geological Survey of Canada, Memoir 338, 85 p.
- Dufresne, C.**
1952: A study of the Kaniapiskau System in the Burnt Creek -Goodwood Area, New Quebec and Labrador, Newfoundland; Ph.D. thesis, McGill University, Montreal, P.Q., 211 p.

- Eugster, H.P.**
1969: Inorganic bedded cherts from the Magadi area, Kenya; *Contributions Mineralogy and Petrology*, v. 22, p. 1-31.
- Eugster, H.P. and Chou, I.**
1973: The Depositional Environment of Precambrian Banded Iron - Formations; *Economic Geology*, v. 68, p. 1144-1168.
- Eugster, H.P. and Jones, B.F.**
1968: Gels Composed of Sodium-Aluminum Silicate, Lake Magadi, Kenya; *Science*, v. 161, p. 160-163.
- Evans, J.L.**
1978: The Geology and Geochemistry of the Dyke Lake area (parts of 23J/8,9), Labrador; Newfoundland Department of Mines, Report 78-4, 39 p.
- Folk, R.L.**
1974: *Petrology of Sedimentary Rocks*, Hemphill Publishing Co., Austin, Texas, 182 p.
- Gross, G.A.**
1968: Geology and Iron Deposits in Canada, Volume III, Iron Ranges of the Labrador Geosyncline; Geological Survey of Canada, Economic Geology Report no. 22, 179 p.
- Harrison, J.M., Howell, J.E., and Fahrig, W.F.**
1972: A geological cross-section of the Labrador Miogeosyncline near Schefferville, Quebec; Geological Survey of Canada Paper 70-37, 34 p.
- Heckel, P.H.**
1972: Recognition of ancient shallow marine environments; in *Recognition of ancient sedimentary environments*, J.K. Rigby and W.K. Hamblin (ed.), Society of Economic Paleontologists and Mineralogists Special Publication no. 16, p. 226-286.
- Hoffman, P.H.**
1987: Early Proterozoic foredeeps, foredeep magmatism, and superior-type iron formations of the Canadian Shield; in *Proterozoic lithospheric evolution*, A. KrÖner, (ed.), *Geodynamics Series*, 17, p. 85-98.
- Holland, H.D.**
1984: The chemical evolution of the atmosphere and oceans; in the *Collection Princeton series in geochemistry*, Princeton University Press, Princeton, N.J., United States, 582 p.
- Howell, J.E.**
1954: Silicification in the Knob Lake Group of the Labrador Iron Belt; Ph.D. thesis, University of Wisconsin, U.S.A., 89 p.
- Keene, J.B.**
1983: Chalcedonic quartz and occurrence of quartzine (length-slow chalcedony) in pelagic sediments; *Sedimentology*, v. 30, p. 449-454.
- Kempe, S. and Degens, E.T.**
1985: An early soda ocean?; *Chemical Geology*, v. 53, p. 95-108.
- Klein, C., and Fink, R.P.**
1976: Petrology of the Sokoman Iron Formation in the Howells River Area, at the Western Edge of the Labrador Trough; *Economic Geology*, v. 71, p. 453-487.
- Krauskopf, K.B.**
1967: *Introduction To Geochemistry*; McGraw-Hill Book Company, New York, 721 p.
- Perrault, G.**
1952: Dyke Lake Area, Labrador; Private report to the Iron Ore Co. of Canada, Newfoundland Department of Energy, Mines and Resources, Assessment Report 023J-0016, 77 p.
- Peterson, M.N.A. and von der Borch, C.C.**
1965: Chert: Modern Inorganic Deposition in a Carbonate-Precipitating Locality; *Science*, v. 149, p. 1501-1503.
- Sheppard, R.A. and Gude, A.J.**
1986: Magadi-type chert-A distinctive variety from lacustrine deposits; in *Studies in Diagenesis*, F.A. Mumpton, (ed.) U.S. Geological Survey Bulletin 1578, p. 335-345.
- Siever, R.**
1962: Silica solubility, 0°-200°C and diagenesis of siliceous sediments; *Journal of Geology*, v. 61, p. 127-150.
1982: Fleming chert breccia: a probable hot spring plumbing system in the 2 billion year-old Labrador Trough (Abstract); *Geological Society of America Program with abstracts*, v. 14, p. 618.
1985: Sedimentology of cherts in the Early Proterozoic Wishart Formation, Quebec-Newfoundland, Canada; *Sedimentology*, v. 32, p. 23-40.
1985b: Sedimentological constraints on the origins of Precambrian iron-formations; *Geological Society of America Bulletin*, v. 96, p. 244-252.
1987: Early silica cementation and subsequent diagenesis in arenites from four Early Proterozoic iron formations of North America; *Journal of Sedimentary Petrology*, v. 57, p. 494-511.
- Surdam, R.C. and Eugster, H.P.**
1976: Mineral reactions in the sedimentary deposits of the Lake Magadi region, Kenya; *Geological Society of America Bulletin*, v. 87, p. 1739-1752.
- Taylor, S.R. and Gorton, M.P.**
1977: Geochemical application of spark source mass spectrography - III. Element sensitivity, precision and accuracy; *Geochimica et Cosmochimica Acta*, v. 41, p. 1375-1380.
- Trendall, A.F.**
1968: Three great basins of Precambrian banded iron formation deposition: a systematic comparison; *Geological Society of America Bulletin*, v. 79, p. 1527-1544
- Tucker, M.E.**
1982: Precambrian dolomites: petrography and isotopic evidence that they differ from Phanerozoic dolomites; *Geology*, v. 10, p. 7-12.
- Wardle, R.J.**
1982: Geology of the south-central Labrador Trough; Newfoundland Department of Mines, Maps 82-5 and 82-6.
- Wardle, R.J., and Bailey, D.G.**
1981: Early Proterozoic Sequences in Labrador; in *Proterozoic Basins of Canada*, F.H.A. Campbell (ed.) Geological Survey of Canada Paper 81-10, p. 331-358.
- Zajac, I.S.**
1974: The Stratigraphy and Mineralogy of the Sokoman Formation in the Knob Lake Area, Quebec and Newfoundland; *Geological Survey of Canada, Bulletin 220*, 159 p.

APPENDIX 1

Location and description of samples not plotted on figures

Sample	Location	Description
3-1	north of Knox Mine	mottled chert, chert breccia
3-2	north of Knox Mine	quartz-chert arenite, chert breccia, mottled, micaceous matrix
3-3	north of Knox Mine	quartz-chert arenite
4-1	north of Knox Mine	quartz-chert arenite, mottled
4-3	north of Knox Mine	quartz siltstone
4-5	north of Knox Mine	chert pebble conglomerate
4-6	north of Knox Mine	chert breccia, quartz-chert sand sized matrix
5-1A	north of Knox Mine	chert breccia, quartz-chert sand sized matrix, jasper cement
5-1B	north of Knox Mine	chert breccia, quartz-chert sand sized matrix, jasper cement
5-2A	north of Knox Mine	chert breccia
5-4	north of Knox Mine	chert breccia, jasper cement
27-1	northern Marble Lake	quartz arenite
27-2	northern Marble Lake	quartz-chert arenite
27-3	northern Marble Lake	massive chert
28-2	north end of Marble Lake	chert breccia, chert-quartz sand matrix
28-3A	north end of Marble Lake	quartz-chert siltstone
28-4	north end of Marble Lake	brecciated chert with quartz sand matrix
28-10	north end of Marble Lake	quartz-chert arenite
29-4B	west shore of Marble Lake	mottled chert with dolomite
29-5B	west shore of Marble Lake	mottled chert with dolomite
29-6	west shore of Marble Lake	mottled chert with dolomite
29-7	west shore of Marble Lake	mottled chert with dolomite
29-8	west shore of Marble Lake	mottled chert breccia
BOB-1	ridge north of Bath Lake	brecciated chert
BOB-2	ridge north of Bath Lake	chert silt to sand
E1-3	basal Fleming to west of grid at Elizabeth Lake	chert breccia, silt matrix
E1-4A	basal Fleming to west of grid at Elizabeth Lake	quartz-chert arenite, phosphatic grains and cement
E1-4B	basal Fleming to west of grid at Elizabeth Lake	chert-quartz siltstone, phosphatic grains and cement
E1-4C	basal Fleming to west of grid at Elizabeth Lake	chert-quartz siltstone, phosphatic grains and cement

Sample	Location	Description
E1-5	west of grid at Elizabeth Lake	chert breccia, quartz sand matrix
E1-8	Elizabeth Lake	chert breccia, micaceous matrix
E1-9	Elizabeth Lake	massive, faintly banded chert
E1-10	Elizabeth Lake	quartz-chert sand with detrital K-feldspar
E1-11	Elizabeth Lake	chert-quartz arenite to chert breccia
E2-5	ridge 3.5 km north of Elizabeth Lake	quartz-chert arenite, carbonate cement
F1-1	ridge immediately east of Elizabeth Lake	chert breccia, quartz sand matrix, jasper cement
F1-2	ridge immediately east of Elizabeth Lake	mottled chert
F1-3	ridge immediately east of Elizabeth Lake	chert breccia, minor quartz sand
L1+2.5	north of Knox Mine, south of grid	chert breccia, quartz sand matrix
L1+25	north of Knox Mine, south of grid	chert breccia, quartz sand matrix
L1+36	north of Knox Mine, south of grid	chert breccia, jasper cement
L1+51	north of Knox Mine, south of grid	chert breccia, micaceous matrix
EL-1	Elizabeth Lake, to north of grid (Fig. 15)	chert breccia micaceous matrix
EL-2	Elizabeth Lake, to north of grid (Fig. 15)	chert breccia
EL-3	Elizabeth Lake, to north of grid (Fig. 15)	chert breccia
KR-1	crest of Knob Ridge	"crystallized gel texture" chert
KR-2	crest of Knob Ridge	"crystallized gel texture" chert
KR-3	crest of Knob Ridge	"crystallized gel texture" chert
SS-1	rail cut south of Schefferville	shale below Fleming Formation
SS-2	rail cut south of Schefferville	shale above Fleming Formation
SS-3	rail cut south of Schefferville	Fleming Formation chert breccia

APPENDIX 2

Analytical data

Table 1. Major-element analyses of samples from the Fleming Formation and related rocks

Sample	3-1	3-2	3-3	4-1	4-3	4-5	4-6	5-1A	5-1B	5-2A
SiO ₂	97.60	90.40	97.50	96.30	93.70	87.40	96.60	89.10	95.00	90.60
TiO ₂	0.06	0.70	0.08	0.11	0.17	0.23	0.10	0.13	0.07	0.11
Al ₂ O ₃	0.97	5.22	1.10	1.56	3.87	7.81	0.83	1.90	0.84	2.29
Fe ₂ O ₃	0.62	0.09	0.06	0.72	0.16	0.63	1.42	4.94	2.17	5.50
FeO	0.05	0.05	0.05				0.80	3.00	1.10	0.30
MnO	0.01	0.01	0.01	0.01	0.01	0.01	0.01	0.02	0.01	0.01
MgO	0.15	0.14	0.11	0.01	0.05	0.12	0.28	0.48	0.26	0.13
CaO	0.05	0.03	0.03	0.05	0.05	0.04	0.03	0.96	0.29	0.10
Na ₂ O	ND	ND	ND	ND	ND	0.01	ND	ND	ND	0.04
K ₂ O	0.20	1.37	0.31	0.34	1.11	2.17	0.03	0.02	0.02	0.05
P ₂ O ₅	0.04	0.05	0.02	0.05	0.03	0.06	0.03	0.65	0.20	0.22
LOI	0.54	1.39	0.54	0.62	0.93	1.62	0.62	1.70	1.23	
H ₂ O	0.30	0.70	0.20	0.30	0.50	1.00	0.40	1.10	0.60	1.00
CO ₂	ND	ND	ND	0.02	0.02	ND	ND	ND	ND	0.20
SUM	100.30	99.50	99.80	99.80	100.10	100.20	100.00	99.90	100.10	100.60
Sample	5-4	27-1	27-2	27-3	28-2	28-3A	28-4	28-8	28-9	28-10
SiO ₂	92.10	96.40	96.40	96.20	95.20	89.90	96.20	94.70	95.20	94.10
TiO ₂	0.12	ND	0.06	0.09	0.10	0.19	0.05	0.08	0.14	0.17
Al ₂ O ₃	2.00	0.71	1.44	1.59	2.01	5.52	0.82	1.71	2.09	3.08
Fe ₂ O ₃	3.67	0.75	0.10	0.08	0.68	0.73	0.27	0.85	0.65	0.65
FeO	1.90									
MnO	0.02	0.01	0.02	0.01	0.01	0.01	0.01	ND	ND	0.01
MgO	0.49	0.01	ND	ND	0.05	0.13	0.02	0.04	0.06	0.04
CaO	0.22	0.12	0.02	0.01	0.04	0.28	0.05	0.44	0.06	0.02
Na ₂ O	ND	ND	ND	ND	ND	ND	ND	ND	ND	ND
K ₂ O	0.06	0.19	0.42	0.46	0.46	1.49	0.21	0.40	0.52	0.78
P ₂ O ₅	0.07	0.10	0.02	0.22	0.04	0.17	0.04			0.03
LOI	1.31	1.31	0.70	1.08	0.85	1.23	0.93	1.16	0.77	0.85
H ₂ O	1.00	0.30	0.30	0.30	0.50	0.80	0.30	0.40	0.50	0.60
CO ₂	0.14	ND	ND	ND	ND	ND	ND	ND	0.05	ND
SUM	100.10	99.70	99.20	99.60	99.50	99.70	98.60	99.70	99.60	99.70
Sample	29-4B	29-5B	29-6	29-7	29-8	BOB-1	BOB-2	E1-3	E1-4A	
SiO ₂	38.80	72.90	85.20	87.00	97.20	93.10	91.00	96.20	54.10	
TiO ₂	0.01	0.02	0.02	0.02	0.02	0.11	0.15	0.10	0.27	
Al ₂ O ₃	0.06	0.22	0.08	0.18	0.33	5.94	4.02	3.01	8.43	
Fe ₂ O ₃	0.47	0.22	0.14	0.14	0.09	0.10	1.58	0.80	0.26	
FeO						0.00	1.10	0.10	0.30	
MnO	0.05	0.03	0.02	0.02	0.01	ND	0.01	0.01	0.00	
MgO	13.30	5.62	2.87	2.70	0.27	0.04	0.39	0.25	0.70	
CaO	19.20	8.55	4.40	4.17	0.47	0.04	0.23	0.05	18.80	
Na ₂ O	ND	ND	ND	ND	ND	0.05	ND	0.03	0.00	
K ₂ O	0.05	0.09	0.05	0.08	0.14	1.53	0.96	0.81	2.75	
P ₂ O ₅	0.03	0.11	0.03	0.05	0.03	0.03	0.16	0.04	13.30	
LOI	28.30	12.50	6.93	6.00	1.00		1.16		2.08	
H ₂ O	0.10	0.10	0.10	0.10	0.10	0.80	0.70	0.50	1.20	
CO ₂	27.90	11.80	6.21	5.72	0.61	0.20	0.05	0.40	0.35	
SUM	100.30	100.20	99.70	100.40	99.60	101.90	99.70	102.30	100.70	

Table 1. Continued

Sample	E1-4C	E1-8	E1-9	E1-10	E1-11	E2-5	F1-1	F1-2	F1-3
SiO ₂	38.90	88.90	95.40	95.50	98.50	85.60	94.40	98.60	96.90
TiO ₂	0.34	0.24	0.02	0.06	0.02	0.06	0.09	0.03	0.04
Al ₂ O ₃	9.01	4.83	1.45	1.93	0.83	0.74	1.54	0.04	0.82
Fe ₂ O ₃	0.30	2.67	1.10	0.32	0.40	9.88	2.52	0.07	1.31
FeO	0.20	0.80	1.00	0.10	0.10	1.40	0.20	ND	0.80
MnO	0.01	0.01	0.01	0.01	ND	0.41	0.01	0.01	0.01
MgO	0.55	0.36	0.20	0.11	0.05	0.43	0.11	0.11	0.24
CaO	25.50	0.47	0.05	0.07	0.04	0.16	0.05	0.09	0.13
Na ₂ O	0.06	ND	0.02	ND	0.02	ND	ND	ND	ND
K ₂ O	2.80	1.07	0.07	0.52	0.11	0.02	0.12	0.01	0.06
P ₂ O ₅	19.80	0.40	0.05	0.03	0.03	0.10	0.05	0.03	0.09
LOI		1.54		1.47		2.47	0.77	1.00	0.70
H ₂ O	2.10	1.20	0.70	0.60	0.70	1.50	0.50	0.10	0.40
CO ₂	0.50	0.03	0.10	ND	1.30	0.63	ND	0.06	ND
SUM	100.10	100.50	100.20	100.00	102.10	99.90	99.70	100.00	100.30
Sample	L1+2.5	L1+25	L1+36	L1+51	EL-1	EL-2	EL-3	KR-1	KR-2
SiO ₂	95.50	96.00	95.70	97.00	94.50	97.80	99.30	98.10	99.30
TiO ₂	0.06	0.07	0.05	0.09	0.11	0.02	0.02	0.02	0.01
Al ₂ O ₃	2.87	3.46	0.82	1.42	3.00	0.04	0.02	0.58	0.07
Fe ₂ O ₃	0.90	0.20	2.28	0.15	0.11	0.24	0.14	0.07	0.09
FeO	0.20	ND	0.10	0.10					
MnO	0.01	0.01	0.01	0.01	ND	0.01	ND	ND	ND
MgO	0.07	0.05	0.16	0.12	0.18	0.07	ND	0.02	ND
CaO	0.04	0.18	0.08	0.02	0.19	0.44	0.08	0.09	0.07
Na ₂ O	0.04	0.06	ND	ND	0.06	0.03	0.02	0.04	0.03
K ₂ O	0.05	0.85	0.26	0.41	0.95	0.01	ND	0.16	0.03
P ₂ O ₅	0.05	0.16	0.05	0.04	0.02	0.02	0.01	0.02	0.01
LOI			0.77	0.39	0.85	0.54	0.54	0.31	0.31
H ₂ O	0.80	0.60	0.40				0.20		
CO ₂	0.90	0.60	0.04				ND		
SUM	101.90	102.20	100.20	99.70	100.00	99.20	100.10	99.40	99.90
Sample	KR-3	SS-1	SS-2	SS-3					
SiO ₂	98.10	66.50	67.70	97.00					
TiO ₂	0.03	0.52	0.63	0.05					
Al ₂ O ₃	0.88	15.90	19.30	1.31					
Fe ₂ O ₃	0.17	1.95	0.94	0.22					
MnO	0.01	ND	ND	ND					
MgO	0.03	1.34	1.19	0.10					
CaO	0.18	0.08	0.09	0.20					
Na ₂ O	0.04	0.09	0.11	0.05					
K ₂ O	0.25	7.24	6.19	0.44					
P ₂ O ₅	0.09	0.07	0.03	0.09					
LOI	0.31	6.31	3.00	0.31					
SUM	100.10	100.10	99.30	99.80					
<p>In samples where FeO is not reported, all iron is reported as ferric oxide. ND = NOT DETECTED, generally below 0.01 weight percent of the oxide in question.</p>									

Table 2. Trace-element analyses of samples from the Fleming Formation and related rocks

Sample	3-1	3-2	3-3	4-1	4-3	4-5	4-6	5-1A	L1+51	EL-1	EL-2
Cr(ppm)	40	30	30				30	110	20	28	29
Rb(ppm)	20	50	20	40	50	100	20	20	10	34	17
Sr(ppm)	ND	60	ND	ND	ND	20	ND	ND	ND	ND	ND
Y(ppm)	ND	20	ND	10	20	20	20	ND	20	37	ND
Nb(ppm)	20	ND	ND	20	10	10	20	20	10	12	11
Zr(ppm)	30	880	90	50	50	380	110	40	10	42	26
Ba(ppm)	70	90	70	80	100	90	90	90	100	66	141
Th(ppm)	2.0	37.0	4.0	6.9	3.3	3.8		2.6	1.2		
U(ppm)	1.3	2.9	0.8	0.9	1.2	1.2		11.5	0.9		
Au(ppb)	2	ND	ND	ND	1	ND	10	1	4		
Sample	EL-3	KR-1	KR-2	KR-3	SS-1	SS-2	SS-3				
Cr(ppm)	28	27	24	24	119	217	27				
Rb(ppm)	14	18	ND	22	239	223	43				
Sr(ppm)	ND	ND	ND	ND	ND	11	ND				
Y(ppm)	ND	25	ND	21	39	50	30				
Nb(ppm)	ND	19	ND	ND	ND	14	ND				
Zr(ppm)	ND	ND	12	ND	84	113	ND				
Ba(ppm)	53	44	59	66	489	222	56				
Sample	5-1B	5-2A	5-4	27-1	27-2	27-3	28-2	28-3A	28-3B	28-4	28-8
Li(ppm)		14		5	4	ND	7	1		1	4
Be(ppm)		0.3		1.0	2.0	2.0	2.0	2.0		2.0	ND
Ni(ppm)		15									
Cr(ppm)	40	3*	40	30	40	30	30	40		30	30
Cu(ppm)		20									
Zn(ppm)						6					
Rb(ppm)	ND		10	10	20	20	30	40		20	10
Sr(ppm)	ND		ND	10	ND	ND	ND	ND		ND	ND
Y(ppm)	ND		ND	ND	ND	10	ND	30		ND	10
Nb(ppm)	10		20	10	10	10	30	10		20	20
Zr(ppm)	10		60	20	40	ND	10	60		ND	ND
Ba(ppm)	110	1	100	100	90	70	80	180		40	100
La(ppm)		11		4	12	5	12	35		5	9
Ce(ppm)				7	23	9	17	43		6	11
Th(ppm)	1.1		3.3	2.0	4.2	1.6	2.3	3.4		0.7	
U(ppm)	3.3		2.6	0.9	0.9	0.8	0.9	2.3		0.6	
Au(ppb)	ND		1	ND	ND	1	ND	1		ND	3
Sample	28-9	28-10									
Li(ppm)	3	3									
Be(ppm)	ND	0.5									
Ni(ppm)											
Cr(ppm)	30	30									
Cu(ppm)											
Zn(ppm)											
Rb(ppm)	20	20									
Sr(ppm)	ND	ND									
Y(ppm)	ND	ND									
Nb(ppm)	10	10									
Zr(ppm)	20	30									
Ba(ppm)	90	60									
La(ppm)	10	17									
Ce(ppm)	14	24									
Th(ppm)		3.7									
U(ppm)		1.5									
Au(ppb)	ND	ND									

Table 2. Continued

Sample	29-4B	29-5B	29-6	29-7	29-8	BOB-1	BOB-2	E1-3	E1-4A	E1-4B	E1-4C
Li(ppm)	1	2	ND	ND	ND	6		9			17
Be(ppm)	0.5	0.5	0.5	0.5	0.5	0.1		0.7			3.2
Cr(ppm)	ND	20	20	20	40	17	20	7	ND	ND	21
Ni(ppm)						4		7			21
Cu(ppm)						8		9			16
Zn(ppm)						0.5		38			25
Rb(ppm)	ND	10	ND	10	10		40		100	100	
Sr(ppm)	ND	ND	ND	ND	ND		ND		30	40	
Y(ppm)	10	10	10	ND	ND		20		60	70	
Nb(ppm)	ND	10	ND	10	10		20		ND	10	
Zr(ppm)	ND	ND	ND	ND	ND		40		60	90	
Ba(ppm)	ND	30	70	50	50	0.5	70	10	ND	ND	50
La(ppm)	0.5	2	0.5	1	0.5	14		0.5			38
Ce(ppm)	ND	ND	ND	ND	ND						
Th(ppm)	0.25	0.25	0.25	0.25		3.0	2.5	1.7	0.9	5.4	6.2
U(ppm)	0.6	0.7	0.6	0.6		1.4	2.0	1.6	1.4	10.1	10.5
Au(ppb)	1	ND	5	2	3		ND		2	1	
Sample	E1-8	E1-9	E1-10	E1-11	E2-5	F1-1	F1-2	F1-3	L1+2.5	L1+36	
Li(ppm)		14		6					9		
Be(ppm)		0.1		0.1					0.2		
Cr(ppm)	40	4	30	3	30	20	20	20	8	20	
Ni(ppm)		30		3					10		
Cu(ppm)		5		6					8		
Zn(ppm)		2		2					5		
Rb(ppm)	20		40		10	10	10	10		20	
Sr(ppm)	10		ND		ND	10	ND	ND		ND	
Y(ppm)	30		ND		ND	40	ND	ND		ND	
Nb(ppm)	10		10		20	10	20	ND		10	
Zr(ppm)	40		ND		10	40	ND	ND		ND	
Ba(ppm)	90	0.5	160	ND	30	70	90	90	ND	80	
La(ppm)		1		5				26			
Th(ppm)	4.3	0.25	1.6	0.9		7.7		8.0	4.6	0.25	
U(ppm)	1.1	2.0	ND	1.0		ND		ND	0.70	0.50	
Au(ppb)	ND		5		3					ND	

ND = NOT DETECTED, generally a concentration of less than 10 parts per million of the element, except: Li and La = (1 ppm); Th, Ba, and U = (0.5 ppm); Be = (0.1 ppm) and Au = (1ppb) for most samples.
Blanks in the table indicate that the element was not analyzed.
Sample locations are either plotted on Figures or described in Appendix 1.
Pyrite separated from sample 27-1 was analyzed for sulphur isotopes at the Ottawa-Carleton Centre for Geoscience Studies-Geological Survey of Canada stable isotope facility. The samples yielded sulphur of $\delta^{34} = +21.7\text{‰}$.

Table 3. Replicate analyses of sample LI-55m

Laboratory	A	B	C	D	E	F
Analytical Methodology	XRF	XRF	XRF	ICP	ICP	XRF
H ₂ O		0.0	0.1	0.0	0.1	
Li	< 1					3
Be	2			0.0	0.0	< 1
B	30	5.4 ³	5.2 ³			< 10
CO ₂		0.1	0.1	0.02	0.02	
F	60	< 50 ³	< 50 ³			
Na ₂ O	< 100 ¹	0.0	0.0	0.03	0.03	<0.01
MgO	100 ¹	0.0	0.0	0.04	0.04	0.02
Al ₂ O ₃	0.45	0.5	0.4	0.47	0.47	0.46
SiO ₂	98.9	99.1	99.0	97.9	97.0	98.8
P ₂ O ₅	40 ¹	0.00	0.00	0.02	0.02	0.02
S		0.00	0.01	0.00	0.01	
Cl	< 50	< 100 ³	< 100 ³			
K ₂ O	700 ¹	0.12	0.12	0.10	0.10	0.11
CaO	100 ¹	0.00	0.00	0.03	0.05	0.02
Sc						0.55
TiO ₂	70.0 ¹	0.02	0.02	0.01	0.01	0.04
V	< 2			1	1	2
Cr	2	0.00	0.00	2	2	3.4
MnO	32 ¹	0.01	0.01	0.01	0.01	34 ¹
Fe ₂ O ₃		0.00	0.00	0.0	0.0	
FeO	0.1	0.2	0.2	0.2	0.2	
FeO ¹	1200 ¹					0.10
Co	< 1			0	0	0.4
Ni	< 1			2	1	1
Cu	2.5			0	0	4.5
Zn	2.0			11	16	1.5
Ga						< 1
Ge	< 10					< 10
As	0.2	0	5			< 1
Se		< 0.5 ³	< 0.5 ³			< 0.5
Br		1	0			0.9
Rb	30	1	2			10
Sr	<10	2	3			< 10
Y	40	17	19	12	12	30
Zr	<10	7	7			< 10
Nb	10	3	2			10
Mo	<1	2	2			< 2
Pd						< 2
Ag	< 0.5	< 0.5 ³	< 0.5 ³			< 0.5
Cd	< 1	< 0.5 ³	< 0.5 ³			0.4
Sb	0.4	< 0.5 ³	< 0.5 ³			< 0.1
Te		< 0.5 ³	< 0.5 ³			
Cs						0.3
Ba	100	65	72	0	0	120
La				1.9	1.9	2.2
Ce		2.9 ²	2.3 ²	2.2	2.3	3

Laboratory	A	B	C	D	E	F
Analytical Methodology	XRF	XRF	XRF	ICP	ICP	XRF
Nd		2.5 ²	2.7 ²	0.5	3.0	< 3
Sm		0.4 ²	0.4 ²	0.3	0.2	0.47
Eu		0.1 ²	0.1 ²	0.1	0.1	0.22
Gd		1.0 ²	1.1 ²	0.9	0.8	
Tb						0.2
Dy		1.3 ²	1.3 ²	1.0	0.9	0.6
Yb		0.6 ²	0.6 ²	2.5	2.6	0.67
Lu						0.09
Hf						< 0.2
Ta						< 0.5
W						< 1
Pt						< 10
Au	<2	< 1.0 ³	1.3 ³			< 1
Pb	4	< 5 ³	< 5 ³			< 1
Bi		< 0.5 ³	< 0.5 ³			0.2
Th		0	2			0.3
U		0	0			0.7
LOI	0.54					0.39
SUM	100.3	100.0	100.0	98.8	98.1	100.0

UNITS

OXIDES AND S [Sulphur] as weight per cent
 ELEMENTS as parts per million (ppm) by weight EXCEPT Au, Pt, Pd as parts per billion (ppb) by weight
 FeO¹ is total iron as FeO

LABORATORY/SOURCES OF DATA

- A X-RAY ASSAY LABORATORIES LIMITED
- B GEOLOGICAL SURVEY OF CANADA
- C GEOLOGICAL SURVEY OF CANADA
- D GEOLOGICAL SURVEY OF CANADA
- E GEOLOGICAL SURVEY OF CANADA
- F X-RAY ASSAY LABORATORIES LIMITED

ANALYTICAL METHODOLOGY

XRF X-Ray Fluorescence Spectrometry
 ICP Inductively Coupled Plasma Emission Spectrometry

SUPERSCRIPTS

- ¹ ppm element
- ² Geological Survey of Canada Inductively Coupled Plasma Emission Spectrometry
- ³ Geological Survey of Canada Geochemistry Laboratory including:

- F, Cl, As = Pyrohydrolysis-Ion Chromatography
- Se, Sb, Te = Hydride generation Atomic Absorption
- Ag = Air-Acetylene Flame Atomic Absorption
- Cd = Pressurized HF Atomic Absorption
- B = Fusion 1 Inductively Coupled Plasma Emission Spectrometry
- Au = MIBK extraction Graphite Furnace Atomic Absorption

Table 4. Neutron activation analyses of samples of the Fleming Formation

Element (ppm)	Limit	E1-3	E1-4A	E1-4B	E1-4C	E1-5	E1-8	E1-9	E1-10	E1-11	3-1	3-2	3-3	4-1	4-5
Sc	0.05	1.2	7.9	7.3	10	1.5	4.9	0.52	0.81	0.54	1.1	5.2	1.1	12	13
Cs	0.2	< 0.2	0.79	0.76	1	< 0.2	0.37	< 0.2	0.28	< 0.2	< 0.2	0.28	< 0.2	1.4	1.8
La	0.5	1.2	26	29	40	5.5	14	1.8	2.4	5.9	6.7	65	9.8	48	44
Ce	2	< 2	39	39	55	7.4	23	< 2	5	6.7	14	121	19	86	102
Nd	2	< 2	26	27	36	4.5	12	< 2	< 0.2	4.3	6.4	38	8.5	42	60
Sm	0.05	0.096	5.9	6.5	7.5	0.8	2.1	0.1	0.3	0.76	1.2	5.5	1.4	8.8	12
Eu	0.1	< 0.1	1.6	1.8	2	0.22	0.56	< 0.1	< 0.1	0.17	0.18	0.67	0.26	2.6	3.3
Tb	0.1	< 0.1	0.9	0.95	1.1	0.14	0.39	< 0.1	< 0.1	0.17	0.12	0.57	0.14	0.94	1.2
Ho	0.5	< 0.5	1.8	1.9	1.9	< 0.5	0.64	< 0.5	< 0.5	< 0.5	< 0.5	0.71	< 0.5	1.3	1.3
Tm	0.2	< 0.2	0.41	< 0.2	0.26	< 0.2	< 0.2	< 0.2	< 0.2	< 0.2	< 0.2	< 0.2	< 0.2	0.31	0.46
Yb	0.2	< 0.2	2.1	2.4	2.4	0.36	1.1	< 0.2	< 0.2	0.59	0.26	1.7	0.36	2.9	2.7
Lu	0.05	< .05	0.29	0.32	0.33	0.052	0.16	<0.05	< 0.05	0.07	<0.05	0.27	<0.05	0.48	0.42
Hf	0.2	0.67	2	2.7	2.3	0.53	1.3	< 0.2	0.86	0.47	0.98	21	2.3	4.6	5.4
Ta	0.1	0.11	0.38	0.28	0.4	< 0.1	0.29	< 0.1	< 0.1	< 0.1	< 0.1	0.35	< 0.1	1.8	2.9
Th	0.2	1.4	5.	5.1	6	0.91	3.6	0.28	1.4	0.8	1.7	32	3.2	5.8	3.9
U	0.5	1.4	7.7	9.9	10	1.5	0.79	1.7	< 0.5	0.91	0.96	2.7	0.59	0.8	0.99
Element (ppm)	5-1B	5-2	5-4	27-1	27-2	27-3	28-3A	28-4	28-10	29-4B	29-5B	BOB-1	BOB-2	L4-4M	L1-36M
Sc	0.65	1.7	1.6	0.88	0.87	1	4.1	0.75	2.7	0.34	0.31	2.3	3.1	2.3	0.72
Cs	< 0.2	< 0.2	< 0.2	< 0.2	< 0.2	< 0.2	0.37	< 0.2	< 0.2	< 0.2	< 0.2	< 0.2	< 0.2	< 0.2	< 0.2
La	1.4	11	10	3.5	9.7	4.2	29	3.3	14	0.7	1.6	16	9	27	1.7
Ce	2.3	20	18	5.6	18	7.3	40	4.5	21	<2	< 2	21	14	42	2.2
Nd	3	9.8	8.4	4.2	8.2	3	26	2.6	11	<2	< 2	13	6.7	25	< 2
Sm	1	2	1.3	0.69	1.3	0.62	4	0.5	1.8	0.15	0.29	2.1	1.6	3.5	0.22
Eu	0.27	0.38	0.19	0.19	0.16	0.14	0.83	0.11	0.33	< 0.1	< 0.1	0.47	0.4	0.55	< 0.1
Tb	0.18	0.28	0.14	0.19	0.13	< 0.1	0.45	< 0.1	0.14	< 0.1	< 0.1	0.23	0.34	0.21	< 0.1
Ho	< 0.5	< 0.5	< 0.5	< 0.5	< 0.5	< 0.5	0.65	< 0.5	< 0.5	< 0.5	< 0.5	< 0.5	0.54	< 0.5	< 0.5
Tm	< 0.2	< 0.2	< 0.2	< 0.2	< 0.2	< 0.2	< 0.2	< 0.2	< 0.2	< 0.2	< 0.2	< 0.2	< 0.2	< 0.2	< 0.2
Yb	0.37	0.88	0.55	0.44	0.26	0.42	1	< 0.2	0.48	< 0.2	< 0.2	0.67	0.66	0.89	0.21
Lu	0.058	0.11	0.076	<0.05	0.05	<0.05	0.14	0.051	0.069	<0.05	<0.05	0.1	0.1	0.12	<0.05
Hf	0.44	1.8	1.6	0.76	1.2	0.58	1.5	0.3	1.1	< 0.2	< 0.2	1.1	1.4	1.4	< 0.2
Ta	< 0.1	0.17	0.19	< 0.1	< 0.1	< 0.1	0.2	< 0.1	0.22	< 0.1	< 0.1	0.16	0.15	0.21	< 0.1
Th	0.89	3	2.8	1.6	4.1	1.3	2.8	0.51	2.9	< 0.2	< 0.2	2.9	2.4	2.9	0.36
U	2.6	4.3	2	0.74	0.58	<0.5	1.9	< 0.5	1.3	< 0.5	0.59	1.2	1.6	1.2	< 0.5

Column marked LIMIT lists elemental limits of detection.

